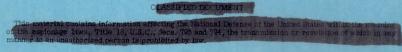# NACA

RESEARCH MEMORANDUM

SUMMARY OF NACA RESEARCH ON AFTERBURNERS

FOR TURBOJET ENGINES

By Bruce T. Lundin, David S. Gabriel, and William A. Fleming

Lewis Flight Propulsion Laboratory
Cleveland, Ohio

NATIONAL ADVISORY COMMITTEE
FOR AERONAUTICS
WASHINGTON
March 23, 1956

TABLE OF CONTENTS

3701

CONFIDENTIAL

DECLASSIFIED

CONFIDENTIAL

3701

NATIONAL ADVISORY COMMITTEE FOR AERONAUTICS

RESEARCH MEMORANDUM

SUMMARY OF NACA RESEARCH ON AFTERBURNERS

FOR TURBOJET ENGINES

By Bruce T. Lundin, David S. Gabriel
and William A. Fleming

SUMMARY

NACA research on afterburners for turbojet engines during the past 5 years is summarized. Although most of this work has been directed toward the development of specific afterburners for various engines rather than toward the accumulation of systematic data, it has, nevertheless, provided a large fund of experimental data and experience in the field. The references cited present over 1000 afterburner configurations and some 3500 hours of operation. In the treatment of the material of this summary, the principal effort has been to convey to the reader the "know-how" acquired by research engineers in the course of the work rather than to formulate a set of design rules.

Material is presented on the following general topics of afterburner design: burner-inlet diffusers, fuel-injection systems, flameholders, combustion space (burner length and shape), combustion instability (screech), starting and transient performance, effects of diluents, and burner-shell cooling. The section on burner-inlet diffusers considers the effect of diffuser length and shape, as well as the use of flow-control devices such as vanes and vortex generators, on both burner-inlet velocity profile and diffuser pressure drop. The fuel-injection system discussed is primarily that of radial spray bars. The effects of spray-bar design and installation on the fuel-air-ratio distribution in the burner, and the resulting influence of these distributions on afterburner performance is presented. The discussion of flameholders includes considerations of flameholder cross-sectional shape, gutter width, number of gutters, and over-all blockage on combustion efficiency, stability limits, and pressure drop. Afterburner-length requirements and the effects of shell taper and flameholder location for various operating conditions are presented in the section on combustion space. The work summarized on combustion screech includes experiments related to the aerodynamics of the flow approaching the combustion zone, the identification of the nature of pressure oscillation, and the use of

screech-prevention methods such as perforated liners. The starting
methods discussed are spark plugs, spontaneous ignition, and hot-streak
ignition. Also considered in this section are the transient performance
characteristics of typical afterburners and control systems. The dilu-
ents considered are water-alcohol mixtures and ammonia; their effects
on both combustor efficiency and stability limits are presented. The
burner-shell cooling methods discussed are variation in internal geom-
etry of fuel systems and flameholders, inner liners, ceramic coatings,
external forced-convection air shrouds, and transpiration or porous-
wall cooling.

INTRODUCTION

Afterburners for turbojet engines have been under development in
this country since the early days of the turbojet engine. Work on full-
scale afterburners was started at the Lewis laboratory as early as 1944,
and test results of successful afterburners were first published in
1946. Within this past decade, afterburners for turbojet engines, paced
by research and development effort in expanded laboratory facilities,
have found increasing application in service aircraft. Practically all
engines manufactured today are equipped with afterburners, and their use
has increased from what was originally a short-period thrust-augmentation
application into an essential feature of the turbojet propulsion system
for flight at supersonic speeds.

A summary of NACA research in this field up to 1950 is presented
in reference 1. Since that time, full-scale afterburner research and
development have continued at a steady pace. Results of this more re-
cent work, covering more than 1000 burner configurations and some 3500
hours of burner operation, are, however, scattered throughout many sep-
arate reports. Many of these reports are, furthermore, not generally
available because of their proprietary nature. It is the purpose of
the present report, therefore, to summarize and to make generally avail-
able the highlights of this past 5 years of afterburner research and de-
velopment at the NACA.

A principal difficulty facing both the designer of afterburners
and the authors of summary reports in this field is that there exists
no really adequate theoretical background for the combustion process
or for combustor design. A further difficulty is that most of the ex-
perimental investigations that have been conducted were directed, for
the most part, toward the development of specific afterburners for var-
ious engines rather than to the accumulation of systematic data. This
work has, nonetheless, provided not only very substantial improvements
in the general performance of afterburners, but also a large fund of
experimental data and an extensive background and experience in the
field.

CONFIDENTIAL

3701

CU-1 back

Afterburner design being, therefore, more of an art than a science, and necessarily based more on experience than theory, the present report is largely confined to a summary of the many, and frequently unrelated, experimental investigations that have been conducted rather than to the formulation of a set of design rules. In the treatment of this material an effort has been made, however, to convey to the reader the "know-how" acquired by research engineers in the course of afterburner studies. The material presented is divided into the following topics:

(1) Experimental procedures

(2) Afterburner-inlet diffusers

(3) Fuel-injection systems

(4) Flameholder design

(5) Combustion space

(6) Effect of operating variables on performance

(7) Combustion instability (screech)

(8) Ignition, starting, and transient performance

(9) Effects of diluents on performance

(10) Shell cooling

Each topic is treated somewhat independently, although interacting considerations are discussed where known or important. A brief summary of most of these topics is also presented at the close of the report. Numerous references are listed for the convenience of those who may desire more detailed treatment than is possible herein.

No attempt is made to describe the details of the apparatus and test procedures used, although they are available in many of the references. The general range of afterburner operating conditions discussed comprises burner-inlet velocities from 400 to 600 feet per second, burner-inlet pressures from 500 to 3500 pounds per square foot absolute, inlet temperatures of approximately 1700° R, and afterburner fuel-air ratios from about 0.03 to about 0.08. Most of the data were obtained with afterburners operating on full-scale engines in either an altitude test chamber or in the altitude wind tunnel. Some data were also obtained from a full-scale (26-inch diam.) afterburner installed in a blower-rig setup.

370L

EXPERIMENTAL PROCEDURES

The blower-rig setup was provided with a preheater and an annular burner-inlet diffuser to simulate turbine-outlet conditions and was connected to central laboratory combustion-air and exhaust equipment. A choked, fixed-area exhaust nozzle that discharged into an exhaust plenum chamber was provided at the afterburner outlet. The full-scale turbojet engines used for most of the investigations were installed either in an altitude wind tunnel or in an altitude test chamber; some data were also obtained from static sea-level test stands. All engines were installed on thrust-measuring platforms.

In the engine installations, the principal independent operating variables were afterburner fuel-air ratio and inlet pressure. Variations in fuel-air ratio required simultaneous variation in exhaust-nozzle area by use of either a variable-geometry nozzle or a series of fixed nozzles in order to maintain constant turbine-inlet temperature; control of afterburner-inlet pressure was obtained by varying the simulated altitude of engine operation. Variations in afterburner-inlet velocity could be made independently of other operating variables only by changes in afterburner diameter. Afterburner-inlet temperature was established by engine operating requirements, and was not an independent variable of operation.

Because the operation of the blower rig was not restricted by any engine operating requirements, changes in inlet velocity could be made at constant values of inlet pressure and of fuel-air ratio by variations of the exhaust-nozzle area.

When the afterburner on the engine setups was equipped with a fixed-area exhaust nozzle, the afterburner-outlet temperature was determined by two methods. One is based on flow continuity through the nozzle throat and the other on momentum, or jet-thrust, considerations. With the flow-continuity method, the actual measurements required to compute exhaust temperature are nozzle-outlet total pressure, effective nozzle flow area, and total gas flow; with the momentum method they are nozzle-outlet total pressure, jet thrust, and total gas flow. With proper instrumentation and by use of appropriate gas properties and nozzle coefficients, satisfactory agreement between the two methods is usually obtained. When the afterburner was equipped with a variable-area exhaust nozzle, the outlet temperature was usually computed only by the momentum method, because of the uncertainty of the effective nozzle flow area under all conditions of operation. In the blower-rig setup, the burner thrust was not measured, and outlet temperature was therefore computed only by the flow-continuity method.

CONFIDENTIAL

3701

The combustion efficiency of an afterburner has been computed on at least four different bases in the various references cited. These four definitions of combustion efficiency are: (1) ratio of actual enthalpy rise to heat input in the fuel, (2) ratio of the ideal fuel flow for the actual temperature rise to the actual fuel flow, (3) ratio of the actual temperature rise to the ideal temperature rise for the fuel flow, and (4) ratio of actual enthalpy rise to ideal enthalpy rise based on the corresponding temperature rises. At fuel-air ratios above stoichiometric, methods (3) and (4) give values of efficiency appreciably greater than those computed by methods (1) and (2); at lower fuel-air ratios, all four methods substantially agree. The data presented herein from different sources are, however, either for fuel-air ratios at which the differences in efficiency are only 3 or 4 percent or the results from any one investigation, or within any one figure, are consistent within themselves. It was therefore considered unnecessary, for the purposes of this summary report, to reduce all efficiency data to a common basis. Because of the differences in efficiency calculations, however, and because different types of afterburners in various states of development were used, the results presented herein should not be compared from one unrelated figure to another.

For all calculations, the fuel flow to the afterburner was taken to be the sum of the fuel directly injected into the afterburner and the unburned fuel entering the afterburner because of incomplete combustion in the primary engine combustor. The afterburner is thus made liable for unburned primary-combustor fuel. The afterburner fuel-air ratio is defined as the ratio of this weight of fuel to the weight of unburned air from the primary engine combustor (or preheater).

AFTERBURNER-INLET DIFFUSERS

The aerodynamic characteristics of the diffuser between the turbine exhaust and the afterburner inlet have an important influence on the performance of the afterburner. These characteristics, in conjunction with those of the turbine, determine both the velocity distribution and the mass-flow distribution entering the afterburner. The effectiveness of the diffuser in reducing the gas velocity below the turbine-discharge value is important, because high burner-inlet velocities have a detrimental effect on afterburner performance. The mass-flow distribution determines the required fuel-flow distribution and, hence, the design of the fuel-injection system. In addition, diffuser pressure losses have a first-order effect on thrust.

Turbine-exhaust gases are discharged from the turbine into the annular inlet of the afterburner diffuser at average axial Mach numbers from 0.4 to 0.8, and at flow directions that may be axial or as much as

40° from the axial, depending on the turbine design. To provide satis-
factory velocities at the afterburner inlet, the diffuser is usually re-
quired to have an area ratio between 1.5 and 2.0. Space and weight con-
siderations usually dictate a maximum diffuser length of less than twice
the afterburner diameter.

These are extreme diffuser requirements and in most cases they lie
outside the realm of known diffuser-design techniques. It is not sur-
prising therefore that large pressure and velocity gradients usually
exist at the outlet of an afterburner diffuser, or that an appreciable
loss in total pressure occurs in the diffuser.

<div style="text-align: center;">

Effect of Diffuser-Outlet Velocity on

Afterburner Performance

</div>

No precise criteria are known that relate the performance of an
afterburner to the magnitude of the velocity gradient at the burner in-
let. Experience has shown, however, that afterburner performance is
sensitive to the magnitude of the velocity of the gases flowing around
the flameholders, deteriorating as the gas velocity near the flamehold-
ers increases. A typical example from reference 2 of the effect of ve-
locity on the performance of a highly developed afterburner is shown in
figure 1. The afterburner was about $4\frac{1}{2}$ feet long and had a conventional
V-gutter flameholder and conventional fuel-system components. As shown
in figure 1(a), the inlet velocity at the center of the burner was low
(typical of most afterburner diffusers) compared with the velocity in
the region of the flameholders. When the average velocity through the
afterburner was about 380 feet per second, the velocity near the flame-
holders was approximately 440 feet per second. As the average velocity
increased, the velocity in the center of the burner remained about the
same but the velocity near the flameholders increased. At an average
velocity of 675 feet per second, the velocity near the flameholders was
between 600 and 800 feet per second.

The combustion efficiency, as shown in figure 1(b), decreased con-
siderably as the average inlet velocity increased. At a burner-inlet
pressure of 570 pounds per square foot, the efficiency decreased from
about 0.88 at an average inlet velocity of 380 feet per second to about
0.60 at an average inlet velocity of 680 feet per second. It is appar-
ent that, in this burner, the velocity in the region of the flameholders
may not exceed 450 to 500 feet per second if combustion efficiencies of
0.85 or higher are to be maintained at low afterburner-inlet pressures;
to maintain efficiencies of 0.8, local velocities should not exceed
about 600 feet per second. At high afterburner-inlet pressures, per-
formance is considerably less sensitive to velocity. As shown in the

3701

DECLASSIFIED CONFIDENTIAL

3701

figure, at a burner-inlet pressure of about 1100 pounds per square foot, combustion efficiencies above 0.80 may be obtained with local velocities of about 750 feet per second, corresponding in this case to an average velocity of about 675 feet per second.

Similar trends have been found in other investigations. For example, in one afterburner development (ref. 3) in which the velocity in the region of the flameholder was about 700 feet per second, combustion efficiencies above 0.72 could not be obtained at low burner-inlet pressures, even though a relatively long burner length was used and extensive development effort was expended on the flameholder and fuel system.

A qualitative measure of the merit of an afterburner-inlet diffuser is, therefore, the magnitude of the gas velocities it provides in the region of the flameholder. For an afterburner about $4\frac{1}{2}$ feet long that is to operate at low inlet pressures or high altitudes, the diffuser should provide velocities in the region of the flameholder that do not exceed 500 to 600 feet per second. On the other hand, for high inlet pressures or low altitudes, local velocities as high as 750 feet per second may be acceptable.

In the absence of a rigorous method of diffuser design, two general types of diffuser have developed. One is a long diffuser having a gradually increasing flow area, and the other is a short diffuser in which the inner body ends abruptly at some convenient length. With the short diffuser, the blunt end of the inner body can serve as part of the flame-holding surface. With long diffusers, the average velocity of the gases entering the burner is low, but some combustion length is sacrificed (for a given over-all afterburner length); with short diffusers, combustion length is greater, but gas velocities are higher. It is evident, therefore, that one of the parameters of primary importance in determining the effect of diffuser performance on afterburner performance is diffuser length. Other design features of interest are the shape of the diffuser inner body and the types of control devices, such as vortex generators or vanes, that may be added to improve performance.

Effect of Diffuser Length

The effects of diffuser length on diffuser-outlet velocity profiles and pressure losses are reported in reference 4, which presents the performance of the series of four diffusers represented in figure 2. Diffuser length varied from less than 0.1 to 1.05 diameters; all had an outlet-inlet area ratio of 1.92. Accompanying the variation in length was a variation in the shape of the inner body that, as will be discussed in a subsequent paragraph, probably had little effect on

CONFIDENTIAL

performance. The diffusers were tested in a duct that imposed a diffuser-inlet velocity distribution approximating fully developed pipe flow. This velocity distribution is an approximate simulation of the diffuser-inlet velocity conditions in some engines.

Velocity profile at the diffuser outlet and pressure loss for the four diffusers are shown in figure 3. As discussed in reference 4, because of the errors inherent in measuring total pressures in highly turbulent streams, the values of pressure drop presented should be considered qualitative and indicative of relative losses only. Pressure loss data for diffuser 4 have no intrinsic significance, inasmuch as the diffuser consists simply of a sudden expansion. As diffuser length was increased the loss in total pressure increased but the velocity profile improved.

With diffuser 3 (fig. 3(b)) the velocity in the region in which flameholders would be located was above 0.8 of the diffuser-inlet velocity. If diffuser 3 were to be used with an afterburner, the average burner-inlet velocity could not exceed approximately 400 feet per second (corresponding to a diffuser-inlet velocity of about 700 ft/sec), if velocities in the flameholder region are to be maintained below the 500 to 600 feet per second required for good high-altitude performance. Increasing the length-diameter ratio from 0.51 (diffuser 3) to 1.05 (diffuser 1) would permit an increase in average burner-inlet velocity to approximately 470 feet per second without exceeding velocities of 500 to 600 feet per second in the flameholder region. The average burner-inlet velocity requirement for most modern engines is generally between 450 and 550 feet per second. It is apparent that although the increase in length from 0.51 to 1.05 diameters considerably improves the performance of this series, a length-diameter ratio of 1.0 (at an area ratio of 1.92) is not great enough to assure efficient burner operation at high altitudes for all modern engines.

Data are not available to show directly the effect on velocity profile of increasing the length of the 1.92-area-ratio diffusers beyond the 1.05 length-diameter ratio. Data from several different diffusers of varying area ratio are, however, plotted in figure 4 as the ratio of the average velocity at the burner inlet to the approximate velocity at the flameholder radius against the diffuser length-diameter ratio. As shown by the solid curve, which represents the three diffusers of figure 3, the improvement in this velocity ratio as diffuser length increases is evident. Extrapolation of these data indicates that a diffuser length-diameter ratio of about 1.5 would permit use of average burner-inlet velocities of about 500 feet per second. Figure 4 also presents data for two diffusers having greater values of length-diameter ratio. One, with an area ratio of 1.5, has a length-diameter ratio of 2.35; the other, with an area ratio of 1.3, has a length-diameter ratio

CONFIDENTIAL

3701

CU-2

of 1.85. An improvement in velocity ratio is evident for the longer, lower area-ratio diffusers as compared with the 1.92-area-ratio diffusers. Although a direct quantitative comparison of the data for the five diffusers can not be made because of differences in diffuser-inlet conditions, the improvement undoubtedly results from both the increase in length and the decrease in area ratio. Sufficient data are not available to separate the two effects. It appears, however, that with reasonably uniform diffuser-inlet conditions, maldistribution of velocity at the burner inlet will limit the average velocity that may be tolerated without large performance losses only for installations in which the length-diameter ratio is less than about 2, and the area ratio is greater than $1\frac{1}{2}$.

Diffusers with Truncated Inner Bodies

In many diffusers, the flow separates from the inner body several inches upstream of the diffuser outlet. Such flow separation occurred, for example, in diffusers 2 and 3 (fig. 2). In such cases, the presence of an inner body downstream of the separation point probably has no effect on diffuser performance. The diffuser inner body could therefore have been cut off at the separation point, thus providing a reduction in over-all length without altering the performance. If, however, the inner body is cut off appreciably upstream of the separation point, an effect of length on performance would be expected. Performance of some diffusers altered in this manner is presented in reference 5; the data are summarized in figure 5. This figure presents the pressure losses and the diffuser-outlet velocity profile for truncated diffusers of two lengths and of two inner-body angles (or diffuser area ratio) for a given length.

Increasing the length-diameter ratio from 0.35 to 0.5 resulted in a significant improvement in velocity profile and a reduction in total-pressure losses of over 50 percent. Performance of the two diffusers having a length-diameter ratio of 0.5 was not affected by the small difference in outlet-to-inlet area ratio.

As previously discussed, cutting off the diffuser before the separation point increases the velocity at the diffuser outlet compared with a diffuser that extends to the separation point. The ratio of average burner-inlet velocity to local velocity in the flameholder region for the two longest cut-off diffusers of figure 5 is approximately 0.7. Such diffusers could therefore be used in afterburners with average inlet velocities of about 390 feet per second without sacrifice in altitude performance or increase in burner length. Although the velocity ratio of 0.7 is about the same as that presented in figure 4 for a 1.92-area-ratio diffuser with a length-diameter ratio of 0.51, no generality is implied by the results because of differences in area ratio and diffuser-inlet conditions.

Effect of Inner-Body Shape

As discussed previously, it was assumed in the investigation of diffuser length that the shape of the inner body has a negligible effect on diffuser performance. The validity of this assumption is supported by the results of previously unpublished NACA tests, shown in figures 6 and 7. Figure 6 shows the configurations and axial area variation of two diffusers with different inner bodies that were tested in an afterburning engine. The rate of change of flow area with length was greatly different for the two inner bodies up to a length of about 34 inches. The velocity distribution was measured at the 34-inch station. As shown in figure 7, the velocity profiles were very nearly the same with the two inner bodies. These results indicate that inner-body shape (for a constant diffuser length) has only a minor effect on diffuser-outlet velocity profile. The data also showed pressure losses for the two diffusers to be very nearly the same.

Flow-Control Devices

Of the numerous flow-control devices that have been used in flow passages, only vortex generators have been comprehensively investigated in diffusers suitable for afterburner inlets. Brief investigations have, however, also been made of annular vanes, annular shrouds or splitter ducts, and boundary-layer suction systems.

Vortex generators. - References 4, 6, 7, and 8 discuss tests in which vortex generators were used to energize the boundary layer along the inner cone (and in some cases along the outer shell as well). Their action is to delay flow separation and thereby permit use of slightly shorter diffusers without loss in performance or slightly improve performance for the same diffuser length. It has been found that differences in diffuser-inlet velocity profile, diffuser length, inlet whirl, and diffuser shape all influence the optimum vortex generator configuration. In general, it has been found that effective vortex generators must be placed several chord lengths upstream of the diffuser separation point and must be long enough radially to extend through the boundary layer into the free stream. For diffusers 2 or 3 feet in diameter, from 20 to 40 equally spaced vortex generators are required. Chord length was between 1 and 3 inches and angle of attack was between 13° and 15° in most tests. Within this range, the effectiveness of the vortex generators was not sensitive to chord length or angle of attack. The optimum values of axial location and vortex generator span must be determined experimentally for each configuration.

Typical effects of vortex generators on diffuser performance are shown in figure 8. Outlet-velocity distributions are given for diffusers 1 and 3 of figures 2 and 3. The vortex generator configurations
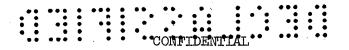
used in these tests were considered to be approximately optimum on the basis of preceding investigations. Twenty-four vortex generators were installed 1 inch upstream of the confluence of the cylindrical section of the diffuser inlet and the curved portion of the inner body. Each was an NACA 0012 untwisted airfoil of 3-inch chord and 1/2-inch span, with the chord skewed 15° to the axis of the diffuser. Alternate vortex generators were skewed to the left, and the intermediate ones skewed to the right. With both long and short diffusers, the vortex generators improved the velocity profile only slightly. The effect of vortex generators on pressure drop has also been found to be very small.

Annular vanes. - Cascades of annular vanes are suggested in reference 9 as a device to improve velocity distribution in diffusers. A brief investigation of annular vanes for afterburner diffusers is reported in reference 7. Three configurations investigated and their outlet-velocity distributions are shown in figure 9. In configuration A, a cascade of five annular vanes was installed, with a blunt inner cone. The vanes were simple, slightly cambered, sheet-metal hoops with rounded leading edges. Successive vanes had slightly different angles of attack, as suggested in reference 9. As shown in figure 9, the outlet-velocity profile with this configuration was fairly uniform, neglecting small gradients caused by wakes off the vanes. The pressure loss of configuration A was very high, however (7 percent of diffuser-inlet total pressure). Configuration B had a longer inner cone, with vortex generators attached, and no annular vanes. Although the pressure loss was only about two-thirds that of configuration A, the velocity profile was poor with a large separated region in the center of the burner. The vortex generators were removed from configuration B and the two upstream vanes of configuration A were installed to form configuration C. Both pressure loss and velocity profile were about the same for configuration C as for configuration B.

On the basis of these preliminary tests, annular cascades appear effective in preventing large gradients in burner-inlet velocity, but only at the expense of large pressure losses. Additional development may produce a more favorable combination of inner body and vanes.

Splitter shrouds. - The use of splitter shrouds to divide the diffuser into two concentric annular passages was briefly investigated in reference 10. The short diffuser represented in figure 10 was tested with and without a splitter shroud surrounding the inner body. The splitter produced a lower velocity in the outer 4 inches of the diffuser outlet, but velocity in the center of the annulus was increased to an undesirably high value. With the splitter, diffuser pressure loss was slightly higher.

3701

These results have been generally confirmed by tests in other types
of diffusers. The use of the splitter reduces the velocity in one pas-
sage, but the reduction is usually accompanied by an increase in veloc-
ity in the other passage to undesirably high values. Although the data
available are by no means conclusive, splitter shrouds seem to be of
doubtful advantage.

Effects of Whirl on Diffuser and Afterburner Performance

Depending on engine design and to some extent on engine operating
conditions, the direction of flow at the turbine outlet (diffuser inlet)
may be as much as 20° to 30° from axial. Typically, as the flow pro-
gresses through the diffuser the angle of whirl increases, with the
greatest increase occurring near the centerbody. As a result, a
diffuser-inlet whirl angle of about 20° may result in an average
diffuser-outlet (afterburner-inlet) whirl angle as high as 40° or 50°
with local whirl angles near the centerbody as high as 70° or 80° (ref.
4). The effects of this whirl on afterburner and diffuser performance
have been investigated in reference 11 and some typical results are re-
viewed in the subsequent paragraphs.

Effects of whirl on afterburner performance. - In figure 11, the
effects of whirling flow on the combustion efficiency of the typical
afterburner of reference 11 are shown. The whirl angles at the diffuser
outlet (without straightening vanes) were greater than 30° (fig. 11(a))
over most of the flow passage. Performance of the afterburner with this
large whirl and with most of the whirl eliminated by straightening vanes
is compared in figure 11(b). It is evident that whirl has no signifi-
cant effect on afterburner combustion efficiency. Similar results were
obtained over a range of altitudes between 30,000 and 50,000 feet. Be-
cause changes in whirl angle result in changes in velocity and mass-flow
distribution at the afterburner inlet, it was necessary to revise the
fuel distribution to obtain an optimum distribution when the whirl angle
was changed. The afterburner was otherwise unchanged for the compara-
tive tests.

Although whirl angle has little effect on combustion efficiency,
large whirl angles can lead to operational problems. In burners with
a large amount of whirl and with fuel injection ahead of inner-body
support struts, flame may seat in the wakes from these struts and cause
warping and buckling of the diffuser parts. To avoid these operational
difficulties, it seems advisable to reduce whirl at the burner inlet.
Experience indicates that whirl angles at the burner inlet up to approx-
imately 20° may be tolerated without operational difficulty.

3701

Flow-straightening vanes. - Airfoil-shaped flow-straightening vanes have been installed at the turbine discharge in several investigations to reduce whirl. Some of the vanes were fabricated from sheet metal and some were cast. Typical effects of straightening vanes on the diffuser-inlet whirl angle are shown in figure 12. Without straightening vanes, whirl angles in excess of 20° (corresponding to diffuser-outlet whirl angles of approximately 40°) occurred over most of the passage. With straightening vanes, the whirl angle was 10° or less. Similar results have been obtained in other investigations (see fig. 11(a)).

The shape of the straightening vanes used is illustrated in figure 13. The vanes, designed to produce an axial discharge, have the leading edge skewed to the diffuser axis at the approximate whirl angle. This inlet angle varies radially to match the local whirl angle, and chord length is greatest in the region of greatest whirl. Maximum effectiveness is obtained with vanes spanning the full passage. A ratio of vane spacing to vane chord of about 3/4 has provided satisfactory performance in several designs.

The presence of vanes in the high-velocity gas stream at the turbine discharge has been found to approximately double the pressure loss in the diffuser-vane combination. However, the reduction in whirl caused by the vanes reduces the resultant velocity over the flameholder (by reduction of the tangential component) and thereby reduces the flameholder pressure loss. As a consequence, it has been found that in most installations the over-all afterburner pressure losses are approximately the same with and without straightening vanes.

FUEL-INJECTION SYSTEMS

The primary function of the fuel-injection system of an afterburner is to provide proper distribution of fuel and air within the burner and adequate preparation of this fuel-air mixture for combustion to occur. Proper distribution requires that fuel be introduced into the gas stream at the correct locations, dependent upon the mass distribution of the turbine-discharge gases and the flameholder-area distribution. Adequate fuel preparation comprises thorough mixing of the fuel with the turbine-discharge gases, and vaporization of the mixture before it reaches the flameholder location, where combustion occurs.

Fuel-Spray Bars and Their Installation

The type of fuel-injection systems used almost exclusively at the Lewis laboratory and that has received widespread industrial acceptance is that of radial spray bars. These bars are located some distance upstream of the flameholder, usually within the turbine-discharge diffuser.

The use of a relatively large number of spray bars, each with several fuel-injection orifices, provides the multiplicity of fuel-injection locations that is necessary for good dispersion of fuel across the gas stream. A distinct research advantage of spray-bar systems is that they can be easily removed for inspection and readily altered in both orifice number and orifice location.

A photograph of a typical fuel-spray bar is presented in figure 14. These spray bars are fabricated from commercial stainless-steel tubing; they are closed at the end and equipped with some means of attachment to the shell of the burner or burner-inlet diffuser. The inside diameter of the spray bar is usually between 1/8 and 1/4 inch; the bars are frequently left round, although in many installations they have been flattened somewhat, as shown in the photograph, to form a more streamlined cross section. The fuel orifices are simply holes drilled through the wall of the tubing at appropriate locations.

As illustrated in figure 15, the spray bars are evenly spaced circumferentially in a single plane across the burner or diffuser. They are usually cantilevered from their point of attachment on the inner or the outer shell; additional structural support is seldom necessary. For simplicity, all the spray bars are usually connected to a single manifold.

In the following presentation, the distribution of fuel-air ratio upstream of the flameholder under burning conditions is discussed for various afterburners. This discussion presents (1) the types of radial and circumferential fuel-air-ratio distribution afforded by various injection systems, and (2) the effects of fuel-air-ratio distribution on the over-all performance of the afterburner. Attention is also given to the degree to which the actual fuel-air-ratio distribution may be predicted from consideration of the injection-system design and the mass-flow profile of turbine exhaust gases. The accuracy of such predictions is not only pertinent to design, but the predictions are useful in evaluating the effects of fuel-air distribution on performance when actual measurements are not available. The effects of fuel mixing length, orifice size, injection pressure, and direction of fuel injection on afterburner performance are also summarized.

Radial Fuel-Air-Ratio Distribution in Afterburner

Measurements of the fuel-air ratio across the gas stream immediately upstream of the flameholder under burning conditions have been of considerable aid to afterburner research and development. These measurements have been obtained with the NACA mixture analyzer described in detail in reference 12. The procedure used consists in obtaining a

3701

sample of the gas mixture with a movable sampling probe, oxidizing the sample in an electrical oxidizer or burner, and measuring the products of combustion in the mixture analyzer. As pointed out in reference 13, it is necessary (1) that the fuel-air mixture be taken into the sampling tube at very nearly free-stream velocity, and (2) that the sample be completely oxidized before going to the mixture analyzer. With proper attention to these points, very satisfactory results have been obtained.

Effect of spray-bar design on distribution. - A typical effect of a change in location of the fuel-injection orifices in a matched set of spray bars on the radial fuel-air distribution is shown in figure 16. These data, obtained from a full-scale afterburner installed on a blower rig (ref. 13), represent the fuel-air distributions measured 22.5 inches downstream of the fuel-spray bars. The fuel was injected in a trans- verse direction from 24 spray bars; this number, as will be illustrated subsequently, provides about the same distribution at all circumferen- tial locations. Sketches of the spray bars, approximately to scale, are included in the figure to show the locations of the fuel-injection orifices.

With the six-orifice spray bar, the fuel-air ratio varied from ap- proximately 0.070 near the center of the burner to less than half this value near the outer shell of the burner. By addition of two orifices near the outer shell of the burner to form the eight-orifice bar, the fuel-air ratio was made nearly the same all the way across the burner. The addition of a pair of orifices to the spray bar thus altered the fuel-air-ratio distribution from a two-to-one variation across the burn- er to an essentially uniform distribution.

Similar data on the effect of orifice location on fuel distribution are shown in figure 17 for a full-scale afterburner operating on a tur- bojet engine. A 16-orifice spray bar, with orifices spaced as shown in the sketch, provided the somewhat uneven fuel-air-ratio distribution shown by the solid curve. To increase the fuel-air ratio near the outer shell of the burner, a second set of spray bars was used that incorpo- rated a closer spacing of fuel orifices near the outer shell. This spray bar, shown in the left portion of the figure, produced the fuel- air-ratio distribution indicated by the dashed curve. Although the fuel-air-ratio distribution obtained with this spray bar was slightly low in the mid-radial location, the fuel-air ratio near the outer shell was substantially increased.

Comparison of measured and calculated distribution. - The data of figures 16 and 17 show that changes in the location of the fuel- injection orifices produce, in at least a qualitative manner, the ex- pected changes in actual fuel-air-ratio distribution. To determine the accuracy with which such changes may be quantitatively predicted, cal- culations of radial fuel-air-ratio distribution were made that were

based on the radial location of the fuel orifice and the measured mass-
flow profile of the turbine exhaust gases at the spray-bar location.
These calculations were thus based on a simple radial proportionment of
fuel and air, neglecting such effects as inertial separation of the fuel
and the air and diffusion of fuel vapor beyond the streamtube of air
passing each orifice.

In figure 18, the results of such a calculation for the two fuel
systems represented in figure 16 are compared with the measured fuel-
air-ratio distribution. Although the minor variations of fuel-air-
ratio distribution across the radius for each separate fuel system are
not closely predicted, the general trends and the differences between
the two fuel systems are predicted with fair accuracy. For both the
uniform distribution of the eight-orifice bar and the decidedly nonuni-
form distribution produced by the six-orifice bar, the calculated fuel-
air ratio is within 0.013 of the measured distribution.

Further evidence that these simple calculations of fuel-air-ratio
distribution will predict general trends but not minor, or detailed,
variations is presented in figure 19. The measured distributions of
this figure are those previously presented in figure 17. Again, the
calculated distributions agree with the measured distributions with re-
gard to both general trend and level; the quantitative agreement is
within about 0.018. Further inspection of these data, as well as other
data not presented herein, shows that the measured fuel-air ratio is
generally greater than the calculated values in the outer one-third of
the burner. This rather general characteristic is attributed to a cen-
trifugal separation of the fuel and air in passing through the annular
diffuser, with the fuel tending to follow the initial axial direction
of gas flow and the gases following more closely the curved walls of
the diffuser inner cone.

From the foregoing, it may be concluded that the gross or principal
effects of changes in spray-bar design on the resulting radial fuel-air-
ratio distribution under burning conditions may be predicted with satis-
factory accuracy from very simple considerations of the radial propor-
tionment of the fuel and air. More detailed considerations of fuel va-
porization and turbulent diffusion such as discussed in reference 14
therefore do not appear necessary for general afterburner development.
In practice, a fuel-injection system for an afterburner is usually de-
veloped in two successive steps. First, the spray bar is designed to
give the desired distribution on the basis of simple calculation of ra-
dial fuel and gas distribution, utilizing for this calculation the ac-
tual, and usually nonuniform, mass-flow profile at the spray-bar loca-
tion. Detailed alterations to the spray bar are then made on the basis
of measurements of the actual fuel-air-ratio distribution. The radial
fuel distribution delivered by a spray bar may, of course, be altered

3701

3701

by changing the location of the fuel orifices, the relative size of the orifices, or by a combination of both. As discussed in reference 13, it has been found that changing the radial location of the fuel orifices produces somewhat more predictable results than does changing the orifice size.

Effect of Radial Fuel-Air-Ratio Distribution on Performance

The effect of distribution of fuel-air ratio on the combustion performance of afterburners has been noted by many investigators over the past 4 or 5 years. This research was, until recently, conducted without the aid of actual measurements of the fuel-air-ratio distribution existing within the burner. It was generally observed, however, that fuel systems which would be expected on the basis of their design to provide most uniform distribution provided the highest combustion efficiency at high over-all fuel-air ratios, and hence provided highest maximum exhaust-gas temperatures. Some early work reported in both references 1 and 15 indicated that progressive alterations to the fuel injectors made to obtain a more homogeneous mixture of fuel and air raised the peak combustion efficiency and shifted the region of peak efficiency to higher over-all fuel-air ratios. Reference 1 also observed that the attainment of such "homogeneous" mixtures requires that the radial fuel distribution be tailored for each engine because of variations in turbine-outlet mass-flow profiles from one engine to another.

Spray-bar fuel-injection system. - Data showing the effect of a change in the radial distribution of fuel-air ratio on combustion efficiency and exhaust-gas temperature are presented in figures 20 and 21, respectively. A sketch illustrating the radial distribution of fuel-air ratio for one point of operation of each fuel system is included in the figures. The over-all fuel-air ratio at which each of these radial distributions was measured is indicated by the leader from the sketch. From considerations of the spray-bar design (as discussed later) and the constancy of the mass-flow profile of the gases as discussed in reference 13, it is believed that the radial distribution for each system stays about the same throughout the fuel-air ratio range presented. The two fuel systems used for the data of these figures are those previously illustrated in figure 16; they are described in greater detail as fuel-system configurations 1 and 3 in reference 13.

For fuel-air ratios higher than about 0.035, the uniform fuel-air-ratio distribution produced higher values of combustion efficiency and exhaust-gas temperature; for lower fuel-air ratios, the nonuniform fuel-air-ratio distribution gave slightly higher values. The nonuniform distribution also resulted in a slightly lower lean blow-out limit, as indicated by the small cross-hatched regions in the figure. This somewhat

better combustor performance at low fuel-air ratios with the nonuniform
distribution is due to the existence of localized regions within the
burner in which the fuel-air ratio is high enough for good combustion,
even at the low over-all values of fuel-air ratio. These locally rich
regions are also the cause of the reduction in combustion efficiency at
higher fuel-air ratios, because the local fuel-air mixture becomes
greater than stoichiometric and thus too rich to burn completely. It
is evident from these data, as well as from many other similar observa-
tions, that a uniform fuel-air-ratio distribution is desirable except
for an afterburner intended primarily for very low-temperature-rise
operation.

Concentric manifold fuel system. - Data from another series of
tests with a full-scale engine in which the radial distribution of fuel
injection was varied is presented in figure 22. In this afterburner,
fuel was injected from three concentric manifolds, each incorporating a
large number of simple fuel orifices. The three manifolds were so con-
nected to separate fuel throttles that the radial distribution of fuel
could be varied during operation. A more complete description of this
fuel system as well as the complete afterburner may be found in refer-
ence 7. Although the fuel-air-ratio distribution was not measured dur-
ing the tests, the distribution provided by one method of operation rel-
ative to another was computed on the basis of the number and the loca-
tion of fuel-injection orifices in operation; the distributions are il-
lustrated by the sketches in the upper part of the figure. While no
claims can be made for quantitative accuracy of fuel-air-ratio distri-
bution, it is apparent that systems A, B, and C provided progressively
more uniform radial distribution of fuel.

The combustion efficiencies concomitant with the three different
fuel systems are shown in the lower part of the figure. Although the
peak efficiency has the same value for all three systems, the fuel-air
ratio at which peak efficiency occurred shifted to progressively higher
values of over-all fuel-air ratio as the fuel distribution became more
uniform. These data illustrate the desirability of a multiple, or at
least, a dual, orifice system if efficient operation is required over
a wide range of fuel-air ratios. Such a dual orifice system, which
could provide a nonuniform (locally rich) fuel distribution for low-
temperature operation and a uniform mixture for high temperature, is
mentioned in reference 1 also. Dual systems have not been put into
actual use in full-scale afterburners because their primary requirement
is usually that of high thrust output; they have, however, found effec-
tive application to ram-jet combustors where efficient operation over a
wide range of conditions is required (refs. 16 to 18).

Locally rich fuel injection. - A particularly striking, though ex-
treme, example of the good combustion performance that may be obtained

at low values of fuel-air ratio with a nonuniform fuel-air-ratio distribution is shown in figure 23. The fuel-injection system used in this afterburner consisted of 12 radial spray bars, each having four fuel orifices. At an over-all fuel-air ratio of 0.055, the local fuel-air ratio (fig. 23(a)) varied from about 0.02 to 0.11 across the radius of the burner, with the rich region located near the position of the single-ring flameholder. The combustion efficiency of this burner is shown in figure 23(b); the performance of the burner with the uniform distribution of figure 20 is included for comparison. As previously noted, operation with the uniform fuel distribution produced a peak efficiency at a fuel-air ratio of about 0.05 and a lean blow-out limit of about 0.03. With the very nonuniform fuel-air-ratio distribution, on the other hand, lean blow-out did not occur until an over-all fuel-air ratio of 0.004 was reached. Although the combustion efficiency decreased rapidly as the fuel-air ratio was increased, efficiencies approaching 100 percent were measured at the lowest fuel-air ratios.

Summary. - A summary of the manner in which afterburner fuel-air ratio for peak combustion efficiency varies with the degree of uniformity of radial fuel-air-ratio distribution is presented in figure 24. The abscissa of this figure is the integral across the burner of the absolute value of the difference between the local and the average fuel-air ratio, divided by the average fuel-air ratio. A value of zero thus indicates perfect uniformity of fuel-air-ratio distribution, and a value of 0.5, for example, means that the mean deviation of local fuel-air ratios from the average value is 50 percent of the average.

Included in figure 24 are all available data from tests in which the fuel-air-ratio distribution was systematically varied and the fuel-air ratio for peak combustion efficiency was observed. Data from references 13 and 19 are based on actual measurements of fuel-air-ratio distribution within the burner, while that from references 7 and 15 are, in the absence of actual measurements, based upon the arrangement of fuel-injection orifices across the burner flow passage. The greater degree of nonuniformity of distribution indicated by the fuel-injector design compared to the actual measurements is a result of the spreading and softening of the distribution between the point of fuel injection and the flameholder.

For both types of data, a rapid decrease in the fuel-air ratio at which peak efficiency occurs is apparent as the fuel-air-ratio distribution becomes less uniform. In order to have a peak combustion efficiency at a fuel-air ratio between 0.055 and 0.06, or to provide maximum temperature rise and thrust augmentation, the mean deviation in local fuel-air ratio should be no greater than 10 percent of the average value.

Circumferential Distribution of Fuel-Air Ratio in Burner

Just as the radial fuel-air-ratio distribution in an afterburner is determined by the number and location of the fuel orifices in each radial spray bar (if such a fuel system is used), so will the circumferential distribution be affected by the spacing between the spray bars and the amount of crossflow penetration of the fuel jet into the gas stream. The spacing between spray bars is, of course, determined directly by the number of bars used and the burner diameter, while the jet penetration is a function of orifice size, gas velocity, fuel-jet velocity, and other properties affecting the vaporization rate of the fuel. These various factors are not independent but are, instead, closely interrelated. In the following discussion, the effect of the number of spray bars on both the circumferential fuel-air-ratio distribution and the burner performance is first examined at various gas velocities for a given orifice size. The effects of changing the orifice diameter are then presented for two gas velocities and different numbers of bars. Although data covering complete ranges of all the pertinent variables are not available, a review of the available data permits certain general conclusions to be drawn.

Although radial nonuniformity in distribution of fuel-air ratio may be desirable in those applications where efficient operation at low temperature rise is desired, it is logical to assume that the circumferential distribution should always be fairly uniform because of the circumferential symmetry of the flameholders in general use. It remains, therefore, to determine the type of fuel system required to give a sufficiently uniform circumferential distribution of fuel-air ratio at various gas velocities.

Effect of number of spray bars on fuel-air-ratio distribution. - The circumferential distributions of fuel-air ratio provided by 12 and by 24 radial spray bars are compared in figure 25. All spray bars were the same, with eight fuel orifices of 0.030-inch diameter in each. The gas velocity for these tests was between 500 and 600 feet per second; fuel was injected in a radial plane. The burner diameter was approximately 26 inches. A measure of the circumferential distribution of fuel-air ratio is provided in this figure by comparing the fuel-air ratios along two radii some 15 inches downstream from the spray bars; one radius was directly aft of a spray bar, and the other in a plane midway between adjacent spray bars. As indicated in the upper part of the figure, the radial fuel-air-ratio distribution is about the same for both radii when 24 spray bars were used, this result indicating a circumferentially uniform distribution. When 12 spray bars were used, however, the fuel-air ratio along the two radii differed by more than 2 to 1 over most of the area of the burner. As would be expected, the difference was greatest near the outer shell of the burner, where the spray bars

3701

were farther apart, and almost disappeared at the center of the burner. Thus, with 12 spray bars in this afterburner, there existed a combined radial and circumferential distortion in fuel-air-ratio distribution.

It should be noted that the poorer circumferential distribution of fuel with the 12 spray bars existed in spite of the higher fuel-injection pressures associated with the smaller number of fuel orifices. This result is contrary to what would be expected for nonvaporizing liquid jets, inasmuch as the correlation of reference 20 for liquid jets indicates that the higher injection pressures should have essentially offset the greater spacing between the bars for the conditions of this test; therefore, vaporization of the fuel had a significant influence on the circumferential fuel distribution. As might be expected, however, the jet penetrations generally indicated by the data of figure 25 are somewhat greater than would have been predicted from the data of reference 21 for air jets. Although more exact quantitative comparisons are not possible, it is apparent that the penetration characteristics of fuel jets in afterburners are between those of liquid jets and air jets, with the specific characteristics depending on the various factors that influence the vaporization rate of the fuel.

Effect of number of spray bars on performance. - The effects of the nonuniform circumferential fuel-air-ratio distribution illustrated in figure 25 on the combustion efficiency of the afterburner are presented in figure 26. Although the effects of this nonuniformity do not appear to be as large as those resulting from a radial nonuniformity, the combustion efficiency is 7 or 8 percentage points higher with the 24-spray-bar fuel system than with the 12-spray-bar system over most of the range of fuel-air ratio.

The data of figure 26 were obtained at a burner-inlet velocity of 500 to 600 feet per second; they indicate that, for these conditions, the higher fuel-injection pressures associated with the smaller number of spray bars did not provide sufficient penetration to give a uniform fuel distribution. It might be expected, however, that the fuel penetration across the gas stream would be greater at a lower gas velocity and the effect of the number of fuel-spray bars on the performance of the afterburner would be less. That this is actually the case is illustrated in figure 27, where the combustion efficiency at a burner-inlet velocity of 380 to 480 feet per second is shown to be the same for both 12 and 24 spray bars. For comparison, the combustion efficiency obtained at these lower gas velocities with the fuel-air-ratio distribution nonuniform in a radial direction, as obtained for the six-orifice spray bar of figure 16, is included as the dashed curve. In this case, the combustion efficiency decreased very rapidly with increasing fuel-air ratio, as previously discussed. Therefore, while low gas velocities permit the number of spray bars used to be reduced because of greater

fuel penetration across the gas stream, the fuel orifices must be located radially to give good coverage across the burner if good performance is desired at high over-all fuel-air ratios.

Effect of orifice size on performance. - The results presented in the preceding section are for an orifice diameter of 0.030 inch. As was mentioned, a reduction in orifice diameter may increase the rate of fuel vaporization sufficiently to decrease the jet penetration and thereby have an adverse effect on burner performance. This effect would be reduced, of course, if a large number of spray bars were used. Data from reference 13 comparing the combustion efficiency with 0.030- and 0.020-inch-diameter fuel orifices are presented in figure 28; 24 spray bars were used in a 26-inch-diameter afterburner. It is apparent that in this case, the jet penetration was not reduced enough by the reduction in fuel-orifice size to affect the performance appreciably. This result was, furthermore, obtained at the relatively high gas velocity of 500 to 600 feet per second.

If the spacing between spray bars is similar to that provided by 24 bars in a 26-inch-diameter burner, orifice diameters as small as 0.020 inch may, therefore, be used even at high gas velocities. If, on the other hand, only 12 spray bars are used, an orifice diameter of 0.020 inch does not appear to be large enough to provide good fuel distribution, even at gas velocities no higher than 400 feet per second. This conclusion is based on a comparison of figure 27 with figure 29, which is replotted from the data of reference 19. As indicated in figure 29, the spray-bar system for these data comprised 12 long spray bars, each having 8 orifices, and 12 shorter spray bars with 6 orifices per bar. The performance obtained when all 24 spray bars were used is compared with that obtained when only the 12 long spray bars were used. Although an exact comparison between the data of figures 27 and 29 is not possible because different afterburners were used, values of gas velocity, burner-inlet pressure, and burner diameter were about the same. The principal difference is that 0.020-inch orifices were used for the data of figure 29 as compared to the 0.030-inch orifices for the data of figure 27.

Contrary to the satisfactory performance indicated in figure 27 for the 12 spray bars having 0.030-inch orifices, the performance shown in figure 29 for 0.020-inch orifices was appreciably reduced when the number of spray bars was decreased from 24 to 12. Not only was the maximum gas temperature reduced from 3400° to 3000° R, but the combustion efficiency at the condition of maximum temperature was also about 20 percentage points lower. Although the fuel-injection pressure at stoichiometric fuel-air ratio was increased from 25 to 75 pounds per square inch for the smaller number of spray bars, the fuel penetration with the small orifices was obviously inadequate to overcome the wider spacing between the bars.

3701

To recapitulate, the use of as few as 12 spray bars in a 26-inch-diameter afterburner provided good performance only when the gas velocity was relatively low (380 to 480 ft/sec) and the fuel orifices were as much as 0.030 inch in diameter. The performance of the 12-bar system was inferior to that of the 24-bar system at high gas velocities with 0.030-inch orifices, and at low gas velocities with 0.020-inch orifices. A spray-bar spacing corresponding to 24 spray bars in a 26-inch-diameter burner provided good performance at high gas velocities (500 to 600 ft/sec) with either 0.020- or 0.030-inch-diameter orifices. Other combinations of orifice diameter and number of spray bars within these limits should, of course, be possible.

Effect of ratio of orifice size to spray-bar diameter. - The foregoing discussion indicates the possibility of reducing the number of spray bars somewhat if the jet penetration is increased by increasing the orifice diameter. Early fuel vaporization is apparently less with the larger orifices, and the penetration characteristics approach those of a purely liquid jet. (As discussed later, large axial mixing distances permit adequate fuel preparation for combustion.) If the fuel orifice becomes too large relative to the internal diameter of the spray bar, however, the static pressure within the bar and the effective flow area of the several orifices will vary. The effect of this ratio of orifice area to spray-bar area on the proportion of fuel delivered by each orifice is reproduced from the data of reference 13 in figure 30. Plotted against the ratio of total fuel-orifice area to spray-bar flow area is the ratio of fuel flow through each orifice relative to that through the number 1 orifice (at the shank of the spray bar). For each value of total orifice area, all orifices were the same size. As this ratio of total orifice area to spray-bar area increases, the fuel orifices located toward the tip of the spray bar deliver proportionally greater amounts of the total fuel flow. This variation in fuel delivery is a result of the higher static pressure within the bar at the tip and the higher relative flow coefficient of the tip orifices. Although these variations are probably negligible for area ratios of less than 0.5, the tip orifices deliver as much as 50 percent more fuel than the shank orifices for an area ratio of 1.0.

As discussed in reference 13, other factors affecting the amount of fuel delivered by each orifice are the length-diameter ratio of the orifice and the method of drilling the hole. Orifices having small length-diameter ratios, with the hole drilled undersize and reamed to final size, produced the greatest uniformity of flow from one orifice to another. Orifices produced in this manner have flow coefficients in the range of 0.5 to 0.6, based on the fuel pressure in the spray bar.

Effect of direction of fuel injection. - The data presented so far on fuel-injection systems were obtained with the fuel injected in a

370L

transverse direction, that is, across the gas stream. It might be ex-
pected that this direction of injection would be somewhat better than an
upstream or downstream direction, simply because it would provide a bet-
ter fuel coverage of the gas stream. This premise is substantiated in
figure 31, which compares the combustion efficiencies obtained when fuel
was injected alternatively in a transverse, upstream, or downstream di-
rection from an otherwise identical system. Although the effect of the
direction of fuel injection is not large at low fuel-air ratios, the com-
bustion efficiency at the higher fuel-air ratios is considerably higher
when fuel is injected in a transverse direction than when injected ei-
ther upstream or downstream. It should be noted that this rather sig-
nificant effect of the direction of fuel injection was obtained with a
fuel-mixing distance of 29.5 inches; if a shorter fuel-mixing distance
had been used, the effects might have been even greater.

A further comparison of the combustion efficiency of an afterburner
with upstream and with downstream injection is presented in figure 32.
In this burner, three concentric fuel manifolds were used; in one case
fuel was injected in a downstream direction from all three manifolds,
and in the other case the direction of injection of two of the manifolds
was reversed. At the higher burner-inlet pressure, the effect of this
change in direction of fuel injection was not large, but performance at
the pressure of 620 pounds per square foot absolute was considerably
better with upstream injection, particularly at the high fuel-air ra-
tios. The very small fuel-mixing distance used in this afterburner
(1.5 inches) probably accounts for this rather large effect of changing
from a downstream to an upstream direction in this case.

Effect of fuel-mixing distance on performance. - There are few data
indicating the isolated effect of a change in the fuel-mixing distance
(the distance between the fuel injector and the flameholder). It has
been a matter of almost universal experience, however, that relatively
large mixing distances (approaching 2 ft) are required for satisfactory
performance, particularly at low burner-inlet pressures. The summary
report of reference 1, for example, indicates an appreciable improvement
in high-altitude performance of an afterburner when the fuel-mixing
length was increased from $17\frac{1}{2}$ to $25\frac{1}{2}$ inches. The improvement in per-
formance of one series of afterburners relative to that of another se-
ries described in reference 22 is also largely attributed to an increase
in fuel-mixing distance. Although there is probably some basis for the
viewpoint that large mixing distances tend to aggravate the problem of
combustion instability, all available experience with afterburners of
many types indicates that the combustion performance at high altitude
will not be satisfactory with mixing distances of only a few inches.
The fuel-mixing distances of all the afterburners investigated at the
Lewis laboratory that have what might be considered satisfactory high-
altitude performance have been of the order of 20 inches or more.

DECLASSIFIED

37 1

CU-4

FLAMEHOLDER DESIGN

As in most of the various aspects of combustor design, knowledge of flameholder design principles has been accumulated empirically. The first experiments with afterburners showed that various bluff bodies in the air stream successfully anchored flame and provided a source for further propagation of combustion throughout the burner. Following these early results, numerous experiments have been performed to explore the size, shape, and arrangement of bluff-body flameholders with the objective of obtaining high combustion efficiency, high altitude limits, and low pressure drop. Because these experiments were necessarily carried out simultaneously with experiments to improve the design of other parts of afterburners, such as fuel-injection systems and inlet diffusers, the relations among the results of tests on different afterburners are obscure in many cases. Wherever possible, however, the results presented herein are selected from experiments that covered a range of pertinent burner designs. In this manner, the degree of generality of the results is revealed. Although types of flameholders other than bluff bodies (such as pilots and cans) may have considerable merit, the absence of information about them makes it necessary to limit the present discussion to bluff-body flameholders.

The flameholders that will be discussed are all formed of annular rings or gutters constructed in a manner similar to that shown in figure 33. The flameholders are usually attached to the wall of the burner with several streamlined struts. Although several methods of fabrication have been employed, the most satisfactory method from the standpoint of durability and ease of manufacture has usually been to weld sheets of Inconel about 1/8 of an inch thick into the shape required (in this case a V) and smooth off the weld on the external surfaces by grinding. Radial interconnecting gutters are similarly formed and attached by welding.

Effects of Cross-Sectional Shape

In references 23 and 24, a theory is advanced to explain the nature of stabilization of flames on gutters. According to the theory, hot gases from the burning boundaries of the fuel-air mixture surrounding the wake from a bluff body are recirculated upstream and enter the relatively cool boundary near the body. These hot gases increase the temperature of the mixture and carry ignition sources into the mixture. By this process, ignition of fresh mixture is initiated, and a continuous process of ignition is maintained.

<u>Isothermal wake flow</u>. - An experimental evaluation of the effect of cross-sectional shape on the recirculation characteristics of bluff

bodies in isothermal flow is given in reference 25. "Bluffness" of a body is considered to be qualitatively proportional to the sum of the angles between the body's trailing edges and its axis of symmetry. It was reasoned that the recirculation characteristics of a bluff body were directly related to vortex strength (ratio of tangential velocity to vortex radius) and to shedding frequency of the vortices formed in the wake. Bluff bodies of twelve shapes were investigated; with the aid of hot-wire and flow-visualization techniques, the strength and shedding frequency of the vortices were determined. Some of the principal results are shown in figure 34.

In figure 34, the ratio of vortex strength to approaching gas velocity is plotted against the ratio of shedding frequency to gas velocity for five representative shapes. The various shapes investigated are shown in the sketches in the symbol key. The flameholders were circumferentially symmetrical except for the V-gutter flameholder with the vortex generators installed on the upstream splitter plate. The vortex generators of this flameholder were essentially small vanes installed on both the inner and outer surfaces of the splitter vane or projecting cylinder. The vanes were inclined at an angle of about 16° to the axis of the burner and were about 3/4 of an inch high and 1.2 inches in chord. The gutter width of each flameholder at the open end was 3/4 of an inch. In figure 34, the general trend of increasing strength and decreasing frequency with increased bluffness of the flameholder is apparent. The changes in vortex strength and frequency are large.

Combustion efficiency. - To determine the possible relation of these isothermal-wake characteristics to combustion performance, tests were made in a simulated afterburner facility to evaluate combustion efficiency, stability limits, and pressure-loss characteristics of flameholders with cross-sectional shapes similar to those tested in cold flow. The results of this investigation are reported in reference 2 and additional tests of two shapes are reported in reference 26. Typical results are shown in figure 35, where the combustion efficiency is plotted against afterburner-inlet pressure. The two upper curves represent typical data selected from reference 2 and the two lower curves are from the afterburner study of reference 26. Although the efficiency levels of the two afterburners differed by about 25 percent (because of differences in flameholder size, fuel distribution, burner length, and burner-inlet velocity), the changes in efficiency with change in flameholder cross-sectional shape are about the same for both. In both afterburners, combustion efficiency was 2 to 20 percentage points lower with the U-shape gutter than with the V-shape gutter. For both burners, the difference in efficiency was greater at the lower inlet pressures.

In figure 36, the afterburner combustion efficiency is plotted as a function of afterburner-inlet velocity and pressure for various shapes of flameholder gutters. Parts (a) to (c) of this figure are for a fuel-air ratio of 0.047, and parts (d) to (f) for a fuel-air ratio of 0.067. Data are shown for ten flameholder cross-sectional shapes. The general trend of decreasing combustion efficiency with increasing afterburner velocity or decreasing inlet pressure is consistent for all shapes investigated, but scatter of the data obscures any general effect of shape on performance.

To aid in comparing the efficiencies of the various flameholders, the arithmetical average difference between the efficiency observed with the V-shape flameholder and with each of the other shapes was calculated; these differences in efficiency are plotted in the bar graphs of figure 37. Included in the calculations are a large number of data points that cover values of fuel-air ratio between 0.02 and 0.08, burner-inlet velocity between 400 and 700 feet per second, and burner-inlet pressure between 500 and 1200 pounds per square foot. Because insufficient data are available to isolate the effects of these variables, the observed values of efficiency at all operating conditions for a given flameholder were averaged together. In view of the trend of decreasing efficiency difference with increasing pressure shown in figure 35, the over-all average differences shown in figure 37 are probably conservative for low pressures and extreme for high pressures.

The results of figure 37 show that the U-shape flameholder is inferior to the flameholders of other shapes by amounts varying from 4 to 10 percent. Among the several shapes with highest efficiency, differences of only 2 or 3 percent were obtained. Below the bar for each flameholder shape is given the corresponding value of cold-flow vortex strength from reference 25. There is no apparent correlation between combustion efficiency and cold-flow vortex strength. It is evident from these results that although the U-shape gutter is inferior to gutters of most other shapes (particularly at low pressures), only small differences in combustion efficiency are obtained by using flameholders with cross-sectional shapes other than the V-shape.

Blow-out limits. - The effect of cross-sectional shape on operable fuel-air-ratio range is shown for several typical shapes in figure 38. Data from references 2 and 26 are included. The effect of gutter shape on the lean and the rich fuel-air ratio limits is small (0.005 to 0.01). The principal effect of shape appears to be that the minimum pressure for stable combustion is about 200 pounds per square foot higher for the U-shape flameholder than for the other shapes investigated.

Pressure loss. - The effect of flameholder shape on total-pressure loss between burner inlet and outlet (excluding pressure losses in the

diffuser) is shown in figure 39. Without burning (temperature ratio of 1.0), the pressure loss is from 1 to 2 percent of the burner-inlet pressure. With the exception of the flameholder with knife edges mounted on the sides of the gutter (square symbols), the pressure losses are the same with the various flameholders within ±1 percent over the range of burner-temperature ratio investigated. Data for pressure drop with the U-shape gutter are available from reference 2 only for the nonburning condition and are therefore shown for the temperature ratio of 1.0 in figure 39. During cold flow, the pressure drop for the U-shape gutter is approximately the same as for the V-gutter. Data from reference 26 indicate, however, that during burning the pressure-loss ratio is 0.01 to 0.02 less with the U-shape flameholder than with a V-gutter flame-holder of the same size $\left(22\frac{1}{2}\text{-percent blockage}\right)$.

In summary, the experimental investigations have shown that after-burner combustion efficiency may vary as much as 10 percent with flame-holder cross-sectional shape. Of the various shapes investigated, the U-shape flameholder was inferior in both stability limit and combustion efficiency to all others. Combustion efficiency and stability limits of several shapes were comparable to the V-shape flameholder. Pressure losses for most of the shapes were approximately the same.

Effects of Gutter Width, Number of Gutters, and Blockage

on Combustion Performance

The size and arrangement of flameholders is one of the dominant factors affecting afterburner performance. The best arrangement of flameholders is a function of the factors of environment in which the flameholder must operate, such as velocity and fuel-air-ratio distribution at the flameholder and type of wall-cooling system used. It is evident, therefore, that a single optimum location (axial and radial spacing) of flameholders does not exist for all possible environmental conditions. Some general trends and qualitative indications of best location are, however, discussed in a subsequent section. In this section the effects of gutter width, number of gutters, and blockage will be shown for a wide range of environmental conditions; general trends that are to a large degree independent of environment are discussed. All the results are for unstaggered flameholders.

Gutter width. - Some effects of gutter width are illustrated in figure 40. It is, of course, impossible in any experiment to isolate the individual effects of gutter width, gutter diameter, number of gutters, and percent blockage. The effects shown in figure 40 may, therefore, be influenced to some degree by variables other than gutter width and number of gutters. An attempt was made in each test to minimize

the extraneous effects. In most cases, the flameholders were located in regions of nearly uniform afterburner-inlet velocity to avoid large effects of small changes in gutter diameter. Particular emphasis was placed on providing a uniform fuel-air-ratio distribution at the flame-holder location.

In figure 40(a), some results from reference 26 are shown. Combustion efficiency at a fuel-air ratio of 0.04 is plotted against burner-inlet pressure for two flameholders, each having two rings and the same blockage but with gutter widths of 2 and 1.6 inches. The 2-inch-wide gutter produced a combustion efficiency two to five points lower than the 1.6-inch gutter. Tests in the same afterburner showed that with 1/2-inch-wide gutters combustion could not be maintained at all at pressure levels below approximately 1000 pounds per square foot absolute. The data shown in figure 40(b), taken from unpublished NACA tests, are contrary to the width trend indicated in figure 40(a). For this after-burner, a flameholder with a 2-inch-wide gutter had a combustion efficiency 2 to 6 percentage points higher than a flameholder with a $1\frac{5}{8}$-inch-wide gutter. In figure 40(c), the results from reference 27 are shown for two flameholders, each having three V-gutter rings. The $1\frac{1}{2}$-inch-wide gutter had 48-percent blockage, and the 3/4-inch-wide gutter had 29-percent blockage. At inlet pressures near 1000 pounds per square foot absolute, the differences in gutter width and blockage had no appreciable effect on combustion efficiency. At lower pressures, the flameholder with narrower gutters and less blocked area produced a combustion efficiency as much as 5 percentage points less than the wide flameholder. Observation of the flame during the tests showed that at pressures less than 800 pounds per square foot absolute the flame was partially blown out with the 3/4-inch gutter, whereas the flame with the $1\frac{1}{2}$-inch gutter was steady and complete. It is thus indicated that the reduction in efficiency at low pressures was due to the narrow gutters rather than the smaller blocked area.

Although there are inconsistencies in the data, it appears that increases in gutter width above $1\frac{1}{2}$ inches have no large effect on combustion efficiency. Reduction in gutter width from $1\frac{1}{2}$ inches to 3/4 inch has no large effect on combustion efficiency, but may cause instability of the flame at low pressures. Gutter widths of 1/2 inch did not support combustion at inlet pressures less than 1000 pounds per square foot absolute. These results were obtained with several afterburners and are apparently independent of burner-inlet velocity over the range between 450 and 620 feet per second. Because all the burners investigated were 4 feet or more in length, the applicability of the results to shorter afterburners is not known.

Blow-out limits for flameholders having different gutter widths (same afterburners that provided data of figs. 40(a) and (c)) are shown in figure 41. Although the minimum pressure limits are not clearly defined, it is evident from the consistent trends of lean and rich blow-out limits that the minimum pressure for combustion is higher for the narrower gutters. The magnitude of the increase in minimum pressure limit as gutter width decreases from 2 inches to 3/4 inch is probably of the order of 100 pounds per square foot. Effects of number of gutters on blow-out limits for the afterburners investigated in references 26 and 27 were negligible.

Number of gutters. - Some data showing the effects of the number of flameholder gutters or rings on combustion efficiency are presented in figure 42. In this figure, a $1\frac{1}{2}$-inch-wide, three-ring flameholder is compared with a 3/4-inch-wide, three-ring flameholder and a $1\frac{1}{2}$-inch-wide, two-ring flameholder. As discussed previously in connection with the effects of gutter width, the lower efficiency of the 3/4-inch-wide, three-ring flameholder at low pressures relative to the $1\frac{1}{2}$-inch-wide, three-ring flameholder is attributed to partial blow-out (a gutter-width effect) of the narrower gutters. The three-ring, 3/4-inch-wide flameholder and the two-ring, $1\frac{1}{2}$-inch-wide flameholder both had a blockage of 29 percent. The three-ring, $1\frac{1}{2}$-inch-wide flameholder had a blockage of 48 percent. Comparison of these three flameholders shows that except in the region of partial blow-out for the 3/4-inch gutters, there is an improvement of about 5 percentage points in combustion efficiency, if three rather than two flameholder rings are used. It is, of course, not possible to separate completely the effects of blockage from the effects of number of rings. Comparison of the three curves at an inlet pressure of 1000 pounds per square foot (above the region of partial blow-out for the 3/4-inch gutters) indicates that blockage in the range from 29 to 48 percent has no separate effect on combustion efficiency. At lower pressures, the effects of number of gutters and blockage on combustion efficiency are not separable, but as is shown subsequently, it is probable that blockage effects are small.

The observed effects of number of gutters, as pointed out in reference 27, are probably due to the increased average burning time obtained by using three rings (six flame fronts or $1\frac{1}{2}$- or 2-inch spacing between gutters), rather than two rings (four flame fronts or about 3-inch spacing between gutters). If the flame front always extends downstream from the gutter edges at approximately the same angle, it is obvious that the fuel particles will, on the average, encounter a flame

3701

front farther upstream in the case of the three-ring flameholder than in the case of the two-ring flameholder. Hence, the average burning time is greater for the larger number of flame fronts.

Although the available data are meager, it appears that, if the gutters are wide enough $\left(\text{approximately } 1\frac{1}{2} \text{ inches}\right)$ to prevent partial blow-out at low pressures, gains in efficiency of 5 to 7 percent are possible at burner-inlet pressures between 500 and 1000 pounds per square foot, by using three rather than two flameholder rings. Data are not available to determine the magnitude of the effects at higher pressures. In view of the apparent insensitivity of combustion efficiency to flameholder design at high afterburner-inlet pressures, it is probable that an afterburner sufficiently long to operate efficiently at low inlet pressure would not be appreciably improved in performance at high pressure by using three flameholder rings instead of two.

Blockage. - Effects of blockage on afterburner combustion efficiency are shown in figure 43 for several afterburners at a high and a low pressure level. Data for this figure were obtained with six afterburners, of which three were fitted with different flameholders to vary the blockage. The number of flameholder gutters used is indicated by the symbols. Included among the tests are a wide variety of fuel-air-ratio and velocity distributions at the burner inlet, average velocity level at the burner inlet, number of flameholder rings, and gutter widths. All the afterburners are similar, however, in that fuel was injected sufficiently far upstream to ensure adequate mixing and vaporization time and burner lengths were great enough to provide adequate burning time. Although the data at high pressures are few and no one afterburner was investigated over a range of blockages at this high pressure, it is evident that blockage effects at pressure levels near 3000 pounds per square foot are very small. These effects are confirmed by many results, such as those discussed in reference 28, which reports afterburners that operated with high efficiency at burner-inlet pressures of the order of 3000 pounds per square foot with blockages as low as 15 to 20 percent.

At lower pressures (fig. 43(b)), gains in efficiency by increasing blockage beyond 30 percent appear to be negligible. The data for the upper curve of figure 43 are representative of three of the best current afterburner designs (afterburners of refs. 7, 27, and 29) in approximately the same state of development. The small effect of flameholder blockage on combustion efficiency for blockages greater than 30 percent is particularly apparent in these data.

For blockages less than 30 percent, the combustion efficiency decreases as blockage decreases. As indicated in the figure, however, the

decrease in efficiency with blockage is greater when blockage is reduced
by decreasing the number of flameholder gutters than when blockage is
reduced by decreasing the width of the gutters and retaining the same
number of gutters. The reduction in efficiency at the lowest blockage
may, therefore, be due at least in part to the use of single-gutter
flameholders. The lower curve of figure 43(b) is for flameholders hav-
ing two gutters, and it is evident that in this case the decrease in ef-
ficiency as blockage decreases below 30 percent is much less than for
the other two curves. These results are further confirmation of the ef-
fects of number of flameholder gutters discussed previously in connec-
tion with figure 42.

Although the effects of blockage on operable fuel-air-ratio range
and minimum pressure for stable combustion have not been well docu-
mented, isolated observations do not indicate any large or consistent
trend with blockage.

All the results presented in figure 43 are for flameholders with
four to six radial gutters interconnecting the annular gutters. Sev-
eral experiments have shown that these interconnecting gutters have
little effect on combustion efficiency, except at conditions near the
minimum pressure limit. It has been shown that in some cases use of
interconnecting gutters improves combustion efficiency and operating
range of fuel-air ratio at very low inlet pressures without any ap-
preciable penalty in flameholder pressure loss.

Summary. - The number, arrangement, and size of flameholders (of
the V-gutter type) are important design considerations. For stable
and efficient combustion at afterburner-inlet pressures down to 600
pounds per square foot, minimum gutter width appears to be about $1\frac{1}{2}$
inches. At very high burner-inlet pressures, both two- and three-
ring flameholders have about the same combustion efficiency; at in-
termediate and low pressures, three-ring flameholders are superior.
At burner-inlet pressures around 3000 pounds per square foot, change
in flameholder blockage over the range from approximately 25 to 40
percent has negligible effect on combustion efficiency. At low pres-
sures (800 lb/sq ft or less), in order to provide a sufficient number
of flameholder rings of adequate width, blockages of 30 percent or
more must be used for maximum combustion efficiency. Gutter width
has a first-order effect on minimum pressure for stable combustion
and on fuel-air-ratio range of afterburners; radial gutters intercon-
necting the annular flameholder rings have a favorable effect on low-
pressure limits.

3701

CU-5

Effect of Flameholder Blockage on Pressure Drop

The pressure drop in the afterburner is due to losses in the diffuser or cooling liners, to the aerodynamic drag of the flameholders, and to the momentum changes associated with combustion of fuel. Numerous approximate methods of calculation of these pressure drops have been published (e.g., refs. 30 and 31). Some measurements of pressure loss in an afterburner (ref. 27) without burning are shown in figures 44 and 45. The flameholders used were simple nonstaggered V-gutters; the various blockages and sizes are indicated in the keys at the top of the figures. A comparison (fig. 44) of the pressure drop observed with flameholders of the same blockage (29 percent), but having different numbers and sizes of gutters, indicates that number and size have no separate effects on the cold-burner pressure losses. It is evident that velocity has a very large effect on pressure loss and that, in general, there is a value of velocity at which the rate of change of pressure loss with velocity increases very rapidly.

A cross plot of the data of figure 44 is given in figure 45. At each inlet Mach number, pressure losses increase appreciably only after blocked area is increased above about 30 percent. For a blocked area of 35 percent, the pressure loss increases from about 0.007 to 0.024 of the inlet total pressure as burner-inlet Mach number increases from 0.2 (400 ft/sec) to 0.3 (600 ft/sec). It appears that blockages as high as 30 percent may be used at an inlet Mach number of 0.3, or as high as 37 percent at an inlet Mach number of 0.2, with a "cold-pressure" loss of only 1 percent. Pressure losses at a burner-inlet Mach number of 0.306 computed by a method similar to that of reference 31 are shown by the dashed line. The method used in reference 31 employs an analytic solution for the flow conditions at the downstream, or exit, plane of the flameholder and application of empirically determined coefficients to compute the pressure drop. The agreement between the calculations and the experimental data is good for pressure losses of 0.04 or less. It has been previously shown that blockages of 35 percent are adequate for good performance at high altitudes; it is thus apparent that the "cold-pressure" losses introduced by such a flameholder in an afterburner amount to only 1 or 2 percent.

In figure 46(a), the combined pressure losses due to drag of the flameholder and cooling liner and to combustion of fuel are shown. The pressure loss is shown as a function of temperature ratio across the burner for several flameholder blockages. It is apparent that a change in blockage over the range between 22 and 31 percent has little effect on pressure losses during burning. Although the absolute values of the pressure loss shown in figure 46(a) are high because of an unusual cooling liner that was used, the relative effects of flameholder blockage are valid.

In figure 46(b), a comparison is made between the measured pressure loss and the pressure loss computed by the method of reference 31. Good agreement between the measured and calculated values indicates that, in the absence of cooling liners or other extraneous devices, the method of reference 31 is adequate for the prediction of internal afterburner pressure losses during burning.

COMBUSTION SPACE

The combustion efficiency and maximum obtainable temperature rise in an afterburner are, of course, functions of the space available for combustion. As length is reduced, the time available for the completion of combustion (residence time) is reduced and, in addition, the distance available for the spread of flame across the burner from the flameholders is decreased. Inasmuch as burner-inlet conditions influence these combustion processes, it would be expected that the effects of the combustion space on performance would be different for different pressure, temperature, and velocity levels. The arrangement of the flameholders across the burner cross section and the amount of wall taper would also be expected to influence the combustion space requirements. Some of these effects for two different classes of afterburners are discussed in the following paragraphs.

Effects of Afterburner Length

Take-off afterburner. - In some afterburner installations, such as in subsonic bombers, it may be desirable to obtain a moderate amount of thrust augmentation at take-off and to carry the afterburner inoperative at altitude conditions. In these applications, minimum afterburner size is required in order to reduce weight and drag penalties to a minimum; internal pressure losses, with their attendant penalties on engine fuel consumption, are also of greater relative importance than the combustion efficiency.

An afterburner designed for take-off application is shown in figure 47. The diffuser, flameholder, fuel system, and perforated liner were designed for minimum pressure loss, as discussed in reference 5, and in part, elsewhere herein. Flameholder blockage amounted to about 14 percent of the burner cross-sectional area. The length of the burner from the flameholder to the exhaust-nozzle outlet was varied from 20 to 62 inches by adding or removing spool sections in the 31-inch diameter section of the burner. The burner-inlet pressure for the tests was 3800 pounds per square foot absolute, and the burner inlet velocity (at the flameholder location) was 350 feet per second.

The effect of the afterburner length on the combustion efficiency is shown in figure 48(a). As the length was reduced from 62 to 20 inches, the combustion efficiency decreased from over 90 percent to less than 60 percent. Although the efficiency decreased rather rapidly as the length was reduced below 3 feet, such a change may not be important for a take-off application because the afterburner operates for only a short time. Of greater importance is the thrust augmentation obtainable with different burner lengths shown in figure 48(b). For the reduction in length from 62 to 20 inches, the thrust augmentation ratio (ratio of augmented thrust to normal thrust with the standard tail pipe) decreased from about 1.50 to 1.36. It is evident, therefore, that for an after- burner designed for take-off use only, where the burner-inlet pressures are relatively high and combustor efficiency is not of primary impor- tance, a length of 20 to 30 inches may be adequate.

The total pressure losses across this afterburner were relatively low. For nonafterburning operation, the loss in total pressure from turbine outlet to exhaust-nozzle outlet was about 5 percent for the burner lengths investigated. This loss is slightly less than the total-pressure loss that usually occurs in a standard, nonafterburning tail pipe.

Altitude afterburner. - Some effects of afterburner length on per- formance for a limited range of conditions are reported in reference 32; more recent and previously unpublished data over a wider range of condi- tions and with an afterburner designed to have good performance at high- altitude conditions are discussed herein. A sketch of the afterburner used is shown in figure 49. A two-ring V-gutter flameholder of 29.5- percent blockage was installed. Fuel was injected from 24 fuel-spray bars located 32 inches upstream of the flameholder. The afterburner was cylindrical and its length was varied in four equal steps from 30 to 66 inches. With each burner length investigated, burner-inlet total pressure, total temperature, and velocity were varied over a wide range.

The variation of combustion efficiency with burner length is summa- rized in figure 50 for the range of burner-inlet conditions investigated. Although reducing inlet pressure and temperature, or raising inlet veloc- ity, lowered the general level of combustion efficiency, all the data showed the same general trend of increased combustion efficiency with burner length. Increasing burner length from 30 to 66 inches raised the combustion efficiency by 25 to 35 percentage points over the range of conditions investigated. The major portion of this efficiency variation occurred between burner lengths of 30 and 42 inches.

As a result of the sizable drop in combustion efficiency at reduced burner-inlet pressures, it follows that a substantial increase in burner length is required to obtain a given efficiency as burner-inlet pressure

is lowered. For example, maximum combustion efficiency at a burner-
inlet pressure of 750 pounds per square foot was obtained with a burn-
er length of about 66 inches. However, the same efficiency required a
burner length of only about 42 inches at a burner-inlet pressure of
1800 pounds per square foot. In addition, the data of figure 48 indi-
cate the same efficiency was attainable with a burner length of only
about 32 inches at a burner-inlet pressure of 3800 pounds per square
foot.

The data of figures 50(c) and (d) also illustrate the possible
trades between burner length and burner-inlet velocity or temperature
for operation at constant combustion efficiency. With relatively short
burners, an increase in length of only a few inches is required to off-
set the efficiency reduction accompanying a 200° F drop in inlet temper-
ature or a 100-foot-per-second increase in inlet velocity. However, for
burners longer than about 42 inches the added length required to offset
efficiency losses resulting from such changes in inlet conditions be-
comes very large. In fact, if the burner is already relatively long,
further additions in length will fail to restore efficiency losses re-
sulting from increased velocity or reduced temperature.

The pressure loss across this afterburner increased with inlet ve-
locity in the manner indicated in figure 44. As might be expected,
there was a negligible effect of burner length on pressure loss. For a
burner temperature ratio of 2.0 and a burner-inlet temperature of
1200° F, the pressure loss increased from 0.04 to 0.11 of the burner-
inlet total pressure as inlet velocity was increased from 400 to 600
feet per second.

Effect of Flameholder Gutter Diameter

Variations in flameholder gutter diameter have been observed to
significantly influence the combustion efficiency of an afterburner
operating at high altitudes. To demonstrate these effects, a brief
investigation was conducted using the afterburner of figure 49 as the
reference configuration.

Data indicating the effect of flameholder gutter diameter were ob-
tained by using a flameholder with gutter diameters slightly smaller
than the one used in the reference configuration. A comparison of these
two flameholders is shown in figure 51. The advantage of moving the
gutters farther away from the burner wall is that it eases the problem
of shell cooling, as is discussed in a later section.

The combustion efficiency obtained with the modified flameholder
and that for the reference configuration (fig. 50) are compared in

3701

figure 52. The modified flameholder was tested with burner lengths of 42 and 66 inches, and the data for these configurations are shown by the solid symbols. Comparison is made with the performance of the reference flameholder over a range of lengths previously presented in figure 50. Moving the outer gutter away from the burner wall requires added length for the flame front to reach the wall, and thus, as shown here, lowers the combustion efficiency by 5 to 10 percent with the 66-inch burner length and as much as about 30 percent with the 42-inch burner length. This means that moving the flameholder gutters inward to ease shell cooling is equivalent to reducing afterburner length. For the cases investigated, the net effect of the flameholder modification was to reduce the combustion efficiency by about the same amount as would a 15- to 20-inch reduction in length of the reference configuration.

Effect of Afterburner-Shell Taper

To demonstrate the effect of burner-shell taper on performance, the afterburner described in figure 49 was operated with a tapered burner section having a length of 42 inches. A sketch of this configuration is shown in figure 53.

The combustion efficiencies obtained with the 42-inch-long tapered afterburner are compared with those for the cylindrical reference afterburner in figure 54. The data of figure 54(a) indicate that a drop in combustion efficiency of 13 to 18 percent resulted from tapering the burner. The primary reason for this drop in combustion efficiency is reduced residence time, inasmuch as the volume of the tapered burner was only 78 percent of that for the cylindrical burner of equal length. To illustrate this point, the combustion efficiency of the two afterburners are compared in figure 54(b) on the basis of afterburner volume instead of length. For the single point of comparison (and for two pressure levels), the efficiency is the same for a given afterburner volume, independent of the taper of the outer shell. Such agreement indicates that the secondary factors associated with tapering the burner are relatively unimportant.

Because combustion efficiency is relatively insensitive to length variations for burners about 60 inches long, it might be expected that tapering burners of this length would result in a smaller efficiency reduction than was observed with the 42-inch burner. Unfortunately, data for longer afterburners of sufficiently similar design and operating conditions for inclusion on figure 54 are not available. However, some slightly tapered afterburners about 60 inches in length have been found to operate with combustion efficiencies of about 90 percent

at burner-inlet total pressures down to about 1000 pounds per square
foot. These observations, therefore, offer some substantiation to the
premise that tapering of afterburners having a length greater than about
60 inches will have a relatively minor effect on combustion efficiency.

EFFECTS OF OPERATING VARIABLES ON PERFORMANCE

OF A TYPICAL AFTERBURNER

Performance of an afterburner of fixed design is affected by inlet
values of velocity, pressure, temperature, and by fuel-air ratio. The
effects of inlet conditions on afterburner performance are illustrated
to some degree in numerous reports. Reference 2, for example, discusses
effects of inlet pressure and velocity in detail. Because most turbojet
engines operate at about the same turbine-outlet (afterburner-inlet)
temperature, data have not been obtained to show the effect of
afterburner-inlet temperature on afterburner performance. Although the
quantitative effect of these inlet variables on combustion efficiency
differs with afterburner design, as is illustrated elsewhere in this re-
port, the general trends of efficiency with changes in inlet conditions
are similar for all burners. With this generality in mind, only a brief
summary of the principal trends is given here.

The afterburner selected for the discussion is illustrated in fig-
ure 55. The burner is 53 inches long and $25\frac{3}{4}$ inches in diameter. A
two-ring V-gutter with a gutter width of $1\frac{1}{2}$ inches and a blocked area
of 29 percent was used. Fuel was injected through radial spray bars
located approximately 30 inches upstream of the flameholder. Particu-
lar attention was given in the design to achieving reasonably uniform
fuel-air-ratio distribution at the afterburner inlet. The afterburner
had an inlet-velocity distribution (fig. 56) typical of current
afterburners.

In figure 57, the effects of inlet velocity and inlet pressure on
the combustion efficiency of the burner are illustrated. As shown in
figure 57(a), combustion efficiency decreases as burner-inlet pressure
decreases. At an inlet velocity of 450 feet per second, the efficiency
decreases about 5 percentage points as pressure decreases from 1000 to
570 pounds per square foot. At higher velocities, however, the effects
of pressure are greater; at an inlet velocity of 600 feet per second,
the efficiency falls off about 13 percentage points for this decrease
in pressure. As shown in figure 57(b), this divergence continues for
velocities up to 700 feet per second. A loss in efficiency of about
18 percentage points results from decreasing pressure from 1060 to 566
pounds per square foot at an inlet velocity of 650 feet per second.

DECLASSIFIED

CONFIDENTIAL

3701

    Although these results are for a fuel-air ratio of 0.047, similar
trends are obtained at other fuel-air ratios. Because of the manner
in which the particular burner under consideration was operated, indi-
vidual effects of fuel-air ratio at constant values of pressure and ve-
locity were not obtained. Fuel-air-ratio effects are illustrated, how-
ever, for several burners in the section on fuel-injection systems.

    The effect of inlet velocity on the blow-out limits is illustrated
in figure 58. The minimum pressure for stable combustion at a given
fuel-air ratio increases slightly as burner-inlet velocity increases.
The minimum pressure that occurs at a fuel-air ratio of about 0.060 in-
creases from about 350 pounds per square foot at an inlet velocity of
500 feet per second to 400 pounds per square foot at a velocity of 600
feet per second.

    It may be concluded that the effects of inlet velocity on blow-out
limits are small but that the inlet velocity and pressure greatly affect
the combustion efficiency, even in an afterburner of good design. Al-
though changes in inlet velocity and inlet pressure affect the perform-
ance of various burners to different degrees, the trends shown by these
data are general and are probably representative of many current aft-
burner designs.

COMBUSTION INSTABILITY (SCREECH)

    The phenomenon commonly known as "screech" in afterburners is a
combustion instability characterized by high-frequency, high-amplitude
pressure oscillations. Combustion-chamber pressure has been observed
to oscillate in various afterburners at frequencies between 800 and
4000 cycles per second, and with amplitudes between one-third and one-
half the burner-inlet pressure. The oscillations are usually accompa-
nied by increased burner-shell temperature and improved combustion ef-
ficiency. The combination of high burner-shell temperature and high-
frequency pressure variation frequently leads to structural failure.
Numerous failures have been encountered in the afterburner shells,
flameholders, and fuel-system components after only a few minutes of
operation with screeching combustion. A photograph of a typical fail-
ure due to screeching combustion is shown in figure 59. Other oscil-
lations of lower frequency, often referred to as buzz or rumble, some-
times occur in afterburners; but screech is the only type of instability
that has become a severe operational problem.

    The afterburner-inlet conditions at which screech occurs differ
widely for various afterburner designs. The occurrence of screech has
been shown, however, to be consistently related to fuel-air ratio and
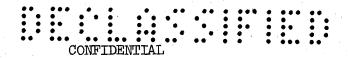
afterburner-inlet pressure. In general, screeching combustion is ob-
served to occur over a wider range of fuel-air ratio as inlet pressure
is increased in the range between 500 and 4000 pounds per square foot.
Recent unpublished data indicate that at pressures above 4000 pounds
per square foot the range of fuel-air ratio for screech may be reduced.
The effects of afterburner-inlet velocity on screech have not been de-
fined completely.

Because of the destructive nature of screeching combustion, con-
siderable effort has been expended in attempts to find methods of sup-
pressing or preventing the occurrence of screech. The principal results
of these investigations are summarized in references 33 and 34; they are
repeated, in part, in the following discussion. Two types of experiment
have been made at the Lewis laboratory to investigate screech. The ear-
liest experiments, which were made before special transient-pressure and
flame-front detection instrumentation was available, consisted of deter-
mining the effects on screech limits (screech limits are defined as the
fuel-air ratio and pressure conditions at which screech starts or stops)
of various systematic changes in the design features of afterburners.
Later experiments, utilizing special transient instrumentation, were
made to identify the mode of oscillation and to develop special devices
for suppressing screech.

Effects of Afterburner Design on Screech Limits

In the earlier experiments on effects of afterburner design on
screech limits, variations in nearly all afterburner components were
investigated. Included in these tests were variations in radial dis-
tribution of fuel-air ratio, in distance between fuel injectors and
flameholder, in shape of the inlet diffuser centerbody, in radial ve-
locity distribution at the flameholder, in radial location of the gut-
ters, in flameholder cross-sectional shape, and in gutter width. Re-
sults of these tests showed that the centerbody shape, the distance
between flameholders, and the distance between the flameholder and the
outer wall had no consistent effect on screech limits.

In contrast to these results, the velocity distribution at the
flameholder influenced the screech limits to a considerable degree in
one afterburner. A high degree of whirl originally existed at the tur-
bine outlet in the particular afterburner investigated. This large
whirl resulted in the velocity distribution at the burner inlet (dif-
fuser outlet) shown by the circled points in figure 60(a). With this
velocity distribution, screech was encountered over a fairly wide range
of fuel-air ratio, as shown in figure 60(b). The addition of antiwhirl
vanes (diamond symbols) eliminated the whirl and also eliminated the
low-velocity region at the inner diffuser wall. With the improved ve-
locity profile, screech was not encountered. To determine whether

3701

CU-6

removal of the whirl or of the low-velocity region had eliminated screech, the flow was tripped off the diffuser inner cone by an obstruction. The resultant velocity profile at the burner inlet was very close to the original profile, but no whirl was present. With this configuration, screech again occurred at approximately the same conditions as with the original configuration. It was concluded that the change in velocity profile rather than the change in whirl was responsible for the improved screech limits. It is evident, therefore, that at least in this case the occurrence of screech was dependent upon the velocity profile at the flameholder.

An effect of the radial distribution of fuel-air ratio on screech limits has been observed in several experiments. The results have, however, been erratic and inconclusive. In some cases, as small a change as 1/8 inch in the immersion of fuel-spray bars eliminated screech at a particular operating condition. In other cases, larger variations in radial fuel distribution have been ineffective in altering the screech limits. Reducing the mixing distance between the fuel injectors and the flameholder has also successfully eliminated screech, but the required reduction in mixing distance has always been so great that altitude performance was sacrificed. Although further research into these effects may reveal some useful design criteria for avoiding screech, it seems unlikely at the present time that alteration in fuel distribution will yield significant benefits in screech suppression without some performance sacrifice.

As illustrated in figure 61, the flameholder gutter width may influence the screech limits. In this figure, the number of times various flameholders of different gutter widths were tested in a particular afterburner is shown; the solid bars represent configurations that screeched, and the open bars those that did not screech. It is thus apparent that the wider the gutter, the greater the probability that screech will occur. No screech was encountered in the particular afterburner investigated if gutters of $1\frac{1}{2}$ inches or less in width were used. This result is not general; other burners using gutters as narrow as 1/2 inch have produced screech, although of lower severity. The general trend of lower screech tendency with narrower gutters has, however, been confirmed in several other investigations. The blockage areas of the flameholders used in these tests were substantially the same. Separate blocked-area effects have not been determined.

A few experiments conducted with various radial locations of the flameholder revealed no effects on screech limits. Similarly, effects of changing the cross-sectional shape from a "V" to a "U" were negligible. However, the addition of an aft splitter plate (such as those shown schematically in fig. 62) to annular V-gutters had appreciable

effect on screech limits. As shown in figure 62, a 9-inch splitter was effective in eliminating screech at some conditions. Other experiments have shown that longer splitter plates are even more effective in preventing screech. Although the 9-inch splitter plate was not adversely affected by the surrounding hot gases, the necessity for cooling longer splitters may make them impractical. The effects of splitter plates on combustion efficiency are not known.

These experiments show that the conditions under which an afterburner will screech may be controlled at least partially by proper design of the diffuser, the fuel system, and the flameholder. Proper selection of these components may enable many afterburners to operate over the required range of inlet conditions without encountering screech. In addition, it appears from the large effects of flameholder design and velocity distribution on screech limits that the origin or mechanism of sustenance of screech is associated with the aerodynamics of the flow upstream of the combustion region as well as with the combustion process itself. It is suggested in reference 35 that vortex shedding from the flameholders may account for the relation between screeching combustion and aerodynamic phenomena. This hypothesis has not been verified.
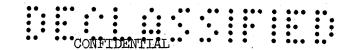
Identification of Mode of Oscillation

The tests to determine the effect of burner configuration on screech limits were ineffective in revealing the origin or nature of the pressure oscillations encountered during screech. To identify the mode of oscillation, additional tests were conducted on two afterburners in which transient-pressure instrumentation was used to measure temporal variations in pressure and to determine the phase relation between components of the pressure oscillations at various stations around the burner circumference and along the burner length.

A typical oscilloscope record from one of these tests is shown in figure 63. A cross-sectional sketch of the burner used showing the relative positions of the pressure pickups around the circumference and the flameholder location is shown at the bottom of the figure. The oscilloscope record shows that the variation of pressure with time is small at stations 1 and 3 and large at stations 2 and 4. It is evident that the pressure pulses at stations 2 and 4 are 180° out of phase. Similar phase relations were measured for other types of flameholders and for burners of different size. Analysis of the possible modes of oscillation (ref. 34) shows that the indicated phase relations can occur only in the mode of pressure oscillation called the first transverse mode.

A diagram schematically illustrating the first transverse mode (fig. 64) indicates that the particle paths are curved transverse

lines. For the first transverse mode, two nodes exist; for higher-order transverse modes, additional nodes exist, with appropriate increases in frequency. Phase and frequency measurements indicate, as shown in figure 65, that for small afterburners (about 6 inches in diam.) without inlet-diffuser centerbodies, the first mode most frequently exists. Modes up to the fourth apparently occur in larger afterburners (up to 36 inches in diam.) with diffuser centerbodies. The shaded areas of figure 65 indicate the ranges of frequencies that are encompassed by the first and fourth modes of oscillation over the range of gas temperature (speed of sound) in the burner. Similar areas, which would lie between the two shown, can be computed for the second and the third modes; they are omitted in figure 65 for clarity.

Oscillation Damping by Perforated Walls

After it was established that screeching combustion is associated with a transverse oscillation, attempts were made to prevent or suppress screech by dampening the oscillation with various devices arranged inside the burner shell. Experiments were made with an afterburner having fins attached to the wall of the burner that extended the entire length of the combustion chamber. The fins were radial and had various heights and circumferential spacings. The fins altered the screech limits and the oscillation frequency, but did not eliminate screech at all operating conditions. Other investigations of the use of fins are reported in reference 36. The results were generally similar to the NACA experience, in that the fins prevented screech in some, but not all, of the configurations investigated. The use of burner-shell taper is also reported in reference 36 to have successfully prevented screech. This result is, however, not supported by similar NACA tests, in which it was found that shell taper of reasonable amounts would not prevent screech. The difference between the results of reference 36 and of the NACA investigation is probably due to differences in flameholder design, fuel-injection systems, and burner-inlet conditions. It may be concluded that the use of fins or shell taper, while beneficial in some cases, will not prevent screech in all burners or under all conditions of operation.

In another attempt to dampen the pressure oscillations, a perforated liner was installed in an afterburner, as shown in figure 66. The liner, spaced concentrically 3/4 inch from the burner wall, had 3/16-inch-diameter holes throughout, spaced on 1/2-inch centers. The liner extended from a few inches upstream of the flameholder to the end of the 24-inch-long combustion chamber. The use of this liner completely prevented screech with several flameholders at burner-inlet pressures up to approximately 3000 pounds per square foot, which was the maximum pressure investigated.

Many additional tests with similar perforated liners in other after-
burners have demonstrated that these liners are effective in eliminat-
ing screech over the full operable range of fuel-air ratio for burner-
inlet pressures up to 6500 pounds per square foot absolute. The
combustion-chamber length of these afterburners was about 5 feet; liner
lengths of 3 feet were sufficient to eliminate screech at all conditions
investigated. Corrugated, louvered liners have appeared to be more ef-
fective than plain cylindrical, perforated liners.

In summary, it is evident that the design of the flameholder, the
fuel system, and the inlet diffuser have an appreciable influence on the
screech limits (conditions of inlet pressure and fuel-air ratio) of aft-
erburners. These facts indicate that the aerodynamics of the flow ap-
proaching the burner are linked with the screech mechanism. By proper
selection of flameholder, fuel system, and diffuser, many burners may
be designed to be screech-free over their required range of operation.
Phase and frequency measurements of pressure oscillations in several
afterburners have led to identification of the modes of oscillation.
The oscillations are transverse and occur in the first to fourth mode
in most afterburners investigated. Perforated combustion-chamber liners
have prevented screeching combustion in every afterburner investigated
over a wide range of fuel-air ratio and pressure conditions.
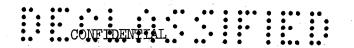
IGNITION, STARTING, AND TRANSIENT PERFORMANCE

The afterburner starting cycle includes three steps: (1) introduc-
tion of the fuel, (2) ignition of the fuel, and (3) control of exhaust-
nozzle area to obtain steady-state afterburner operation. The ignition
phase of afterburner starting has been investigated in somewhat greater
detail than the other two phases because of the need for repeated starts
during afterburner investigations in altitude facilities.

Introduction of Fuel

A significant portion of the time required to start an afterburner
after the control lever is advanced to the afterburning position is con-
sumed in accelerating the fuel pump and filling the afterburner fuel
lines and manifold. The time required to fill the fuel piping and mani-
folds is obviously directly proportional to the volume of the piping
that must be filled at each start and inversely proportional to the
fuel-flow rate set by the starting control. The time required to accel-
erate the conventional turbine-driven fuel pump usually does not exceed
1 second at any flight condition. Likewise, the time required to fill
the afterburner fuel piping at low altitudes where the fuel-flow rates

are high is also very short. At high-altitude conditions, however, the time required to fill a given volume of fuel piping becomes quite significant because of the reduced fuel-flow rate.

The effect of this set, or starting fuel-flow rate on the time required to reach operating manifold pressure is shown in figure 67. Data are presented for a 6000-pound-sea-level-thrust engine (ref. 37) and for a 10,000-pound-thrust engine. The afterburner fuel systems of the two engines were similar and utilized air-turbine-driven fuel pumps, with the turbine driven by compressor bleed air. The volume of piping that had to be filled prior to each start (neglecting any residual fuel downstream of the fuel shut-off valve) was approximately 135 cubic inches for the 6000-pound-thrust engine and 200 cubic inches for the 10,000-pound-thrust engine.

In figure 67, the time required to reach the operating manifold pressure is plotted against the ratio of the fuel-system volume to the starting fuel-flow rate. Data are presented for several flight conditions, which define a single curve. The time required to fill the fuel systems varied from 2 to 9 seconds, with the longer times occurring at the higher altitude conditions, where the flow rates were lowest. Agreement of the two sets of data indicates that the time required to accelerate the fuel pump to delivery speed was about the same for both systems. Measurements on the 10,000-pound-thrust engine showed that about 1 second of the total time was required to accelerate the pump from rest. These data thus indicate that to avoid delays in filling the fuel system before the afterburner can be ignited, it is important to keep to a minimum the volume of fuel piping that must be filled prior to each afterburner start.

Ignition

Three general methods of igniting afterburner fuel have been used: (1) spark ignition, (2) spontaneous ignition, and (3) hot-streak ignition. Some of the early research on these methods of ignition is summarized in reference 1. The spark-ignition method utilizes a spark plug to ignite a combustible mixture provided within a sheltered region of the burner. Spontaneous ignition is obtained in an afterburner when the pressure, temperature, velocity, and fuel-air-ratio conditions within the burner are such that the fuel-air mixture ignites without addition of energy from an outside agency. In the hot-streak method, afterburner ignition is obtained by momentarily increasing the fuel-air ratio in one of the primary engine combustors to about twice the normal operating value. This momentary excess of fuel produces a streak of flame that extends through the turbine and into the afterburner and thus provides the ignition source for the afterburner fuel.

Spark ignition. - Spark-ignition systems were used in a number of the early afterburners investigated at the Lewis laboratory (ref. 38). These afterburners generally incorporated the spark plug in a sheltered region at the downstream end of the afterburner diffuser inner body, as illustrated in figure 68. Experience with this type of system indicated that ignition could seldom be initiated at altitudes above about 30,000 feet, and the systems were not particularly reliable at lower altitudes.

Three factors contribute to the poor reliability of the spark-ignition method. One factor is breakdown of the electrical insulation in the region of high gas temperature, which causes a short circuit in the ignition lead. A second factor is melting or burning of the electrodes during afterburner operation, which prevents reignition of the burner. A third factor often preventing ignition is that the spark is either improperly located or releases too little energy to initiate ignition. The ignition systems used provided a spark energy of only about 0.02 joule per spark at a repetition rate of several hundred sparks per second. Although higher spark energies, such as those provided by recent capacitor-type systems, would be expected to improve the ability of the spark to effect ignition, no good solution to the problems of electrode-insulation breakdown or electrode burning has been obtained. Because other methods of afterburner ignition held promise of being more reliable, further development of a spark system for afterburner ignition was discontinued.

Spontaneous ignition. - Methods of spontaneously igniting the afterburner fuel have been investigated to determine the applicability and degree of effectiveness of this method. Although this method of ignition was seldom employed in gasoline-fueled afterburners without an explosive light-off, the conversion to kerosene and later to JP-3 and JP-4 fuels sufficiently lowered the spontaneous-ignition temperature of the fuel to provide satisfactory spontaneous-ignition characteristics in some afterburners. Many other afterburners of different configurations could not, however, be ignited spontaneously at turbine-outlet temperatures up to current maximum values of 1700° to 1750° R. There are no consistent results available to indicate the specific differences in afterburner design that result in some burners being readily ignitable spontaneously while others are not, although relatively minor alterations in radial fuel distribution of some afterburners have had marked effects on the spontaneous-ignition characteristics. In general, it is believed that the two afterburner design factors having a major influence on the ability to obtain ignition in this manner are the fuel-air-ratio distribution and the velocity profile within the burner. Fuel-air mixtures slightly richer than stoichiometric in a sheltered zone, with low velocities in and near such a zone, are believed to promote spontaneous ignition.

Spontaneous ignition has been obtained at burner-inlet pressures as low as about 500 pounds per square foot absolute; both burner-inlet pressure and burner-inlet temperature have been found to exert a pronounced effect on ignition limits (ref. 39). The effects of inlet pressure and temperature on the limits of spontaneous ignition in one afterburner configuration are shown in figure 69. Each data point on this figure represents a single afterburner start; the fuel-air-ratio value is that at which ignition occurred as the afterburner fuel flow was gradually raised. Each curve thus represents a boundary between the ignition and no-ignition regions at a given pressure. The region to the left of each curve represents the fuel-air ratios at which spontaneous ignition could not be obtained. At a burner-inlet pressure of about 1500 pounds per square foot absolute, the inlet temperature had no effect on the fuel-air ratio required for successful ignition, but at lower pressures, large increases in fuel-air ratio were required to obtain spontaneous ignition as the burner-inlet temperature was reduced. Similarly, these data show that for a given fuel-air ratio a reduction in burner-inlet pressure required a large increase in burner-inlet temperature for spontaneous ignition to occur. Spontaneous ignition of this afterburner was unobtainable at a burner-inlet pressure of 500 pounds per square foot.

The effect of burner-inlet pressure on the fuel-air ratio required to obtain spontaneous ignition for several other afterburner configurations is illustrated in figure 70. As in the previous figure, each data point represents a single afterburner start as afterburner fuel flow was being increased. These data also indicate that higher fuel-air ratios are required to obtain spontaneous ignition as the burner-inlet pressure is reduced. It should also be noted that there are appreciable differences in the required fuel-air ratio among the several configurations. The poor reproducibility of spontaneous-ignition limits is indicated by the wide band of fuel-air ratio over which ignition occurred in the several configurations.

The effect of altitude on the time required for spontaneous ignition to occur after the preset fuel manifold pressure is reached differs greatly among various afterburners. In one installation, the time required for spontaneous ignition increased from about 4 seconds at an altitude of 15,000 feet to 40 seconds at an altitude of 45,000 feet (unpublished NACA data). In contrast to this result, another quite similar afterburner (ref. 37) exhibited little effect of altitude on spontaneous ignition time, with the time for ignition varying between 4 and 8 seconds at altitudes between 30,000 and 50,000 feet.

These data, as well as related experience on other afterburners, indicate that the ability of an afterburner to ignite spontaneously cannot be predicted, nor can any practical modifications necessary to

provide reliable spontaneous ignition in any given afterburner be speci-
fied. Therefore, spontaneous ignition, although it may be fortuitously
obtained in some afterburners, is not a method that can be generally re-
lied upon.

    Hot-streak ignition. - Because of its high degree of reliability
and simplicity, the hot-streak ignition method has received most wide-
spread application in research afterburners at the Lewis laboratory.
The earliest hot-streak ignition systems provided supplemental fuel
through one of the main engine fuel nozzles. The system was operated
manually to supply the excess flow at the discretion of the operator
for a period of about 1 second. This method of injection was subse-
quently modified to isolate the hot-streak fuel from the engine fuel
manifold and thereby simplify the installation. This later system uti-
lized a fuel-injection orifice located about one-half the distance down
the combustor from the main fuel nozzle, as shown in figure 71. Details
of a typical hot-streak-injector installation are shown in figure 72(a).
For can-type combustors, the injector is designed to approximately dou-
ble the fuel-air ratio of the combustor in which it is located. In
annular-type combustors, the injector is designed to provide a similar
increase in local fuel-air ratio and thus handles a flow of 10 to 15
percent of the main engine fuel flow. A large number of afterburners
utilizing this type of system have been consistently ignited at alti-
tudes up to 50,000 or 55,000 feet, which correspond to burner-inlet
pressures down to about 500 pounds per square foot absolute (refs. 1
and 37). The system has been used with equal success on engines hav-
ing one-, two-, or three-stage turbines. In each case it has been found
that once the fuel-air ratio in the afterburner has reached a combusti-
ble level, the hot-streak fuel need be injected for only 1/2 to 1 second
to ignite the afterburner.

    To explore the effect of the hot-streak-injector location on the
ignition limits, the effectiveness of several hot-streak injectors lo-
cated immediately upstream of the turbine nozzle was investigated and
compared with that of the more conventional upstream location. Details
of the turbine-inlet injector installation are shown in figure 72(b).
This injector was also designed to double the fuel-air ratio in one
combustor can. The time required before a burst from the hot-streak
system would ignite the afterburner using both types of hot-streak in-
jectors is compared in figure 73 for altitudes of 30,000 to 50,000 feet.
Also included for comparison is the time required to ignite this after-
burner spontaneously. The time required for ignition is defined as the
period between the time at which full afterburner fuel manifold pressure
was obtained after a throttle burst and (1) the time at which the burner
ignited spontaneously, or (2) the time at which a 1/2- to 1-second burst
of hot-streak fuel flow would provide ignition. Minimum ignition times
for several preset fuel-air ratios are plotted in the figure. Minimum

3701

time for the hot-streak systems was determined by progressively reducing the time between the throttle burst and actuation of the hot-streak ignitor until ignition could no longer be obtained from the burst of hot-streak fuel flow.

In general, the data of figure 73 indicate a relatively minor effect of either afterburner fuel-air ratio or altitude on the time for hot-streak ignition, with about 1 or 2 seconds being required in most cases. At the lower altitudes, ignition occurred slightly sooner with the turbine-inlet fuel injector than with the upstream injector, but at an altitude of 50,000 feet the turbine-inlet injector failed to provide ignition because of the absence of flame through the turbine. Increasing the injector flow two- to threefold did not improve the ignition characteristics of the turbine-inlet injector. Furthermore, when the turbine-inlet injector flow was reduced by one-half or more, afterburner ignition was unobtainable at any altitude investigated.

Failure of the turbine-inlet injector to provide flame through the turbine at high altitude was attributed to insufficient time for the fuel to ignite before entering the turbine. This premise was borne out by the fact that moving the turbine-inlet injector 3 inches farther upstream resulted in ignition characteristics comparable to those observed with the upstream injector.

Although the improvements in ignition that have been described and which result from proper installation of the ignition system are considered to apply to most afterburners, the ignition times shown in figure 73 do not apply to all afterburner designs. In some afterburners subjected to extensive ignition tests, hot-streak ignition has occurred during the process of filling the fuel manifolds so that the ignition time, as defined herein, was essentially zero.

Because the time required to fill the fuel piping and obtain a combustible mixture in the afterburner following a throttle burst varies with altitude and varies from engine to engine, a single burst of hot-streak fuel for a period of 1/2 to 1 second would have to be very accurately scheduled to provide reliable ignition at all flight conditions. However, continuous injection of hot-streak fuel for periods much longer than 1/2 to 1 second would, in all probability, overheat the turbine stator. Therefore, to provide reliable afterburner ignition without endangering turbine life, the hot-streak ignition system should be designed to provide intermittent bursts of fuel for periods of 1/2 to 1 second from the time the throttle burst occurs until the control senses that the afterburner has ignited. Of course, it is important that the control system be designed so that in the event of failure the hot-streak fuel cannot be continuously injected into the engine.

Hundreds of afterburner starts with the hot-streak ignition system injecting fuel into an engine combustor for periods up to 1 second have resulted in no apparent effect on the turbine rotor blades or on the stator blades located in the path of the hot-streak flame. The absence of any rotor or stator blade deterioration attributable to the hot streak indicates that although the gas temperature may suddenly rise as much as 1000° F, the increase in metal temperature is much less because of the thermal capacity of the turbine blades. To support and explain these practical observations, transient metal temperatures were measured at the stator-blade leading edge in a single-stage turbine assembly as large step increases were made in engine fuel flow. The actual response in stator-blade metal temperature to the sudden changes in gas temperature can be characterized by a time constant. Typical values of this time constant, defined as the time to reach 63 percent of the final value in response to a step input, are shown in figure 74; the data cover a range of turbine-inlet pressures from 3000 to 12,500 pounds per square foot absolute. These pressures correspond to an altitude variation from 7000 to 45,000 feet at a Mach number of 0.8 for the engine used.

The significance of these time constants is illustrated by the computed values of stator-blade temperature rise shown in figure 75. These values were computed using the time constants of figure 74, with the assumption that the engine was operating at an average turbine-inlet temperature of 2000° R and that the temperature in the path of the hot-streak flame increased in a stepwise fashion to 3000° R for periods of 1/2 to 1 second. The values of blade-temperature rise thus calculated are seen to be considerably less than the sudden rise in gas temperature in the path of the hot streak.

The turbine rotor-blade temperatures are, of course, affected to a much lesser extent by the hot-streak flame than are the stator blades. This insensitivity of the rotor blades to the hot streak is due to the speed with which the rapidly rotating blades pass through the local hot region.

The foregoing discussion of the hot-streak ignition system indicates that, with proper installations, the system is a simple and reliable method of initiating afterburner ignition. Its use has consequently become standard on all afterburner-equipped engines investigated at the Lewis laboratory. Hot-streak fuel-injection periods no longer than 1 second have caused no problems of turbine deterioration, even with engines subjected to hundreds of hot-streak starts.

Turbine-outlet hot-streak ignition. - In view of the requirement that the preturbine hot-streak fuel be injected for only short intervals to avoid overheating the turbine, and in view of the possibility

3701

that accidental prolongation of the injection period would cause turbine-stator failure, the feasibility of obtaining dependable ignition with a hot-streak ignitor located immediately downstream of the turbine was investigated on one engine. Three hot-streak fuel-injector configurations were investigated. Details of these injectors are shown in figure 76. The principal difference in the fuel injectors was the size, location, and number of fuel orifices. One injector consisted of a straight tube with seven orifices directed toward the turbine, another injector consisted of a bent tube pointed toward the turbine with four orifices in the end of the tube, and the third injector was a similar tube with the end left open to the full inner diameter of the tube. The afterburner on which these injectors were evaluated was of conventional design with a double V-gutter flameholder, having relatively uniform values of fuel-air-ratio distribution and velocity profile upstream of the flameholder.

Afterburner ignition limits of the three turbine-outlet hot-streak fuel injectors are compared in figure 77, which also indicates ignition limits with the conventional preturbine hot streak. Each data point represents an attempt to ignite the afterburner. All starting attempts were made at a turbine-outlet temperature of 1710° R. Although the igniter fuel-air ratio does not represent the fuel-air ratio in the region of the fuel injector, it serves to generalize the igniter fuel flows for all altitudes as a fraction of the engine air flow.

The three turbine-outlet hot-streak injectors were equally effective, although they were inferior to the preturbine hot-streak system. With the turbine-outlet injectors, the maximum altitude for dependable ignition was between 50,000 and 55,000 feet. In comparison, the preturbine hot-streak system ignited this afterburner at altitudes up to 60,000 feet, which was the operating limit of the afterburner.
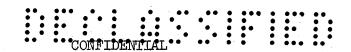
Stabilization of Operation

The greater part of the time consumed in the afterburner starting sequence occurs while the control is stabilizing engine conditions immediately following ignition. This fact is illustrated by the investigation of reference 37, in which a production-type electronic control and a continuously variable exhaust nozzle were used on an engine. An example of how the control and engine variables are affected by the starting cycle is illustrated by a typical oscillograph trace in figure 78. There is a 6- or 7-second interval between advance of the throttle and ignition, followed by 7 or 8 seconds of oscillatory operation of the engine afterburner before steady-state conditions are reached. The oscillations are caused by an interaction of the various loops of the control, in conjunction with the dynamic behavior of the engine. In this

particular control system, engine speed is controlled by primary engine
fuel flow, and turbine-outlet temperature is controlled by exhaust-
nozzle area.

The following sequence of events occurs in the engine afterburner
and the control during ignition and stabilization of operation: the
fuel-air mixture in the afterburner ignites while the exhaust nozzle is
in a closed or nonafterburning position; because the exhaust nozzle re-
stricts flow, the pressure in the afterburner increases, raising the
pressure level throughout the engine and tending to decrease the engine
speed; to maintain engine speed constant, the speed control increases
the primary engine fuel flow; this increase in engine fuel flow, along
with the increase in pressure level at the turbine outlet, tends to
drive the turbine-outlet temperature over the limiting value; this over-
temperature condition then causes the exhaust-nozzle control to open the
exhaust nozzle; because the temperature-error signal is usually large,
the nozzle starts to open very rapidly, which decreases the pressure
level in the afterburner; this decrease in afterburner pressure tends
to make the engine overspeed, which causes the control to reduce the
engine fuel flow; both the increase in nozzle area and the decrease in
engine fuel flow cause the turbine-outlet temperature to decrease rap-
idly and thus reduce the temperature-error signal to the control. The
signal reduction causes the control to stop the nozzle opening and, in
some cases, actually to start closing the nozzle before the required
area is obtained; the turbine-outlet temperature is driven over the
limit and the cycle is again repeated but with diminishing magnitude.
The cycling is continued until the proper nozzle area is reached. Am-
plitude of the oscillations may be reduced by changing the constants
of the control system, but such a modification would make the control
action slower.

The period of oscillation depends on the time constant of the en-
gine and on the control-system constants. Because the engine time con-
stant (rotor inertia divided by change in torque for a given change in
engine speed) increases with altitude, the period of each oscillation
and thus the time to reach equilibrium is greater at altitude. This
increase in duration of the oscillations with altitude is shown in fig-
ure 79 for both hot-streak and spontaneous ignition. With hot-streak
ignition, the duration of the oscillations increased from about 7 to
17 seconds as the altitude was increased from 30,000 to 50,000 feet.
The duration of the unsteady operation was about 2 seconds longer with
spontaneous ignition than with hot-streak ignition at altitudes of
30,000 to 40,000 feet and was as much as 30 seconds longer at an alti-
tude of 50,000 feet. The greater length of time required for the con-
trol to stabilize engine operation following spontaneous ignition is
due to the more violent manner in which the fuel is ignited. The high
fuel-air ratios required to obtain spontaneous ignition, particularly
at high altitude, are probably the main contributors to the violent ig-
nition of the fuel.

3701

Complete Starting Sequence

The time required for each phase of the starting sequence and the total time consumed from throttle burst to stabilized afterburner operation at three altitudes and for both spontaneous and hot-streak ignition are summarized in figure 80. The time required for the complete starting sequence with hot-streak ignition increased from $11\frac{1}{2}$ to 27 seconds as the altitude increased from 30,000 to 50,000 feet. The same altitude variation increased the total starting time with spontaneous ignition from $16\frac{1}{2}$ to 60 seconds.

Of the total time for starting, the time required to obtain preset fuel manifold pressure amounted to only about 2 seconds at an altitude of 30,000 feet, although as long as 8 seconds were required at an altitude of 50,000 feet. After the manifold pressure reached the preset value, only 1 to 2 seconds were required to obtain ignition with the hot-streak system, as compared to 4 to 6 seconds for spontaneous ignition. Although ignition times significantly shorter than that provided by the hot-streak system cannot be expected, reductions in the time required to obtain a preset fuel manifold pressure would be obtainable by reducing the volume of the fuel lines that must be filled prior to each afterburner start.

As mentioned previously, the greatest portion of the starting time at each altitude is consumed in reaching equilibrium following ignition. Although the length of this stabilizing period is significant, it should be noted that the afterburner provides a substantial thrust increase shortly after ignition occurs. During the time that afterburner operation is becoming stabilized, the thrust will be oscillatory and may periodically equal or even exceed the final stabilized value. Because the hot-streak system provided smoother ignition than did spontaneous ignition, particularly at high altitudes, the oscillation was less severe with the hot-streak system; consequently the time required to stabilize operation was appreciably shorter at all altitudes.

EFFECTS OF DILUENTS ON PERFORMANCE

The combined use of afterburning and injection of refrigerants into the compressor or combustion chamber of a turbojet engine may, as discussed in reference 40, result in higher thrust augmentation than can be achieved by either injection or afterburning alone. The over-all augmentation ratio ideally obtainable with the combined systems is approximately the product of the ratios obtainable from the individual systems. Experimental investigations of combined refrigerant injection

and afterburning are reported in references 41 and 42. In these experiments, afterburning was combined with injection of ammonia or a water-alcohol mixture. Alcohol is normally added to the water because it depresses the freezing point of the mixture and because it serves as a convenient source of the additional heat needed to vaporize the water. Because a water-alcohol mixture provides appreciable gains in thrust only at moderately high inlet-air temperatures, tests with these fluids were confined to sea-level, zero-ram conditions. Ammonia injection, on the other hand, provides useful thrust gains at low ambient temperatures and, consequently, tests with ammonia injection were conducted at conditions simulating flight above the tropopause at a Mach number of approximately 1.0.

In reference 41, augmentation ratios as high as 1.7 were obtained by combined water-alcohol injection and afterburning as compared to about 1.5 for afterburning alone and 1.22 for injection alone. In reference 42, appreciable thrust increases with combined ammonia injection and afterburning over that obtainable with either system alone were demonstrated. The thrust increases obtainable by the combined augmentation systems depend, however, on the coolant used, the characteristics of the engine, and the gas-temperature limitations in the afterburner. Because of this dependence of thrust output on factors other than afterburner performance, the effect of the presence of the injected coolants (diluents) on the performance of the afterburner is discussed in this section with regard to operating limits and combustion efficiency of the afterburner rather than with regard to thrust augmentation obtainable.

The afterburners used in the experiments (figs. 81 and 82) were representative of the best current design practices as discussed in other sections of this report. The afterburners were over 5 feet long and had two- or three-ring V-gutter flameholders with blockages of about 35 percent. The fuel-injection systems were located to provide adequate mixing length.

Effect of Water-Alcohol Injection

In figure 83 are shown the effects of the presence of water and alcohol on the combustion efficiency and outlet-gas temperature of the afterburner. The mixture used was 30 percent alcohol and 70 percent water by volume; the alcohol was a blend of 50 percent ethyl and 50 percent methyl alcohol. The value of fuel-air ratio presented in the figure is the weight ratio of fuel flowing to the afterburner (including alcohol not consumed in the engine combustors) to unburned air flowing to the afterburner. Values of equivalence ratio presented are based on total flow of all fuels (engine fuel, afterburner fuel, and alcohol) and total air flow. At each fuel-air ratio, or equivalence

3701

ratio, increasing the flow of coolant decreases the combustion efficiency. These effects are particularly pronounced at the higher equivalence ratios. With an equivalence ratio of 0.93, the efficiency decreases more than 35 percent as the coolant-to-air ratio increases from zero to 0.072. The effects of water-alcohol injection on gas temperature are shown in figure 83(b). Outlet temperature decreases 17 percent over the same range of coolant-to-air ratios. The temperature could not be increased by raising the equivalence ratio beyond the value of 0.93 because the decrease in combustion efficiency offset the increase in fuel flow. The large reduction in combustion efficiency as water-alcohol flow is increased is probably due to a reduction in reaction rate, as discussed in reference 43.

The maximum equivalence ratios that could be used in the engine were limited by afterburner screech. The limits of stable combustion are shown in figure 84. The afterburner fuel-air ratio at which screech occurred was approximately constant over most of the coolant-flow range and occurred at a value greater than the fuel-air ratio for maximum temperature. The over-all equivalence ratio was also nearly constant over the range of injected flows.

Although afterburner blow-out was not encountered in the full-scale work of reference 41, some small-scale combustor work reported in reference 44 indicates that for some burner designs, blow-out limits may be affected by water injection. Results of blow-out tests on a 6-inch-diameter V-gutter combustor (from ref. 44) are shown in figure 85. Afterburner equivalence ratio is plotted against the injected water-air ratio. With the burner operating with JP-3 fuel, the possible range of operation decreases as water-air ratio increases, and operation was not possible at water-air ratios above 0.07.

Also shown in figure 85 are operating points for a slurry fuel of 60 percent magnesium (approximately 3-micron particle size) and 40 percent JP-3 fuel. As indicated by the stable operation obtained at equivalence ratios over 1.0 at water-air ratios as high as 0.15 (limited only by water-pumping capacity), the effect of water injection on blow-out limits is eliminated in the practical range of water injection rates by the use of the slurry fuel.

The small-scale-burner results with the slurry fuel have been partially confirmed in a full-scale afterburner. Unpublished full-scale-afterburner tests with a slurry of 50 percent magnesium and JP-4 fuel have shown that stable screech-free operation is possible with a water-air ratio of about 0.10 at stoichiometric fuel-air ratio in the afterburner.

3701

Effect of Ammonia Injection

The effect on combustion efficiency and outlet-gas temperature of ammonia injection in the afterburner of figure 82 is shown in figure 86. In this afterburner, maximum combustion efficiency and highest gas temperature over the range of equivalence ratios covered occurred at an over-all equivalence ratio of 1.0 for all ammonia flows. Increasing the ammonia-air ratio decreased both the combustion efficiency and the maximum gas temperature. This effect, while quite small at an equivalence ratio of 1.0, became much greater as the equivalence ratio was decreased.

Although screech was not encountered during these tests, the effect of ammonia injection on blow-out limits shown in figure 87 was observed. At the higher ammonia-injection rates, the afterburner was operable over only a very narrow range of equivalence ratios. At ammonia-air ratios above 0.05, afterburner operation was not possible at any equivalence ratio.

The relative effects of water and ammonia on afterburner combustion efficiency cannot be determined by direct comparison of the results because the tests were run on different afterburners with somewhat different inlet conditions. It is probable that the superior performance of the afterburner of figure 82 with ammonia injection as compared to the afterburner in figure 81 with water injection is due, at least in part, to its greater length.

SHELL COOLING

An important problem of afterburner design and operation is that of obtaining sufficient cooling of the burner shell to ensure adequate service life with minimum penalty to aircraft performance. Although continual increases in aircraft performance and installation requirements have steadily increased the severity of this problem, operational gas temperatures of afterburners have always been such that some form of cooling was required. Many different methods of maintaining safe afterburner-shell temperatures have therefore been investigated since the first full-scale afterburner was operated over 10 years ago.

Consideration is first given to typical distributions of gas and shell temperatures in afterburners. Control of shell temperature by variations in the internal arrangement of flameholders or fuel-injection systems is then discussed, together with associated compromises in combustion performance. Most extensively investigated has been the cooling of the afterburner shell by maintaining an adjacent flow of relatively cool air or gas, either by passing turbine-discharge gas through an internal liner or external cooling air through an outer cooling shroud.

Included in the summary of this work is a discussion of the local and over-all heat-transfer coefficients within the afterburner and presentation of a generalized cooling correlation equation. Finally, recent investigations of transpiration cooling, in which cooling air is passed through a porous afterburner shell, are summarized.

Combustion-Gas and Shell Temperature Distributions

Longitudinal temperature profile. - Data that indicate the manner in which the bulk gas temperature varies along the length of an afterburner are presented in figure 88. The data were actually obtained from ram-jet combustion chambers (ref. 45), but the flameholders and fuel systems used were similar to those of afterburners. Applicability of these data to an afterburner was also verified in reference 46 by analysis of longitudinal distributions of static pressure. The data presented cover length-diameter ratios between 5 and 8, a range which is representative of most full-scale afterburners. Afterburners outside this range of length values may, of course, have different temperature patterns.

The rates of increase in gas temperature are compared in the figure with a dashed curve that expresses the longitudinal temperature-rise ratio as a sinusoidal function of the burner-length fraction. (The symbols used in this section are defined in the appendix.) Under practical operating conditions for an afterburner, the measured and calculated values of temperature do not differ by more than 200° F. This rather satisfactory agreement between the measured temperatures and the values given by the equation provides a very simple means of predicting the local rate of change of bulk gas temperature along the burner length.

As would perhaps be expected, the gas temperature increases most rapidly immediately downstream of the flameholder and tends to level off near the exhaust nozzle. At a station midway between the flameholder and the exhaust-nozzle outlet (a value of $x/L = 0.5$), the temperature rise is approximately three-fourths of its final value.

In addition to these measurements of bulk gas temperature, local gas temperatures 1/4 and 1/2 inch from the burner shell have been measured. The longitudinal profiles of these temperatures, as well as those of the shell itself, are presented in figure 89. In contrast to the rapid increase in bulk gas temperature downstream of the flameholder, the gradual spreading of the flame is such that the gas temperatures near the shell do not start to rise rapidly until some distance downstream of the flameholder. The gas temperature 1/4 inch from the burner shell is, in fact, essentially constant from the turbine outlet to a

CONFIDENTIAL

point 24 inches downstream of the flameholder. This fairly constant gas temperature for the first 24 inches of burner length is reported in reference 47 to exist for several radial distributions of fuel-air ratio.

The level of the shell temperatures shown in figure 89 is influenced, of course, by the design of both the internal components of the afterburner and the external cooling-air shroud that was used. The general trend of these shell temperatures, however, follows that of the gas temperatures adjacent to the burner shell. Special cooling of the first foot or two of burner length is therefore not required owing to the nature of the flame spreading from the flameholder. Downstream of this point, however, the cooling requirements increase rapidly.

The data of figure 89 were all obtained at an exhaust-gas bulk temperature of 3811° R. Longitudinal profiles of shell temperature for three exhaust-gas temperatures are presented in figure 90; the trends are similar for the three temperature levels.

Transverse gas-temperature profiles. - Values of combustion gas temperature measured across a diameter of a typical afterburner at a station 48 inches downstream of the flameholder are shown in figure 91 for two values of exhaust-gas bulk temperature. The difference between the general level of the temperatures shown and the exhaust-gas bulk temperature is due to continued combustion of fuel in the 2 feet of burner length aft of the measuring station. As the exhaust-gas bulk temperature was increased, the transverse gas-temperature profile became higher and slightly broader, but did not increase appreciably near the burner shell.

These data were obtained with a fairly typical radial distribution of fuel-air ratio. As noted in reference 47, variations in the fuel-air-ratio distribution can have large effects on this transverse gas-temperature profile.

Circumferential shell-temperature profiles. - The shell temperatures measured at various locations around the circumference of an afterburner near the exhaust nozzle have always been found to vary appreciably. The difference between the maximum and minimum shell temperature at a given station usually amounts to from 400° to 500° F and is frequently as great as 600° F. When average shell temperatures are under discussion, which will be the usual consideration herein, it must therefore be recognized that maximum temperatures are from 200° to 300° F higher.

No real correlation has ever been found between the circumferential temperature pattern and the design of the burner. The circumferential variation in shell temperature is, however, related in reference 47 to

internal gas-temperature variations rather than to external effects such as might be introduced by the cooling system of an engine installation. Furthermore, it has been found in many investigations that a given afterburner holds its general temperature pattern over extended periods of operation and at various gas-temperature levels. In figure 92(a) are presented two circumferential profiles of afterburner shell temperature, one obtained when the afterburner was fairly new and the other after it had been operated more than 9 hours. This operating time was accumulated by many separate runs over a period of several days. The shell temperature of this afterburner varied from a minimum of about 800° F to a maximum of nearly 1300° F under the particular conditions of operation. The circumferential profiles differ by less than 200° F for the two periods of operation.

Two circumferential profiles of shell temperature measured in this afterburner at different exhaust-gas temperatures are presented in figure 92(b). Although the shell temperature is naturally higher for the higher gas temperature, the profile is similar for both gas-temperature levels. At the higher exhaust-gas temperature, the shell temperature is seen to vary from a low of 920° F to a high of 1500° F.

Control of Shell Temperature Through Changes in

Burner Internal Geometry

One method of preventing excessive shell temperatures is to so distribute the fuel injection and position the flameholding elements that no burning takes place near the outer shell. Although this method has been successfully applied in many cases where a high level of thrust augmentation is not required, it loses its effectiveness as higher gas temperatures, and consequently, more uniform fuel-air-ratio distributions, are desired. The problem thus becomes one of compromise in design, to evaluate the gains in cooling against the associated performance losses. Although quantitative data are not available to completely define this choice, some information is available in which either the fuel-injection pattern or the flameholders were independently varied and that provides at least a qualitative picture of their influence on shell temperatures and performance.

Distribution of fuel injection. - The effects of a radial shift in the location of fuel injection away from the afterburner shell on shell temperature and combustion efficiency are shown in figure 93. The afterburner used for these tests had radial fuel-spray bars and a two-gutter flameholder of 30-percent blockage with a radial clearance of $2\frac{7}{8}$ inches between the outer gutter and the afterburner shell. No cooling

liner was used. Two comparative patterns of radial fuel distribution
are sketched in figure 93(a). For configuration A, the fuel orifices
covered the inner 70 percent of diffuser annulus area; while for con-
figuration B, the fuel orifices were confined to the inner 40 percent
of annular area. With the fuel so confined to the inner section of
the burner, the shell temperatures were 100° F lower at the higher
exhaust-gas temperatures. As shown in figure 93(b), however, combus-
tion efficiency of configuration B was considerably below that of con-
figuration A for gas temperatures above 3000° R. Thus, while the shell
temperatures could be significantly reduced by this shift in fuel dis-
tribution, simultaneous losses in combustion performance are likely for
high fuel-air-ratio levels of operation. It is nonetheless noteworthy
that, if, for example, a gas temperature of only 2800° R were desired,
the radial shift in fuel distribution would provide a 75° reduction in
shell temperature without appreciable loss in efficiency.

Similar results were noted in reference 11, which reports that a
shift in the fuel orifices away from the burner shell reduced the shell
temperatures by some 30° F. The altitude limit of this afterburner,
which operated in the fuel-air-ratio range of 0.05 to 0.06, was, how-
ever, reduced from 54,000 to 50,000 feet by the inward shift in fuel
distribution.

Some additional data on shell temperatures with various fuel dis-
tributions are presented in figure 94. In the upper part of the figure
are illustrated the approximate radial distribution of fuel, with con-
figuration A approximately uniform, configuration B with fuel towards
the outer shell, and configuration C with fuel towards the center of
the burner. The longitudinal distributions of shell temperature, shown
in the lower part of the figure, are for an average exhaust-gas temper-
ature of 3230° R. Even at this relatively low temperature, the shell
temperatures differed appreciably at the downstream end of the burner.
With more fuel near the outer wall (configuration B), the shell temper-
atures were about 200° F above those with the uniform injection (con-
figuration A) and about 300° F above those with the fuel near the center
of the burner (configuration C). This variation in fuel distribution
also had an appreciable effect on the combustion performance. Configu-
ration B was characterized by rough burning and the combustion efficien-
cy was about 8 percent lower than that of either configuration A or C at
a fuel-air ratio of about 0.04 and a burner-inlet pressure of 1400
pounds per square foot. Although the combustion efficiency at these
conditions was approximately the same for both configurations A and C
(about 95 percent), the maximum temperature that could be reached by
configuration C was only 3250° R as compared to 3700° R for configura-
tion A.

3701

    The effect that the fuel distribution has on afterburner shell tem-
peratures may be influenced not only by the location of the fuel injec-
tion orifices themselves but also by the aerodynamic characteristics of
the flow in the diffuser. A particularly striking example of this ef-
fect is described in reference 11. Reduction in whirl of the gases
leaving the turbine from about 30° to 10° R by the addition of turning
vanes and vortex generators at the turbine outlet decreased the shell
temperatures between 80° and 120° F at an exhaust-gas temperature of
3100° R. Even greater reductions were considered possible at higher
gas temperatures. This reduction in shell temperature by elimination
of turbine-outlet whirl was attributed to both the decreased tendency
of the fuel to centrifuge toward the outer shell and to the increased
thickness of the boundary layer at the outer shell.

    Distribution of flameholding elements. - Increasing clearance be-
tween the outer gutter of the flameholder and the burner shell obviously
cannot be accomplished without attendant changes in the gutter width,
blocked area, or number of rings. An isolated effect is therefore not
possible. One set of data in which the radial clearance was increased
from $2\frac{7}{8}$ to $3\frac{11}{16}$ inches, together with an attendant increase in both gut-
ter width and blocked area, is presented in figure 95. The shell tem-
peratures at the burner-outlet station (fig. 95(a)) were reduced between
50° and 100° F with this increase in radial clearance. The combustion
efficiency (fig. 95(b)) also increased somewhat with increase in radial
clearance. This increase in efficiency cannot be attributed to the
change in clearance dimension, but rather to the increases in gutter
width and in blockage of the flameholder and possibly to a better aline-
ment of the flame-seat area with the fuel-distribution pattern. In any
event, it is apparent that although no general rules may be stated, some
alleviation of the cooling problem may frequently be possible by alter-
ation of the internal geometry of the burner without sacrifice in
performance.

                              Use of Inner Liner

    Use of an inner liner was one of the first methods used to maintain
the shell of an afterburner at safe temperature levels. Inner liners
are currently finding application in many production engines, frequently
in the same basic form as first used at the Lewis laboratory in 1948. A
photograph of one of these early liners is presented in figure 96. The
liner usually extends from the flameholder station to the exhaust-nozzle
inlet or, in some cases, terminates within the convergent section of the
nozzle. A radial clearance, usually 1/2 inch, is provided between the
liner and outer shell of the afterburner through which 6 to 8 percent of
the turbine-exhaust gases are pumped by virtue of the momentum pressure

drop of combustion. The liners have commonly been made of 0.063-inch sheet Inconel. Attachment to the outer shell must be made in a manner that will permit expansion in both axial and circumferential directions; one type that has been successfully used is illustrated in the insert of figure 96.

Outer-shell temperatures of afterburners equipped with inner liners are presented in references 1, 11, and 48. All available comparative data are presented in figure 97. In this figure, the average temperature of the outer shell and the inner liner at the exhaust-nozzle inlet are plotted against the exhaust-gas bulk temperature. The curve for the temperature of the inner liner was, in the absence of sufficient experimental data, computed from the cooling correlation equation of reference 46, to be discussed subsequently. In this calculation, 6 percent of the exhaust gas was assumed to flow through the liner. Agreement with the single data point available (actually obtained from a cross plot of many data points presented in ref. 1) is very good.

As noted in the figure legend, the three afterburners for which shell temperatures are presented were of about the same length and were operating at about the same turbine-outlet temperature. No external cooling shroud or insulation was used around the afterburners; all were installed bare in the open test chamber or wind tunnel test section. No particular effort was made to pass cooling air over the burner, but the test compartment was sufficiently ventilated to maintain an ambient temperature of the order of 100° F to protect instrumentation and other equipment.

The outer-shell temperatures of the three afterburners show remarkable agreement. Shell temperatures are seen to increase from about 800° F at an exhaust-gas temperature of 2000° R to slightly under 1200° F for a gas temperature of 3500° R. An average liner temperature of 1850° F at the downstream end is indicated for an exhaust-gas temperature of 3500° R. Although the liner has lost much of its strength at these high temperatures, it is not highly stressed and satisfactory life has usually been experienced. If the liner supports permit thermal expansion in both longitudinal and circumferential directions, the liners were usually in a satisfactory condition after as much as 40 or 50 hours of afterburner operation.

The temperature of the outer shell of an afterburner in an actual aircraft installation may, of course, differ appreciably from the values of figure 97, if the afterburner is either insulated or provided with external cooling. Some idea of the effect of an inner liner on the outer-shell temperature may, however, be obtained by comparison of shell temperatures of a given afterburner both with and without a liner. Such a comparison is presented in figure 98 for two different afterburners. For exhaust-gas temperatures of 3000° to 3500° R, the shell temperature is reduced about 150° F by installation of the inner liner.

Ceramic Coatings

The use of a ceramic coating to reduce absorption of radiant energy by the afterburner shell has been considered for many years. Many ceramic coatings, such as the painted coating of Uverite mentioned in reference 49, possess absorptivities that are only one-eighth to one-tenth those of steel at typical shell temperatures. Simple heat-transfer calculations indicate that this reduction in absorptivity should reduce the shell temperature about 100° F for nonluminous radiation and 150° to 200° F for luminous radiation at gas temperatures of 3500° R. Experimental verification of these temperature reductions has, however, been difficult to obtain. The principal difficulty of experimental verification is that either two different afterburners must be tested or a single afterburner must be disassembled for subsequent coating and that the normal variation of shell temperature from one afterburner to another obscures the effects of the coating.

One interesting approach to this problem was the use of a 4-percent solution of ethyl silicate in the fuel (ref. 8). During operation of the engine with this fuel, a thin frosty coating having a milky appearance formed on the inside of the shell. Presented in figure 99 are some shell temperatures observed during a sequence comprising operation with the standard fuel (gasoline), with the ethyl silicate additions, and with the standard fuel; temperatures during the second period of standard-fuel operation were observed 15 minutes after start of the period. The shell temperature was 70° to 100° F lower than the starting value, both during use of the ethyl silicate and for a period of at least 15 minutes after operation on clear fuel was resumed. Data are not available to establish how long this coating may be effective or the effect of operating transients on stability of the coating.

Forced Convection Cooling by External Air Shroud

In addition to the use of an inner liner, or properly designed fuel-injection systems and flameholders previously discussed, most afterburners are also provided with an external air shroud, through which is passed either ram air or compressor bleed air. Because information upon which to base the design of annular cooling systems for small-length-diameter-ratio chambers containing radiant gases was not available in the heat-transfer literature, an investigation of such cooling systems was conducted by the NACA some three years ago. This investigation is reported in references 46, 47, and 50, and some of the salient results are summarized in the following paragraphs.

Inside heat-transfer coefficient. - The convective heat-transfer coefficient h_c at the nozzle-inlet station is plotted in the usual

manner in figure 100. This heat-transfer coefficient was obtained by subtracting the contribution of radiation, utilizing published emissivities and absorptivities, from the measured heat-flow rate through the burner shell and dividing by the applicable temperature difference. The fluid properties appearing in the various dimensionless parameters were evaluated at the film conditions. The symbols used are defined in the appendix.

The correlation represented by the line drawn in the plot and expressed by the inserted equation is that given in reference 51 for air in smooth tubes at high temperatures. The present data agree with this line within ±0.15. As is pointed out in reference 50, this agreement between the present data and that of reference 51 is probably the result of the similarity of the transverse temperature profiles of the afterburner with those of fully developed turbulent flow in pipes.

The heat-transfer coefficient of figure 100 is, as previously mentioned, for convective heat transfer. To obtain the total inside coefficient, the contribution of radiant heat transfer is added to this coefficient. The magnitude of this radiation will, of course, depend on the pressure level in the burner and the operating fuel-air ratio, that is, whether the radiation is predominantly luminous or nonluminous. The present data were obtained over a range of pressures from 750 to 1400 pounds per square foot absolute and the flame was translucent, varying from a light blue-violet to turquoise with no yellow luminosity. The flame was therefore nonluminous.

The combined inside heat-transfer coefficient for a burner-inlet pressure of 1400 pounds per square foot absolute is plotted in figure 101 against the distance downstream from the flameholder, with the difference between the gas and shell temperatures as a parameter. Typical operating lines for two different outlet gas temperatures are superimposed on this map. Along the operating lines, the combined coefficient h_{cr} decreases from about 22 to a minimum of 17 at the midpoint of the afterburner and then increases to about 26 at the end of the afterburner. Because radiation is slight in the upstream portion of the burner, the combined coefficient decreases in this section in much the same manner that the convective coefficient does in the entrance section of a pipe before fully developed turbulent flow is established. The subsequent increase in the combined coefficient is due to increases both in the nonluminous radiation and in the convective coefficient as the temperature gradients near the wall increase. As is discussed later, the radiant heat-transfer coefficient at the downstream end of the burner was about one-fourth of the combined coefficient.

Over-all heat-transfer coefficient. - The measured over-all heat-transfer coefficient, including both the outside-shell coefficient adjacent to the cooling air (which may be computed from information in the

heat-transfer literature) and the combined inside coefficient, is presented in figure 102. This plot is similar to that of figure 101, with burner length as the abscissa, temperature difference from gas to shell as a parameter, and with typical operating lines superimposed for two exhaust-gas temperatures. The longitudinal variation of this over-all coefficient is similar to that of the combined inside coefficient h_{cr} because the controlling resistance to heat transfer is that of the inside film.

The relative magnitudes of the various heat-transfer coefficients at the exhaust-nozzle inlet station and for a gas-to-shell temperature difference of 1600° F are indicated for some typical operating conditions in the following table:

Burner-inlet static pressure, lb/sq ft abs	Heat-transfer coefficient, Btu/(hr)(°F)(sq ft)			
	Convective	Radiation	Combined inside	Over-all
850	12.3	4.2	16.5	11.5
1400	18.5	6.0	24.5	17.5

The heat transferred by nonluminous radiation was about one-fourth of the total heat transferred to the shell for the conditions investigated. The presence of luminous radiation, which is usually observed in afterburners operating at high gas temperatures and at combustion chamber pressures of two atmospheres or higher, would obviously considerably increase the amount of heat radiated. Additional research is, however, necessary to establish the magnitude of the luminous radiation under these conditions and to formulate convenient methods for its prediction. The over-all heat-transfer coefficient was approximately 0.7 of the combined inside heat-transfer coefficient.

Cooling correlation equation. - To provide a convenient and rapid method of calculating the shell temperature of an afterburner from commonly known performance parameters, a semiempirical correlation equation is derived in reference 46. The form of the equation was analytically derived, and data from references 47 and 50 were used to evaluate the constants in the equation. The final plot of this evaluation, which determines the correlation equation, is presented in figure 103. For convenience, the equation is repeated:

$$\frac{T_g - T_s}{T_s - T_{a,2}} = 30 \left(\frac{T_{a,2}}{T_g}\right)^{0.73} \left(\frac{W_a}{W_g}\right)^{0.8}$$

where

$T_{a,2}$ outlet cooling-air temperature, °R

T_g bulk temperature of combustion gas at exhaust-nozzle inlet, °R

T_s average shell temperature at exhaust-nozzle inlet, °R

W_a cooling-air flow, lb/sec

W_g combustion-gas flow, lb/sec

    This equation relates the average shell temperature at the down-stream end of the combustor to the outlet gas temperature, the outlet cooling-air temperature, and the mass-flow ratio of cooling air to combustion gas. As previously noted, the maximum shell temperature will usually be from 200° to 300° F higher than these average temperatures. The pertinent dimensions of the afterburner used to establish this correlation were a length of 5 feet, an internal diameter of 26 inches, and a cooling-passage height of 1/2 inch. Charts for determining the outlet-air temperature $T_{a,2}$ from the more commonly known inlet-air temperature and other known parameters are presented in reference 46. The equation has, of course, the limitations regarding the relative influence of convective and radiant heat transfer discussed previously. It also was obtained from an afterburner with essentially one fuel-air-ratio distribution; although, as discussed in reference 46, changes in fuel-air distribution sufficient to cause marked deviation from the equation resulted in poor combustion performance. The equation may be considered a good approximation for present types of afterburners without an inner liner up to gas temperatures of 3500° R at flight conditions where luminous radiation is not significant. The deviation of shell temperature from the correlation values for either afterburners with an inner liner or those specially designed for maximum thrust (high-temperature afterburners) is illustrated later herein.

    An indication of the degree to which the correlation equation accounts for the effect of all significant variables is presented in figure 104 in which values of shell temperature computed from the equation are plotted against measured temperatures. Principal variables covered by the tests included exhaust-gas temperatures from 2850° to 3500° R, pressures from 850 to 1400 pounds per square foot absolute, cooling-air mass-flow ratios from 0.067 to 0.191, inlet cooling-air temperatures from 500° to 1587° R, and afterburner-inlet temperatures from 1340° to 1630° R. Agreement between the measured and calculated values of shell temperature is within ±50° R.

3701

CU-9 back

For convenience, the shell temperatures computed by the correlation equation are plotted in figure 105 against the coolant-flow ratio, for a range of exhaust-gas temperatures at an inlet cooling-air temperature of 80° F. This plot shows, for example, that an average shell temperature of 1500° F would be obtained for a coolant mass-flow ratio of 0.08 and a gas temperature of 3500° R. Doubling the coolant flow ratio (to 0.16) would decrease the shell temperatures about 350° F, to 1150° F. For most of the region of practical interest, the shell temperature is changed by 250° to 300° F for a 500° R change in gas temperature, other conditions remaining constant.

Shell temperatures computed from the correlation equation are compared with measured temperatures from several afterburners in figure 106. The measured temperatures are superimposed on the computed curves presented in figure 105. To represent an extreme set of conditions, data are presented for two high-temperature afterburners (refs. 8 and 19) and for a moderate-temperature afterburner fitted with an inner liner (ref. 52). The high-temperature burners of references 8 and 19 were operated at a burner-inlet pressure of 2450 and 1800 pounds per square foot absolute, respectively; with both, considerable effort was made to achieve the very uniform fuel-air distribution necessary to burn all the turbine-exhaust gases and thus reach high bulk gas temperatures.

For the afterburner with the inner liner, the shell temperatures are 200° to 300° F lower than predicted by the correlation equation. As previously discussed, the largest part of this difference may be attributed to the liner itself. Shell temperatures of the high-temperature afterburners are some 250° to 300° F higher than predicted by the equation; a cooling-air flow 30 to 40 percent greater than that computed would be required to maintain the same shell temperatures. This difference is undoubtedly largely due to the injection of fuel closer to the shell of the high-temperature afterburners than was the case for the afterburner of the correlation equation, and possibly due to the greater contribution of radiant heat transfer at the somewhat higher pressure level of operation. In any event, the correlation equation appears to be fairly accurate for conventional afterburners operating at gas temperatures up to 3500° R at pressures up to 1 atmosphere; in more extreme cases, such as those illustrated in figure 106, deviations in shell temperature of up to 200° to 300° F may be expected.

Transpiration Cooling

To avoid the considerable losses in net thrust resulting from the large amounts of cooling air required for high-temperature afterburners at supersonic flight conditions, more effective cooling by means of transpiration, or air passage through porous walls, has been investigated. In this type of cooling, the cooling air is allowed to pass through

a porous wall that forms the afterburner shell, thus providing both an intimate contact of the cooling air with the burner shell and a constantly replenished insulating layer of cool air on the inside surface of the shell. A preliminary investigation of this method of cooling an afterburner with a sintered porous stainless steel shell is reported in reference 53. Although promising cooling characteristics were obtained, the sintered material that was used was considered unsatisfactory from the standpoint of strength, control of permeability, and fabrication difficulties. Although sintered materials of considerably improved characteristics have since been developed, their unavailability at the time lead to the choice of a wire cloth material for the subsequent investigations reported in references 54 and 55.

The wire cloth used was Monel 21 × 70 twilled Dutch weave that was sprayed with silver solder and brazed and rolled to a 35-percent reduction in thickness for control of permeability. The burner shell was formed by spot-welding strips of this cloth to a structural framework. The various channels of wire cloth formed in this manner, which were 4 inches wide and about 1/2 inch deep and extended the length of the burner, are apparent in the photographs of figure 107. After initial operation, the channels were bulged between 1/4 and 3/8 inch at the midspan, a result which reduced the tensile stresses caused by the pressure forces. This burner shell successfully withstood the pressure surges of a number of afterburner starts as well as the usual pulsations during normal steady-state operation. Air-flow calibrations taken during the investigation (afterburning operation of 4 hours and 10 minutes) revealed no discernable variation with time.

Typical longitudinal profiles of temperature and pressure for a given exhaust-gas temperature and coolant-flow ratio are shown in figure 108. Temperature profiles for the combustion gas, the afterburner porous wall, and the cooling air are shown in figure 108(a). Data for the porous wall and the cooling-air temperature are presented for the hottest and coolest of the 20 separate channels. A considerable difference in temperature between these two channels was obtained, largely because of a nonuniform pressure distribution from the inlet plenum chamber that was used. It is believed that a better plenum chamber, the addition of cross-flow holes in the structural angles that supported the wire cloth, or a better selection of wall permeability would have largely eliminated these temperature variations. On the average, the wall temperature did not increase a great deal along the length of the burner but rather tended to follow the nearly constant temperature of the cooling air.

The pressure of the cooling air in one channel and the combustion gas pressure are shown in figure 108(b). The cooling-air pressure rises

along the length of the channel because of the deceleration of the flow
associated with the continuous bleeding of air through the shell. The
gas pressure decreases along the length of the burner because of the in-
ternal pressure drop of the afterburner, thus providing an increasing
pressure differential along the wall. The single curve of figure 108(c)
shows that the longitudinal addition of cooling air into the slightly
tapered burner was nearly linear.

To permit application of these data to other afterburners or other
operating conditions, a correlation is presented in reference 55 that is
summarized in figure 109. In this correlation, the temperature-
difference ratio $(T_{s,l} - T_{a,l})/(T_{g,l} - T_{a,l})$ is plotted against the
coolant-flow ratio $(\rho V)_a/(\rho U)_g$ for constant values of bulk Reynolds
number. The length used in the Reynolds number is the distance from the
leading or upstream edge of the porous wall. Consequently, the
temperature-difference ratios and the coolant-flow ratios are local val-
ues corresponding to the local Reynolds numbers. The quantity $(\rho U)_g$
was assumed identical to the local one-dimensional value of total weight
flow per unit of combustion-chamber flow area. The porous-wall temper-
ature $T_{s,l}$ was measured on the cooling-air side of the wire cloth, but
can be considered practically to represent the temperature on the hot-
gas side because of the small difference in measured temperatures across
the wire cloth.

The correlation presented in figure 109 includes data from both the
hottest and coolest channels; these data define a single curve for a
given Reynolds number. For coolant-flow ratios less than about 0.007,
the Reynolds number has no effect on the correlation. For higher
coolant-flow ratios, however, the temperature-difference ratio, and
hence the wall temperature for fixed cooling-air and gas temperatures,
decreases as the Reynolds number is increased. A partial comparison of
this correlation with the approximate theories of references 56 and 57
is presented in reference 55.

The coolant-flow ratio $(\rho V)_a/(\rho U)_g$, or more specifically the cool-
ant flow $(\rho V)_a$, is a function of the permeability of the wire cloth and
the pressure difference across the cloth. Information relating the de-
sign and fabrication of the cloth to its permeability is presented in
reference 54. This information, together with the correlation of fig-
ure 109, permits determination of porous-wall temperatures of an after-
burner for various values of total, or over-all, coolant-flow ratio
W_a/W_g. The results of a sample calculation are presented in figure 110,
together with comparative curves for conventional forced-convection
cooling.

Because the longitudinal profiles of both the static pressure of
the cooling air and the combustion gas are functions of flight condi-
tion, the temperature curves obtained for transpiration cooling vary
somewhat from one flight condition to another. As discussed in refer-
ence 55, however, these variations are small and the curves presented
in figure 110 may be considered representative of operation of a typi-
cal, present-day turbojet engine operating over a range of flight speeds
between Mach numbers of zero and 2.0. The operable range of transpira-
tion cooling is limited by the allowable pressure drop across the porous
wall. As an example, the upper tick on each curve corresponds to an as-
sumed minimum pressure drop across the wall of 1 pound per square inch
at the leading edge. The lower tick corresponds to an assumed maximum
pressure drop of 6 pounds per square inch at the trailing edge. Because
of these limits on wall pressure drop, together with the drop in
combustion-chamber pressure along the length of the burner, the cooling-
air pressure must be accurately controlled.

The maximum temperature limit for the porous cloth that was used
was about 950° F because of oxidation of the brazing alloy. With a
temperature margin of 200° F allowed for normal circumferential vari-
ations in gas temperature and random variations in permeability of the
cloth, a safe operating temperature of 750° F may be used for the pres-
ent material. Reference to the curves of figure 110 shows that this
wall temperature could be maintained with a coolant-flow ratio of 0.033
for a gas temperature of 3700° R and an inlet cooling-air temperature
of 200° to 250° F. For a maximum operating temperature of 1400° F for
a forced-convection-cooled shell of stainless steel, a coolant-flow ra-
tio of 0.15 would be required for forced-convection cooling at the same
gas temperature. Cooling-air requirements for a transpiration-cooled
afterburner wall are thus of the order of one-fifth those required for
a convection-cooled shell. Even lower cooling-air flow rates and, of
perhaps more importance, higher permissible shell temperatures and re-
laxation of air-pressure control requirements for transpiration cooling
may be expected from several possible improvements in design and mate-
rials. These improvements would include closer quality control of wall
permeability, the use of stainless steel or Inconel instead of Monel
wires, the use of high-temperature brazing alloys, and methods of con-
struction that would provide a more uniform circumferential distribution
of cooling air and a somewhat higher pressure drop across the wall.

SUMMARY OF RESULTS

Burner-Inlet Diffusers

Typical afterburner-inlet diffusers produce varying degrees of non-
uniformity in the velocity profile at the burner inlet, with high veloc-
ities near the outer wall in the region of the flameholders and lower

DECLASSIFIED

velocities in the center of the burner. Because the gas velocity at the flameholder is usually limited by combustion considerations, the allowable average burner-inlet velocity, and hence the burner diameter, is largely a function of the uniformity of this velocity profile. One of the most significant diffuser design variables affecting the outlet velocity distribution is burner length. Although data are not available to provide detailed design rules, several investigations have demonstrated that increasing diffuser length results in a more uniform velocity profile, but with some increase in pressure loss. For a diffuser area ratio of about 2.0, a length-to-outlet diameter ratio of 1.0 should provide a velocity profile suitable for achieving good combustion performance at high altitude for an average burner-inlet velocity of 450 to 500 feet per second. With a length-diameter ratio of 2.0 and an area ratio of 1.5, the velocity profile should be sufficiently uniform to provide an average burner-inlet velocity of over 0.9 of the velocity in the flameholder region. The shape of the diffuser inner body has no appreciable effect on afterburner performance. Vortex generators provide small improvements in diffuser velocity profile, but other flow control devices such as annular vanes and splitter ducts have not been successfully applied. Afterburner-inlet whirl has a negligible effect on combustion efficiency but may lead to burning in the wakes of support struts and attendant overheating and warping of adjacent parts of the diffuser. Turbine-outlet whirl may be reduced to acceptable values by relatively simple straightening vanes.

Fuel-Injection Systems

To obtain high combustion efficiency at moderate-to-high over-all fuel-air ratios, the fuel-injection system of an afterburner must provide a uniform fuel-air-ratio distribution across the burner in both a radial and a circumferential direction. If maximum efficiency is required at fuel-air ratios of 0.055 to 0.060, for example, the mean deviation of local fuel-air ratio must be less than 10 percent of the average value. If a maximum combustion efficiency at low fuel-air ratios is desired, the fuel distribution should be nonuniform. With the usual type of circular-gutter flameholder, this nonuniformity, or the locally rich regions, should be oriented in a radial rather than in a circumferential direction. The radial fuel-air-ratio distribution provided by a fuel-injection system can be predicted with satisfactory accuracy by simple considerations of the radial proportionment of the injected fuel and gas flow. The uniformity of the circumferential pattern of fuel-air ratio will depend on both the spacing of the radial fuel-spray bars and the penetration characteristics of the fuel jet across the gas stream. The penetration characteristics of fuel jets in afterburners appears to be between those of pure liquid jets and those of air jets, with the relative position depending on the factors that influence the rate of
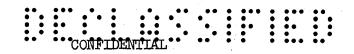
fuel vaporization. To obtain a uniform circumferential fuel-air-ratio distribution, the spray bars should be no more than 3 inches apart at the burner shell if the gas velocities are high (500 to 600 ft/sec). For lower gas velocities, the spray-bar spacing may be increased some-what, provided that the fuel orifices are at least 0.030 inch in diame-ter. Highest combustion efficiency at high fuel-air ratios is obtained with fuel injected in a direction transverse to the gas stream, and with a mixing distance of at least 12 to 15 inches between the point of in-jection and the flameholder.

Flameholder Design

Of the cross-sectional gutter shapes investigated, all provided about the same combustion performance except the U-shaped gutter, which was inferior in both combustion efficiency and blow-out limits. The num-ber, arrangement, and size of flameholder gutters are important design factors. Gutter widths of approximately $1\frac{1}{2}$ inches are necessary for good combustion at inlet pressures of 600 to 1000 pounds per square foot absolute, although smaller gutters are satisfactory at higher pressures. At low and intermediate pressure, three-gutter flameholders appear to be superior to one- or two-gutter flameholders. In order to provide a suf-ficient number of gutters of adequate width to give good flame stability and good efficiency at low pressures (below 1000 lb/sq ft abs), flame-holder blockage should be at least 30 percent. Gains in efficiency by increasing blockage above 30 or 35 percent appear to be negligible. Ra-dial gutters that interconnect the annular gutters have a favorable ef-fect on low-pressure blow-out limits. Although the pressure drop across a flameholder increases rapidly with increasing velocity and blockage, the isothermal pressure drop of typical installations, having 30 to 35 percent blockage and for velocities from 400 to 600 feet per second, is only of the order of 1 to 2 percent of the inlet pressure. Both the isothermal and burning pressure drop may be calculated with good accuracy.

Combustion Space

For afterburners designed to operate at high-altitude conditions, an increase in afterburner length from 30 to 50 inches provides a large increase in combustion efficiency for various conditions of fuel-air ratio, inlet pressure, inlet velocity, and inlet temperature. Gains in performance by increasing the length beyond 5 feet were, however, small. The effect of shell taper was found, in the one case investigated, to be nearly the same as reducing the length of a cylindrical afterburner by an amount providing the same reduction in burner volume; thus the effect of shell taper may be large for short lengths and relatively minor for

long lengths. Reducing the diameter of the flameholder relative to the burner shell, which reduces the combustion volume by increasing the distance for the flame front to reach the shell and hence fill the combustor, was found to decrease the combustor efficiency significantly. For low-inlet-velocity and high-inlet-pressure conditions, such as for an afterburner intended only for take-off, considerable reductions in burner length are possible. Good take-off thrust augmentation, of the order of 40 percent, was obtainable in a low-pressure-drop afterburner with a length of only 20 to 30 inches.

Combustion Instability (Screech)

The origin and basic mechanism of combustion screech in afterburners, a destructive, high-frequency, high-amplitude pressure oscillation, are not known. Dependance of the occurrence of screeching combustion on the design of the inlet diffuser and of the flameholder suggests that it is associated with the aerodynamics of the flow approaching the burning region as well as with the combustion process itself. The pressure oscillations that occur with screech have been identified as a transverse oscillation of between the first and fourth mode. This identification of the mode of oscillation has led to the successful use of perforated cylindrical liners for the prevention or elimination of screeching combustion. These perforated liners, which are located about 3/4 inch inside the burner shell and extend at least 60 percent of the combustion chamber length, have eliminated screech in all afterburners investigated over the full operable range of fuel-air ratio and for pressures up to 6500 pounds per square foot absolute.

Ignition, Starting, and Transient Performance

The complete starting cycle of an afterburner consists of filling the fuel pipes and manifolds with fuel, igniting the fuel, and establishing equilibrium engine-afterburner operation. The time required to accelerate the fuel pump from rest and reach the operating fuel-manifold pressure increased from 2 to 9 seconds as altitude was increased from 30,000 to 50,000 feet for two typical afterburner installations. Ignition of the fuel by means of a spark plug is unreliable, and spontaneous ignition, while successful and consistent in some afterburners, cannot be considered a generally reliable method. Hot-streak ignition, which produces a torch of flame into the afterburner by momentary augmentation of fuel flow to a primary combustor, has been very successful in many types of afterburners. The time required to obtain ignition by this method varies from 1 to 3 seconds. The greatest length of time in the complete starting cycle is involved in establishing equilibrium operation of the engine-afterburner combination following ignition of the fuel. With a representative current control system, the

time required for oscillations in the exhaust-nozzle area, the primary engine fuel flow, and other engine variables to reach their final steady-state values increased from 11 to 27 seconds as altitude was increased from 30,000 to 50,000 feet.

Effect of Diluents on Performance

Injection of a water-alcohol mixture or ammonia into the compressor or combustor of the engine to obtain high thrust augmentation has been found to have a detrimental effect on the combustion performance of afterburners. Large decreases in the combustion efficiency and maximum outlet-gas temperature occur as the water-alcohol injection rate is increased, particularly for high over-all equivalence ratios. Both small-scale work and some full-scale afterburner experience indicate a large improvement in range of stable operation of the burner if a magnesium slurry fuel is used instead of JP-3 fuel. Compressor injection of ammonia also decreases afterburner combustion efficiency for a given over-all equivalence ratio, although the effects are small at high equivalence ratios. Afterburner blow-out limits also decrease as ammonia injection is increased.

Shell Cooling

Circumferential variations in shell temperatures of 400° to 600° F exist at the downstream end of most afterburners. These temperature patterns are maintained, for a given afterburner, at various operating conditions and over considerable periods of time. The shell temperature may be reduced at least 100° F by changing the radial fuel distribution from uniform to nonuniform (away from the shell) but usually at the expense of a loss in combustion efficiency at high fuel-air ratios. Increasing the clearance between the flameholder gutter and the afterburner shell can also considerably reduce the shell temperature, but with uncertain effects on the combustion performance. The use of an inner liner will reduce the shell temperature about 150° F for typical operating conditions. Although such liners operate at high temperatures (up to 1900° F), they have satisfactory life if installed to permit expansion. The heat transferred to the burner shell by radiation is about one-fourth of the total heat flux under nonluminous conditions. For cooling by a forced-convection cooling-air shroud, a correlation equation permits prediction of the temperature of the inside surface of typical, moderate-temperature afterburners within about 50° for a wide range of operating conditions. For special high-temperature afterburners (outlet-gas temperature above 3500° R) shell temperatures may be 200° to 300° F higher than predicted by the equation. An afterburner using transpiration cooling (with a wire cloth shell) required about
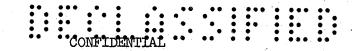
one-fifth as much cooling air as a comparable convective-cooled after-
burner, even for the low (750° F) temperature limits of the present
material.

Lewis Flight Propulsion Laboratory
　　National Advisory Committee for Aeronautics
　　　　Cleveland, Ohio, December 21, 1955

APPENDIX - SYMBOLS

A cross-sectional area, sq ft

$A_{g,y}$ combustion chamber flow area at distance y from upstream
                edge of porous shell, sq ft

$c_{p,f}$ specific heat of gas at constant pressure and film temper-
                ature, Btu/(lb)(^{O}R)

D afterburner diameter, ft

f/a fuel-air ratio

h_c convective gas-side heat-transfer coefficient,
                Btu/(hr)(^{O}R)(sq ft)

h_{cr} combined convection and radiation heat-transfer coeffi-
                cient, Btu/(hr)(^{O}R)(sq ft)

k_f thermal conductivity of gas at film temperature,
                Btu/(hr)(^{O}R)(ft)

L distance from flameholder to exhaust-nozzle outlet, ft

$T_{a,2}$ outlet cooling-air temperature, ^{O}R

$T_{a,l}$ local value of cooling-air temperature, ^{O}R

T_f film temperature, arithmetic mean of bulk and shell tem-
                perature, ^{O}R

T_g bulk gas temperature, ^{O}R

T_s average shell temperature, ^{O}R

V_b flow velocity based on bulk temperature, ft/sec

W_a cooling-air flow, lb/sec

W_g combustion-gas flow, lb/sec

x distance from flameholder to station x, ft

y distance from upstream edge of porous wall, ft

μ_f absolute viscosity of gas at film temperature, lb/(ft)(sec)

ρ_f density of gas at film temperature, lb/cu ft

$(\rho U)_g$ total weight flow per unit of combustion chamber flow area
                   $(W_g + \Sigma W_a)/A_{g,y}$, lb/(sec)(sq ft)

$(\rho V)_a/(\rho U)_g$ coolant-flow ratio

Subscripts:

av   average

L   exhaust-nozzle inlet

l local

x   station x

0   flameholder

REFERENCES

1. Fleming, W. A., Conrad, E. William, and Young, A. W.: Experimental
   Investigation of Tail-Pipe-Burner Design Variables. NACA RM
   E50K22, 1951.

2. Nakanishi, S., Velie, W. W., and Bryant, L.: An Investigation of
   Effects of Flame-Holder Gutter Shape on Afterburner Performance.
   NACA RM E53J14, 1954.

3. Schulze, F. W., Bloomer, H. E., and Miller, R. R.: Altitude-Wind-
   Tunnel Investigation of Several Afterburner Configurations Having
   Moderately High Burner-Inlet Velocities. NACA RM E54G22, 1954.

4. Wood, Charles C., and Higgenbotham, James T.: Effects of Diffuser
   and Center-Body Length on Performance of Annular Diffusers with
   Constant-Diameter Outer Walls and with Vortex-Generator Flow Con-
   trols. NACA RM L54G21, 1954.

5. Ciepluch, Carl C., Velie, Wallace W., and Burley, Richard R.: A
   Low-Pressure-Loss Short Afterburner for Sea-Level Thrust Augmen-
   tation. NACA RM E55D26, 1955.

6. Wood, Charles C.: Preliminary Investigation of the Effects of Rec-
   tangular Vortex Generators on the Performance of a Short 1.9:1
   Straight-Wall Annular Diffuser. NACA RM L51G09, 1951.

7. Conrad, E. William, Schulze, Frederick W., and Usow, Karl H.: Effect
   of Diffuser Design, Diffuser-Exit Velocity Profile, and Fuel Dis-
   tribution on Altitude Performance of Several Afterburner Configura-
   tions. NACA RM E53A30, 1953.

8. Conrad, E. William, and Campbell, Carl E.: Altitude Wind Tunnel In-
   vestigation of High-Temperature Afterburners. NACA RM E51L07, 1952.

9. Patterson, G. N.: Modern Diffuser Design: Aircraft Eng., vol. x,
   no. 115, Sept. 1938, pp. 267-273.

10. Mallett, William E., and Harp, James L., Jr.: Performance Character-
    istics of Several Short Annular Diffusers for Turbojet Engine After-
    burners. NACA RM E54B09, 1954.

11. Braithwaite, Willis M., Walker, Curtis L., and Sivo, Joseph N.: Al-
    titude Evaluation of Several Afterburner Design Variables on a
    J47-GE-17 Turbojet Engine. NACA RM E53F10, 1953.

12. Gerrish, Harold C., Meem, J. Lawrence, Jr., Scadron, Marvin D., and
    Colnar, Anthony: The NACA Mixture Analyzer and Its Application to
    Mixture-Distribution Measurement in Flight. NACA TN 1238, 1947.

13. Jansen, Emmert T., Velie, Wallace W., and Wilsted, H. Dean: Experi-
    mental Investigation of the Effect of Fuel-Injection-System Design
    Variables on Afterburner Performance. NACA RM E53K16, 1954.

14. Longwell, John P., and Weiss, Malcolm A.: Mixing and Distribution
    of Liquids in High-Velocity Air Streams. Ind. and Eng. Chem.,
    vol. 45, no. 3, Mar. 1953, pp. 667-677.

15. Johnson, LaVern A., and Meyer, Carl L.: Altitude Performance Char-
    acteristics of Turbojet-Engine Tail-Pipe Burner with Variable-Area
    Exhaust Nozzle Using Several Fuel Systems and Flame Holders. NACA
    RM E50F28, 1950.

16. Trout, Arthur M., and Wentworth, Carl B.: Altitude Investigation
    of a 20-Inch Ram-Jet Combustor with a Rich Inner Zone of Combustion
    for Improved Low-Temperature-Ratio Operation. NACA RM E52L26, 1953.

17. Henzel, James G., Jr., and Wentworth, Carl B.: Free-Jet Investiga-
    tion of 20-Inch Ram-Jet Combustor Utilizing High-Heat-Release Pilot
    Burner. NACA RM E53H14, 1953.

18. Dangle, E. E., Friedman, Robert, and Cervenka, A. J.: Analytical
    and Experimental Studies of a Divided-Flow Ram-Jet Combustor.
    NACA RM E53K04, 1954.

3701

19. Huntley, S. C., Auble, Carmon M., and Useller, James W.: Altitude Performance Investigation of a High-Temperature Afterburner. NACA RM E53D22, 1953.

20. Chelko, Louis J.: Penetration of Liquid Jets into a High-Velocity Air Stream. NACA RM E50F21, 1950.

21. Callaghan, Edmund E., and Ruggeri, Robert S.: Investigation of the Penetration of an Air Jet Directed Perpendicularly to an Air Stream. NACA TN 1615, 1948.

22. Huntley, S. C., and Wilsted, H. D.: Altitude Performance Investigation of Two Flame-Holder and Fuel-System Configurations in Short Afterburner. NACA RM E52B25, 1952.

23. Nicholson, H. M., and Field, J. P.: Some Experimental Techniques for the Investigation of the Mechanism of Flame Stabilization in the Wakes of Bluff Bodies. Third Symposium on Combustion and Flame and Explosion Phenomena, The Williams & Wilkins Co. (Baltimore), 1949, pp. 44-68.

24. Williams, Glenn C.: Basic Studies on Flame Stabilization. Jour. Aero., Sci., vol. 16, no. 12, Dec. 1949, pp. 714-722.

25. Younger, George G., Gabriel, David S., and Mickelsen, William R.: Experimental Study of Isothermal Wake-Flow Characteristics of Various Flame-Holder Shapes. NACA RM E51K07, 1952.

26. Renas, Paul E., and Jansen, Emmert T.: Effect of Flame-Holder Design on Altitude Performance of Louvered-Liner Afterburner. NACA RM E53H15, 1953.

27. Henzel, James G., Jr., and Bryant, Lively: Investigation of Effect of Number and Width of Annular Flame-Holder Gutters on Afterburner Performance. NACA RM E54C30, 1954.

28. Lundin, Bruce T., Dowman, Harry W., and Gabriel, David S.: Experimental Investigation of Thrust Augmentation of a Turbojet Engine at Zero Ram by Means of Tail-Pipe Burning. NACA RM E6J21, 1947.

29. Braithwaite, Willis M., Renas, Paul E., and Jansen, Emmert T.: Altitude Investigation of Three Flame-Holder and Fuel-Systems Configurations in a Short Converging Afterburner on a Turbojet Engine. NACA RM E52G29, 1952.

30. Hawthorne, W. R., and Cohen, H.: Pressure Losses and Velocity Changes Due to Heat Release and Mixing in Frictionless, Compressible Flow. Rep. No. E.3997, British R.A.E., Jan. 1944.

31. Sterbentz, William H.:   Analysis and Experimental Observation of
    Pressure Losses in Ram-Jet Combustion Chambers.   NACA RM E9H19,
    1949.

32. Useller, James W., Braithwaite, Willis M., and Rudey, Carl J.:   In-
    fluence of Combustion-Chamber Length on Afterburner Performance.
    NACA RM E54E06, 1954.

33. Harp, James L., Jr., Velie, Wallace W., and Bryant, Lively: Inves-
    tigation of Combustion Screech and a Method of Its Control.   NACA
    RM E53L24b, 1954.

34. Lewis Laboratory Staff.   A Summary of Preliminary Investigations
    into the Characteristics of Combustion Screech in Ducted Burners.
    NACA RM E54B02, 1954.

35. Bragdon, Thomas A., Lewis, George D., and King, Charles H.:   In-
    terim Report on Experimental Investigation of High Frequency Os-
    cillations in Ramjet Combustion Chambers.   M.I.T. Meteor Rep.
    UAC-53, Res. Dept., United Aircraft Corp., Oct. 1951.   (BuOrd
    Contract NOrd 9845.)

36. Newton, R. T., and Truman, J. C.:   An Approach to the Problem of
    Screech in Ducted Burners.   General Eng. Lab., General Electric
    Co., Schenectady (N.Y.), Mar. 12, 1954.

37. Renas, P. E., Harvey, R. W., Sr., and Jansen, E. T.:   Altitude
    Starting Characteristics of an Afterburner with Autoignition
    and Hot-Streak Ignition.   NACA RM E53B02, 1953.

38. Thorman, H. Carl, and Campbell, Carl E.:   Altitude-Wind-Tunnel In-
    vestigation of Tail-Pipe Burner with Converging Conical Burner
    Section on J35-A-5 Turbojet Engine.   NACA RM E9I16, 1950.

39. Conrad, E. William, Bloomer, Harry E., and Sobolewski, Adam E.:   Al-
    titude Operational Characteristics of a Prototype Model of the J47D
    (RX1-1 and RX1-3) Turbojet Engines with Integrated Electronic Con-
    trol.   NACA RM E51E08, 1952.

40. Hall, Eldon W., and Wilcox, E. Clinton: Theoretical Comparison of
    Several Methods of Thrust Augmentation for Turbojet Engines.   NACA
    Rep. 992, 1950.   (Supersedes NACA RM E8H11.)

41. Useller, James W., and Povolny, John H.:   Experimental Investigation
    of Turbojet-Engine Thrust Augmentation by Combined Compressor Cool-
    ant Injection and Tail-Pipe Burning.   NACA RM E51H16, 1951.

3701
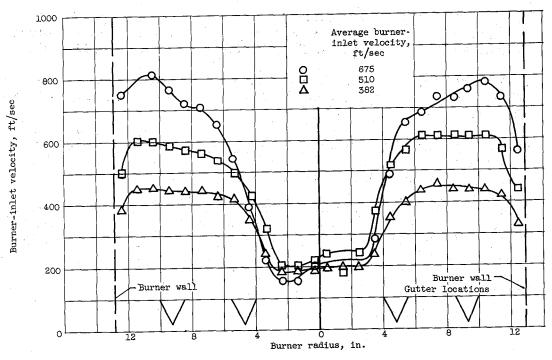
42. Useller, James W., Harp, James L., Jr., and Fenn, David B.:
    Turbojet-Engine Thrust Augmentation at Altitude by Combined
    Ammonia Injection into the Compressor Inlet and Afterburning.
    NACA RM E52L19, 1953.

43. Kapp, N. M., Snow, B., and Wohl, K.: The Effect of Water Vapor on
    the Normal Burning Velocity and on the Stability of Butane-Air
    Flames Burning above Tubes in Free Air. Meteor Rep. UAC-30,
    United Aircraft Corp., Nov. 1948. (U.S. Navy, BuOrd Contract
    NOrd 9845 with M.I.T.)

44. Tower, Leonard K.: Effect of Water Vapor on Combustion of
    Magnesium-Hydrocarbon Slurry Fuels in Small-Scale Afterburner.
    NACA RM E52H25, 1952.

45. Pinkel, I. Irving: Determination of Ram-Jet Combustion-Chamber
    Temperatures by Means of Total-Pressure Surveys. NACA TN 2526,
    1952. (Supersedes NACA RM E7C03.)

46. Koffel, William K., and Kaufman, Harold R.: Empirical Cooling Cor-
    relation for an Experimental Afterburner with an Annular Cooling
    Passage. NACA RM E52C13, 1952.

47. Koffel, William K., and Kaufman, Harold R.: Cooling Characteris-
    tics of an Experimental Tail-Pipe Burner with an Annular Cooling-
    Air Passage. NACA RM E51K23, 1952.

48. Conrad, E. William, and Jansen, Emmert T.: Effects of Internal
    Configuration on Afterburner Shell Temperatures. NACA RM E51I07,
    1952.

49. Bennett, I. G.: Suppression of Radiation at High Temperatures by
    Means of Ceramic Coatings. Jour. Am. Ceramic Soc., vol. 30, no.
    10, Oct. 1, 1947, pp. 297-305.

50. Koffel, William K., and Kaufman, Harold R.: Investigation of Heat-
    Transfer Coefficients in an Afterburner. NACA RM E52D11, 1952.

51. Humble, Leroy V., Lowdermilk, Warren H., and Desmon, Leland G.:
    Measurements of Average Heat-Transfer and Friction Coefficients
    for Subsonic Flow of Air in Smooth Tubes at High Surface and
    Fluid Temperatures. NACA Rep. 1020, 1951. (Supersedes NACA
    RM's E7L31, E8L03, E50E23, and E50H23.)

52. Wallner, Lewis E., and Jansen, Emmert T.: Full-Scale Investigation
    of Cooling Shroud and Ejector Nozzle for a Turbojet Engine -
    Afterburner Installation. NACA RM E51J04, 1951.
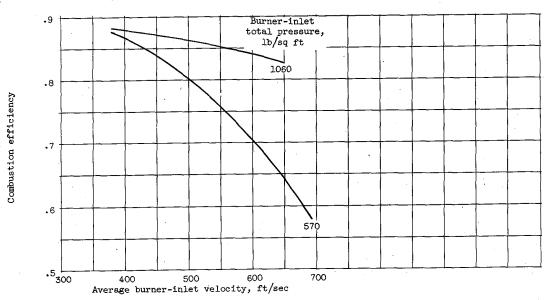
53. Koffel, William K.: Preliminary Experimental Investigation of
    Transpiration Cooling for an Afterburner with a Sintered, Porous
    Stainless-Steel Combustion-Chamber Wall. NACA RM E53D08, 1953.

54. Koffel, William K.: Air-Flow Characteristics of Brazed and Rolled
    Wire Filter Cloth for Transpiration-Cooled Afterburners. NACA RM
    E53H24, 1953.

55. Koffel, William K.: Cooling Characteristics of a Transpiration-
    Cooled Afterburner with a Porous Wall of Brazed and Rolled Wire
    Cloth. NACA RM E54E25, 1954.

56. Rannie, W. D.: A Simplified Theory of Porous Wall Cooling. Prog.
    Rep. 4-50, Power Plant Lab., Jet Prop. Lab., C.I.T., Nov. 24,
    1947. (AMC Contract No. W-535-ac-20260, Ord. Dept. Contract No.
    W-04-200-ORD-455.)

57. Friedman, Joseph: A Theoretical and Experimental Investigation of
    Rocket-Motor Sweat Cooling. Jour. Am. Rocket Soc., no. 79, Dec.
    1949, pp. 147-154.

3701

CU-11 back

3701

(a) Velocity profiles.

(b) Combustion efficiency at fuel-air ratio of 0.047.

Figure 1. - Effect of velocity in region of flameholders on afterburner performance.
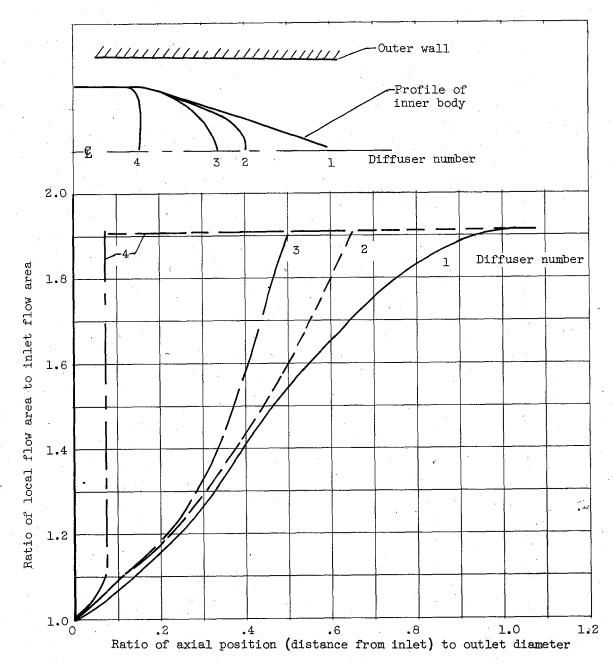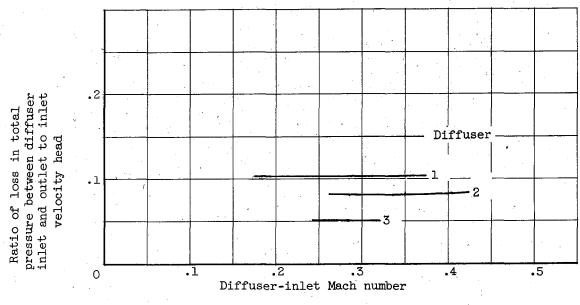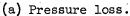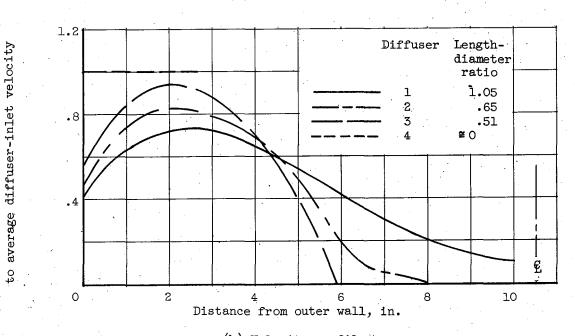
Figure 2. - Geometric relations of diffusers investigated to determine length effects.

CONFIDENTIAL

3701

(a) Pressure loss.

(b) Velocity profile.

Figure 3. - Performance of four diffusers of different length.
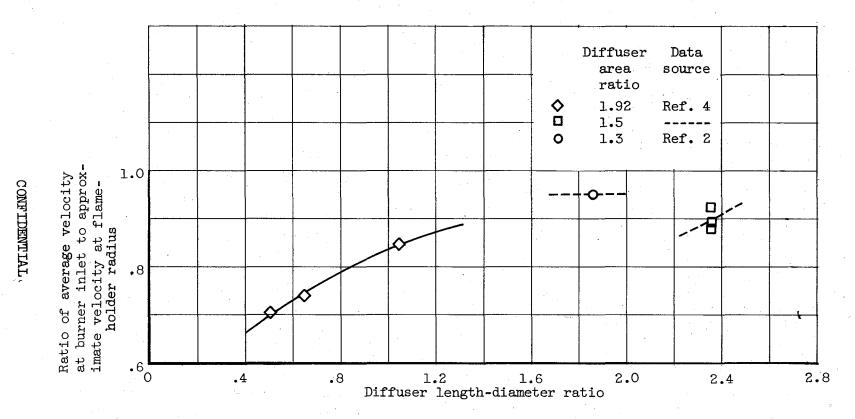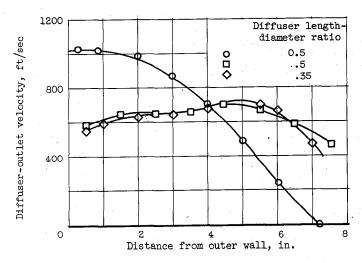
Figure 4. - Effect of diffuser length-diameter ratio on velocity near flameholder.

3701

(a) Velocity profiles.

(b) Pressure loss.
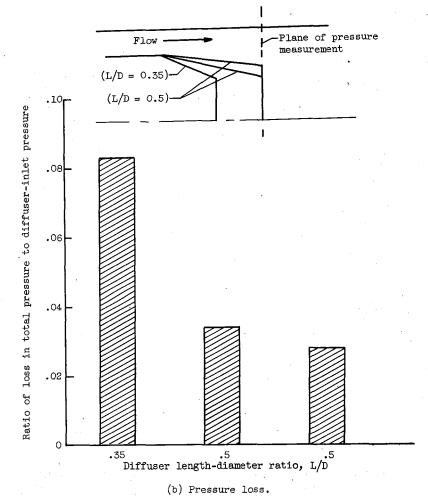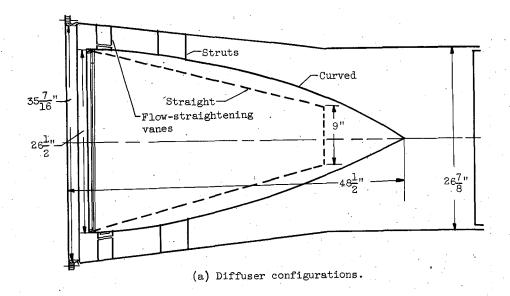
Figure 5. - Effect of length on diffuser performance.

(a) Diffuser configurations.

(b) Diffuser area variation.
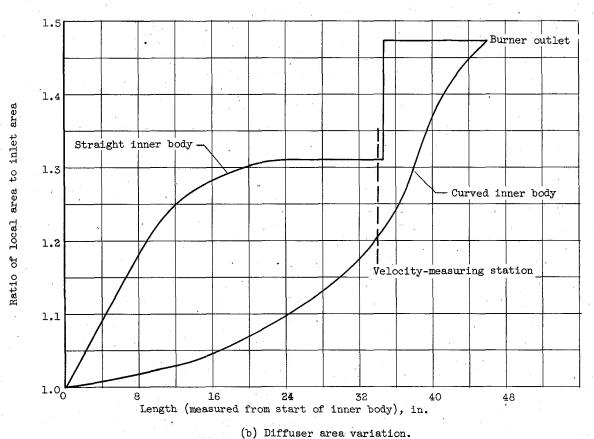
Figure 6. - Diffusers used in investigation of inner-body shape.

Figure 7. - Radial velocity profiles 34 inches from diffuser inlet with two inner-body shapes.

3701

Outer wall

1"

$7\frac{1}{4}$"

$10\frac{1}{2}$"

$26\frac{1}{2}$"

Profile sketch of diffuser 1 with vortex generators

1.2

———— Without vortex generators
- - - - - With vortex generators

.8

.4

0

(a) Diffuser 1.

Outer wall

1"

$7\frac{1}{4}$"

$10\frac{1}{2}$"

$14\frac{5}{8}$"

Profile sketch of diffuser 2 with vortex generators

1.2

.8

.4

Ratio of local velocity to average diffuser-inlet velocity

0   2   4   6   8   10

Distance from outer wall, in.

(b) Diffuser 2.
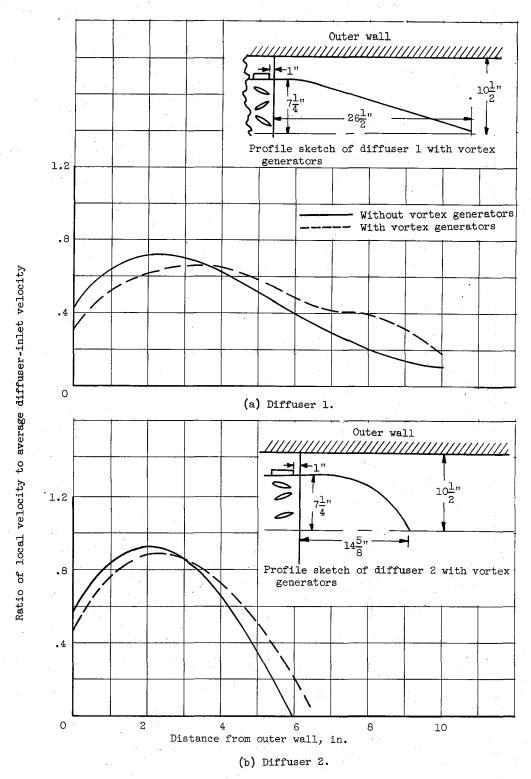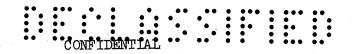
Figure 8. - Effect of vortex generators on diffuser-outlet velocity profiles.

DECLASSIFIED

CU-12 back   3701
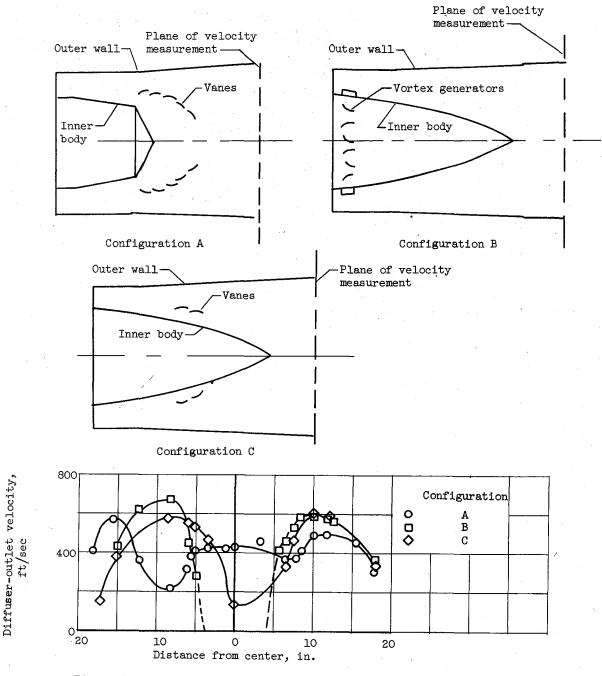
Figure 9. - Effect of annular vanes on diffuser-outlet velocity profiles.
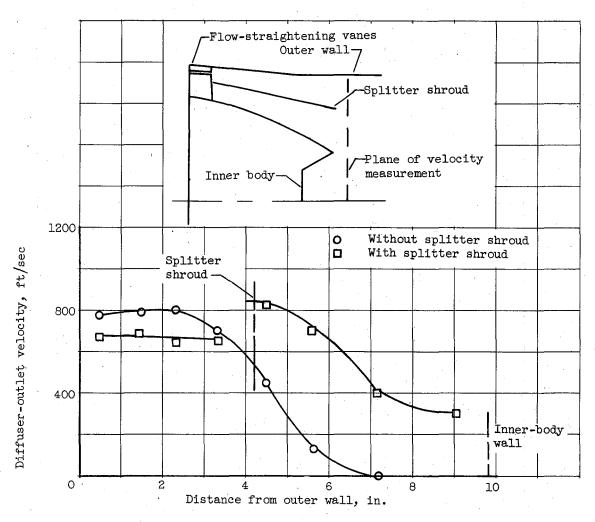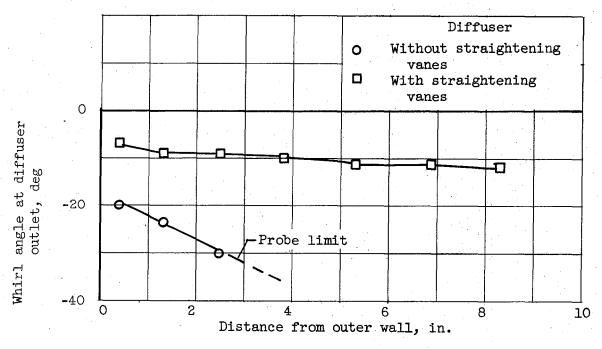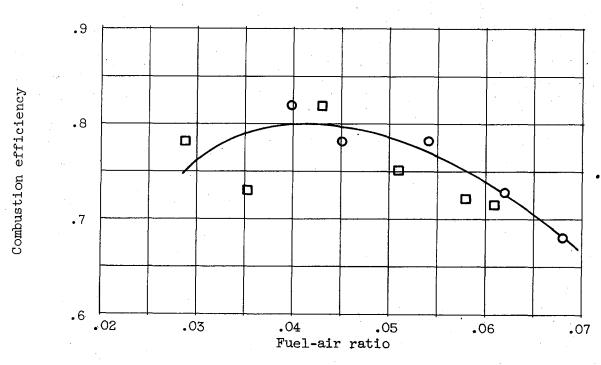
Figure 10. - Effect of splitter shroud on diffuser-outlet velocity profile.

DECLASSIFIED

3701

(a) Representative diffuser-outlet whirl angles.

(b) Effect of diffuser-outlet whirl on combustion efficiency at altitude.

Figure 11. - Effect of diffuser-outlet whirl on afterburner performance.
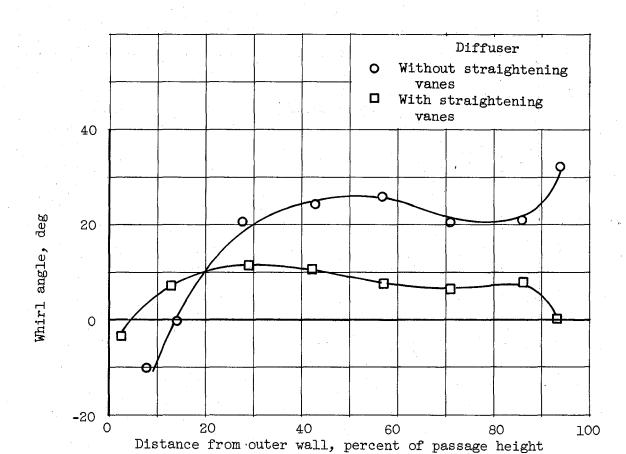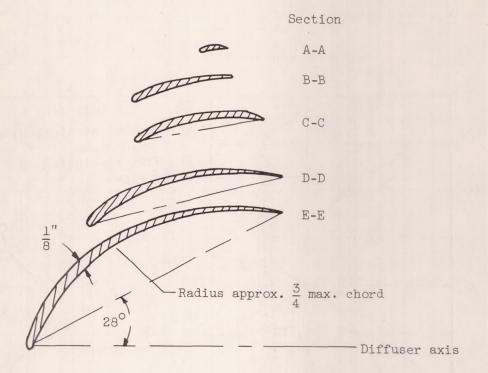
Figure 12. - Effect of straightening vanes on whirl angles near diffuser inlet.

Section

A-A

B-B

C-C

D-D

E-E

$\frac{1}{8}$"

Radius approx. $\frac{3}{4}$ max. chord

28°

Diffuser axis

A-A

B-B

Diffuser outer wall

C-C

D-D

E-E

Inner body

Max. chord

Elevation
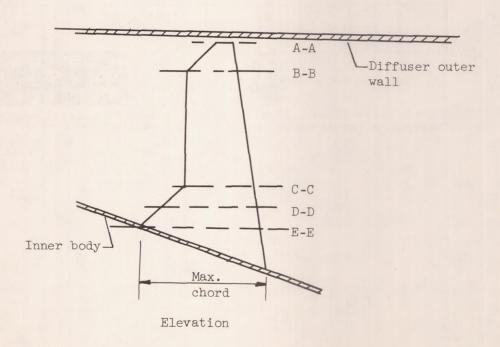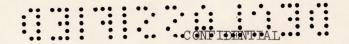
Figure 13. - Typical flow-straightening vane at turbine outlet.
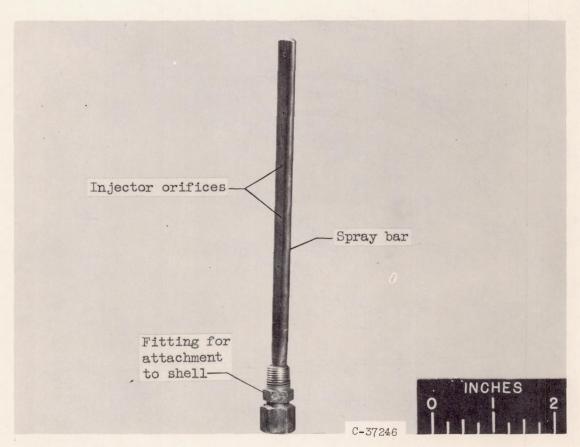
Figure 14. - Typical fuel-spray bar for full-scale afterburner.

C-39998
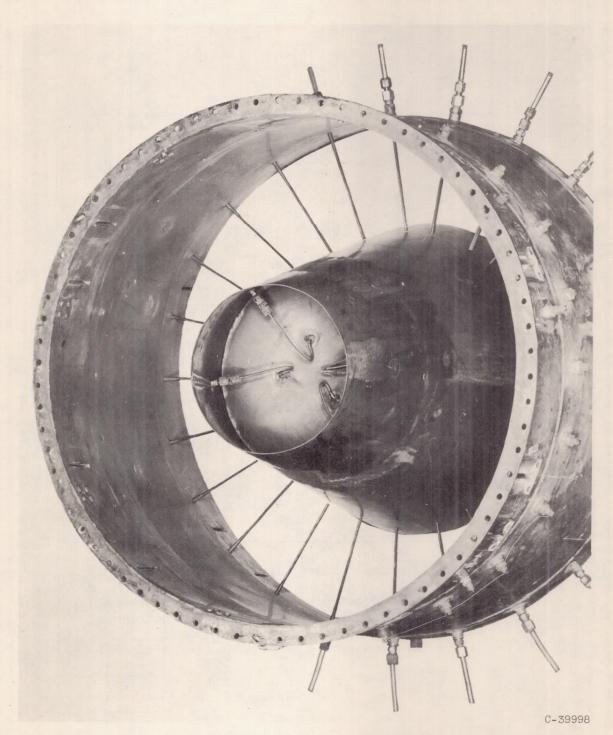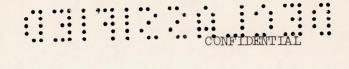
Figure 15. - Upstream view of spray-bar installation. Burner section removed.
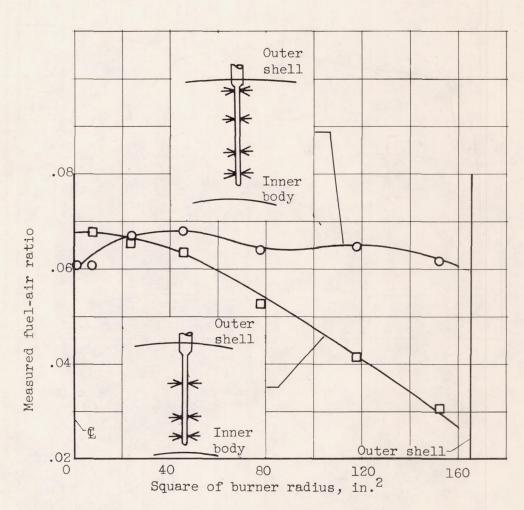
Figure 16. - Effect of spray-bar design on fuel-
air-ratio distribution 22.5 inches downstream
of spray bars. Transverse injection from 24
spray bars having 0.030-inch-diameter orifices.
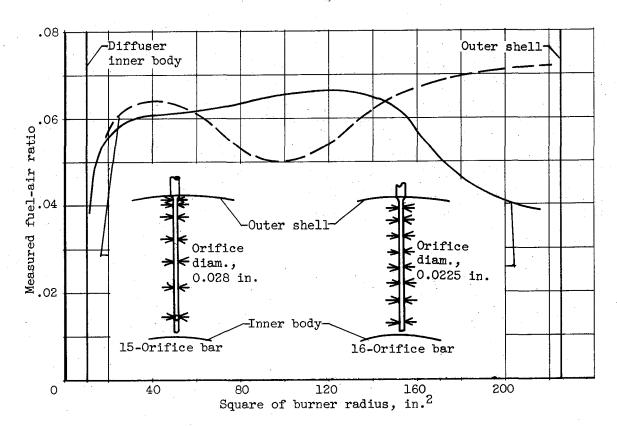
Figure 17. - Effect of radial location of fuel orifices on fuel-air-ratio distribution 15 inches downstream of spray bars. Transverse injection from 20 spray bars.
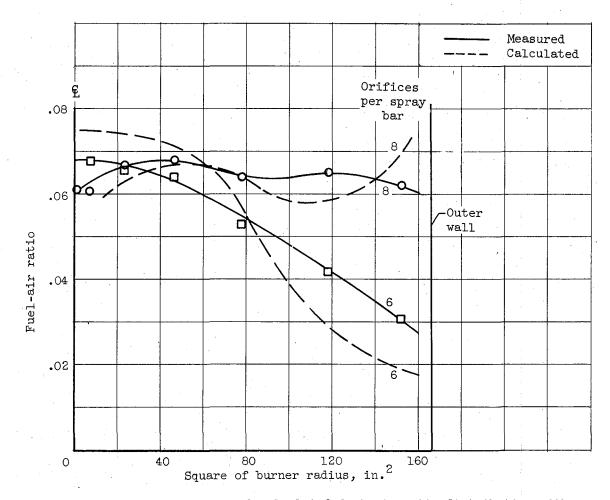
Figure 18. - Comparison of calculated fuel-air-ratio distribution with measured values from figure 16. Fuel mixing distance, 22.5 inches.
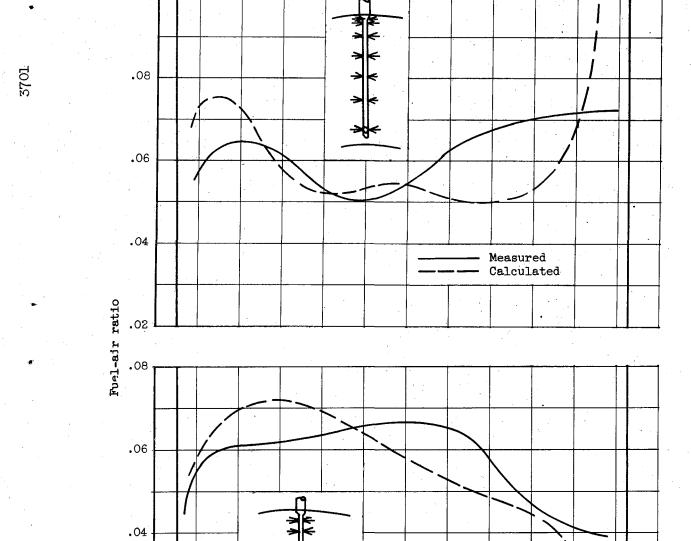
Figure 19. - Comparison of calculated fuel-air-ratio distribution with measured values of figure 17. Fuel mixing distance, 15 inches.

Figure 20. - Effect of radial fuel-air-ratio distribution on combustion efficiency.
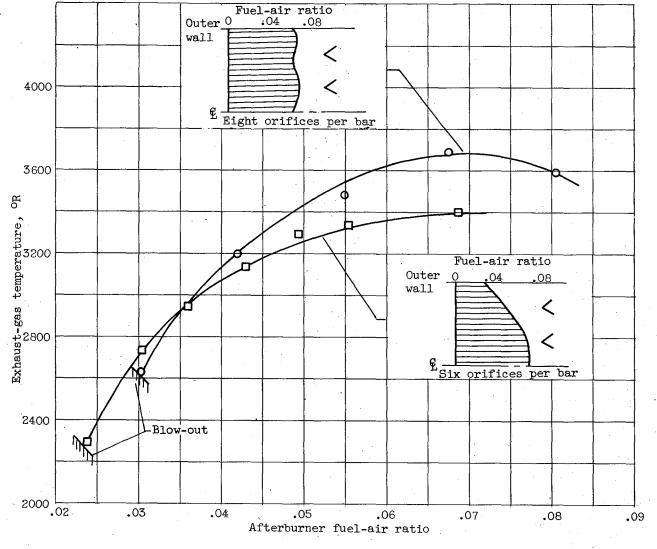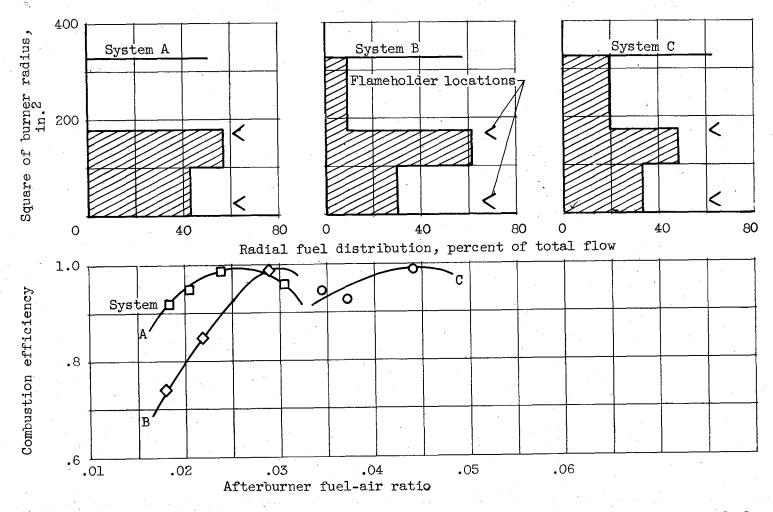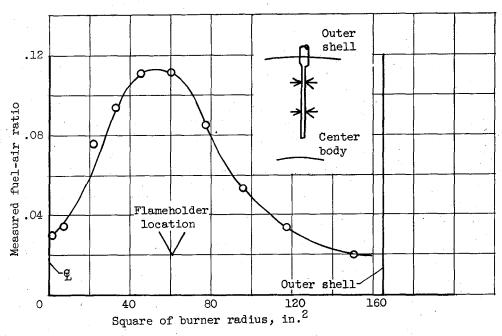
Figure 21. - Effect of radial fuel-air-ratio distribution on exhaust-gas temperature.
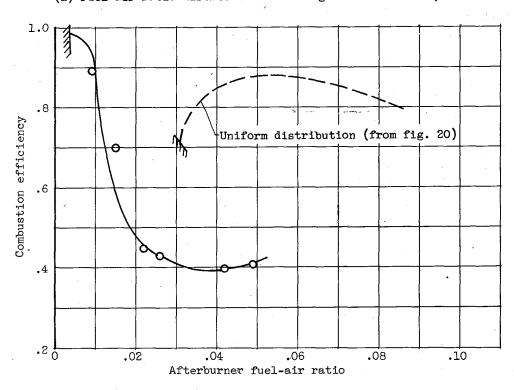
Figure 22. - Effect on combustion efficiency of varying radial distribution of fuel.

DECLASSIFIED

(a) Fuel-air-ratio distribution. Average fuel-air ratio, 0.055.

Measured fuel-air ratio

.12

.08

.04

Outer shell

Center body

Flameholder location

Outer shell

0   40   80   120   160

Square of burner radius, in.^{2}

(b) Combustion efficiency.

Combustion efficiency

1.0

.8

.6

.4

.2

Uniform distribution (from fig. 20)

0   .02   .04   .06   .08   .10

Afterburner fuel-air ratio

Figure 23. - Combustion performance of afterburner with locally rich fuel injection. Transverse fuel injection from 12 bars having four 0.030-inch-diameter orifices.

::: ::::: ::::: :::::::: CONFIDENTIAL ::::::::: NACA RM E55L12

3701
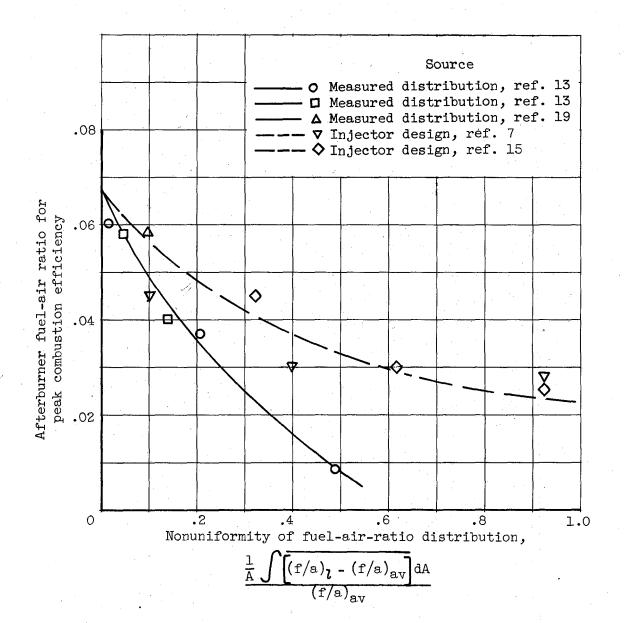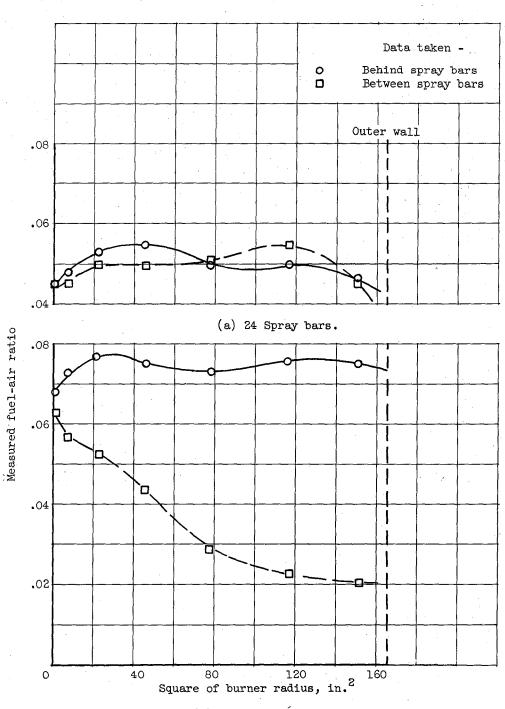
Figure 24. - Variation of fuel-air ratio at which peak combustion efficiency occurs with uniformity of fuel-air ratio distribution.

(a) 24 Spray bars.

(b) 12 Spray bars.

Figure 25. - Effect of number of spray bars on circumferential fuel-
air-ratio distribution. Transverse injection from eight 0.030-
inch-diameter orifices in each bar. Gas velocity, 500 to 600 feet
per second; burner diameter, 26 inches.
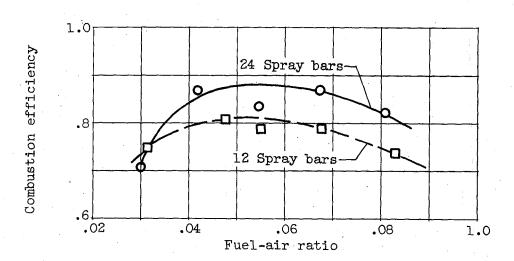
Figure 26. - Effect of number of spray bars on combustion efficiency. Transverse injection. Eight 0.030-inch-diameter orifices per spray bar; gas velocity, 500 to 600 feet per second.
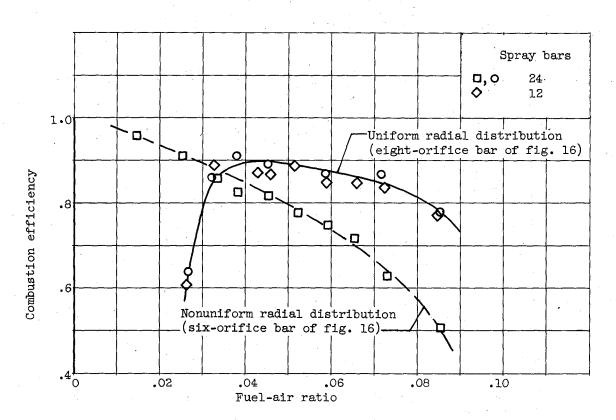
Figure 27. - Effect of radial and circumferential fuel-air-ratio distribution on combustion efficiency. Orifice diameter, 0.030 inch; burner-inlet velocity, 380 to 480 feet per second.

3701
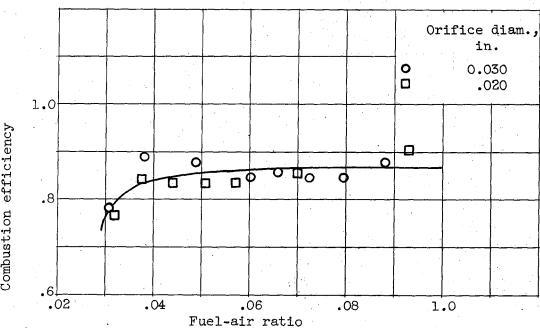
Figure 28. - Effect of spray-bar-orifice size on combustion
    efficiency. Transverse injection from 24 spray bars, each
    having eight orifices. Gas velocity, 500 to 600 feet per
    second; burner diameter, 26 inches.

(a) Exhaust-gas temperature.

(b) Combustion efficiency.
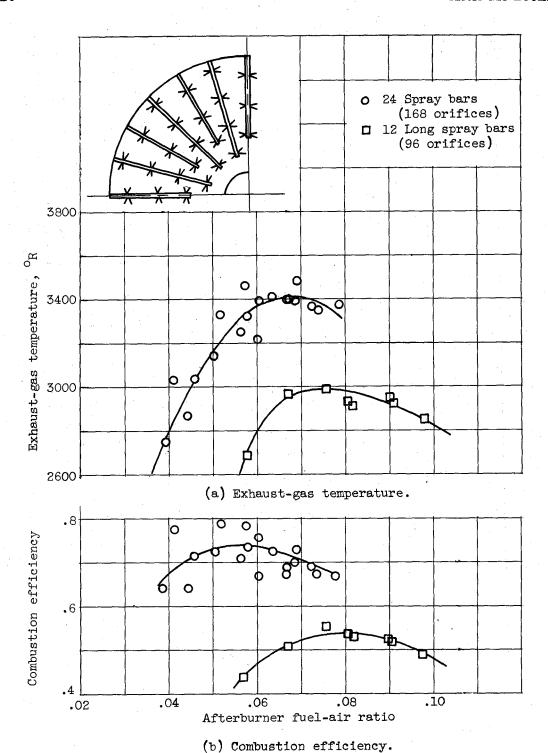
Figure 29. - Effect of number of fuel-spray bars on combustion efficiency and exhaust-gas temperature. Burner-inlet velocity, approximately 400 feet per second; diameter of transverse injection orifice, 0.020 inch.
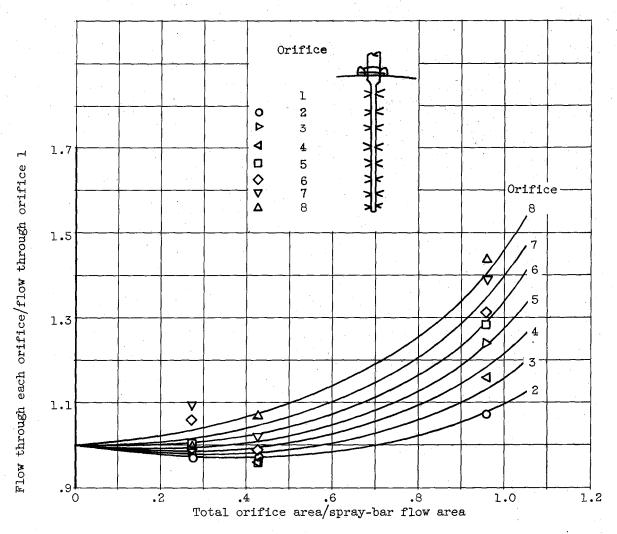
Figure 30. - Flow distribution among orifices of spray bars having various ratios of total orifice area to spray-bar flow area.
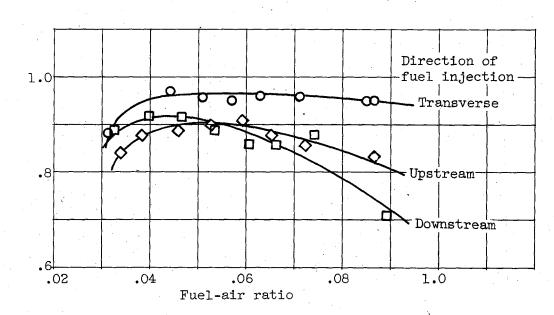
Figure 31. - Effect of direction of fuel injection on com-
bustion efficiency. Twenty-four fuel-spray bars with eight
orifices per bar; gas velocity, 460 to 540 feet per second;
burner-inlet pressure, 1060 to 1350 pounds per square foot
absolute.
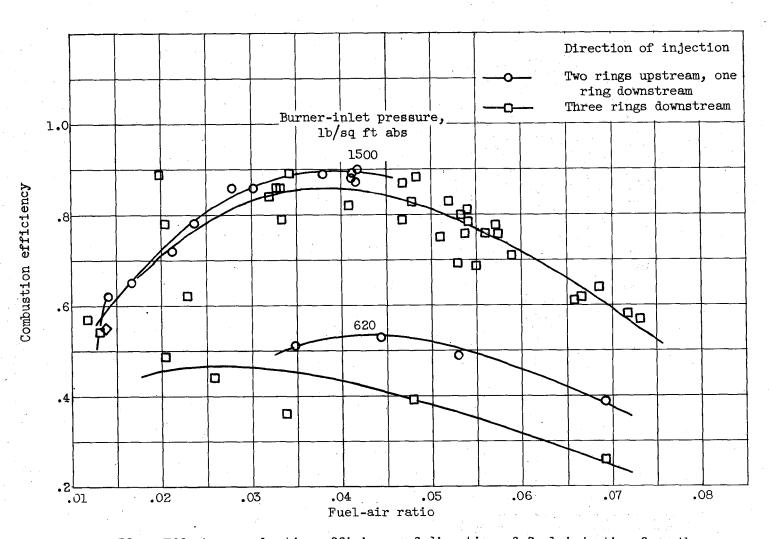
Figure 32. - Effect on combustion efficiency of direction of fuel injection from three con-
centric manifold rings. Orifice diameter, 0.041 inch; total number of fuel orifices, 144.

3701

Gutters

Interconnecting gutter

Section A-A   Downstream view
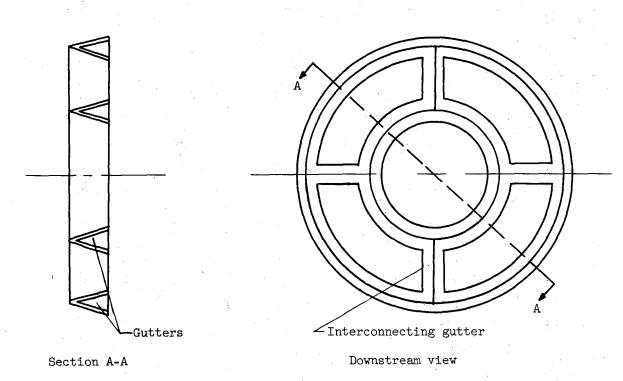
Figure 33. - Typical two-ring V-gutter flameholder.
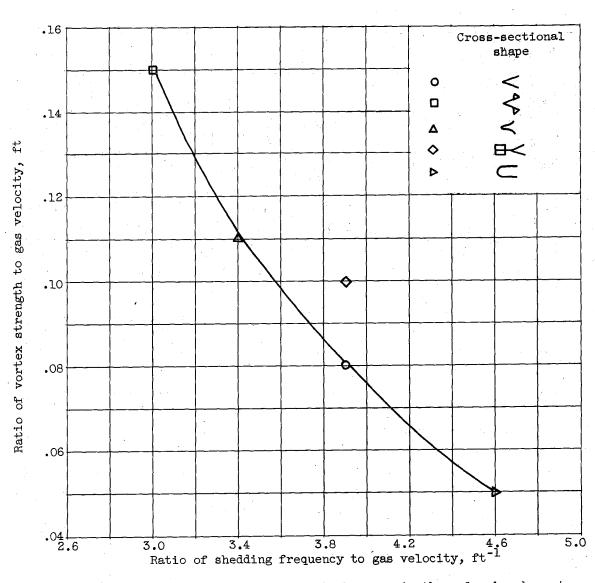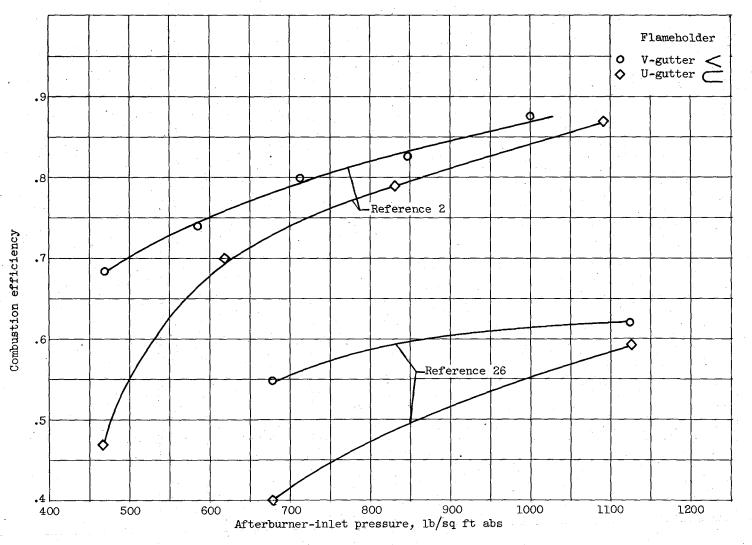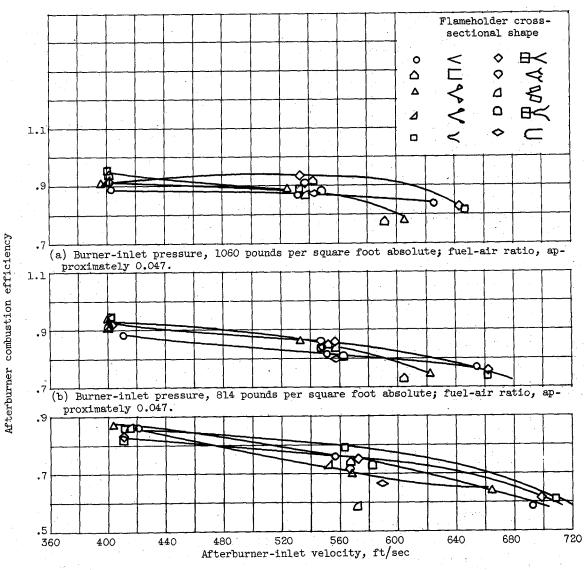
Figure 34. - Effect of cross-sectional shape on isothermal wake character-
istics. Gutter width, 3/4 inch.

Figure 35. - Effect of flameholder cross-sectional shape on afterburner combustion efficiency as function of afterburner-inlet pressure. Afterburner fuel-air ratio, approximately 0.045.

DECLASSIFIED

CONFIDENTIAL

Flameholder cross-
sectional shape

(a) Burner-inlet pressure, 1060 pounds per square foot absolute; fuel-air ratio, approximately 0.047.

(b) Burner-inlet pressure, 814 pounds per square foot absolute; fuel-air ratio, approximately 0.047.

Afterburner combustion efficiency

Afterburner-inlet velocity, ft/sec

(c) Burner-inlet pressure, 566 pounds per square foot absolute; fuel-air ratio, approximately, 0.047.

Figure 36. - Effect of flameholder cross-sectional shape on afterburner as function of afterburner-inlet velocity.

3701

(d) Burner-inlet pressure, 1060 pounds per square foot absolute, fuel-air ratio, approximately 0.067.

(e) Burner-inlet pressure, 814 pounds per square foot absolute, fuel-air ratio, approximately 0.067.

(f) Burner-inlet pressure, 566 pounds per square foot absolute; fuel-air ratio, approximately 0.067.
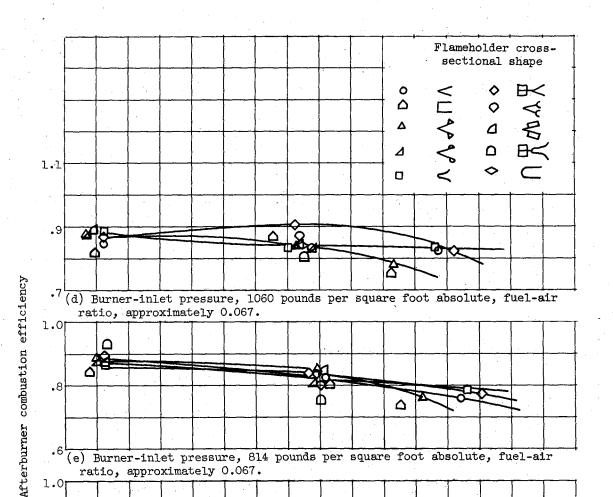
Figure 36. - Concluded. Effect of flameholder cross-sectional shape on afterburner as function of afterburner-inlet velocity.
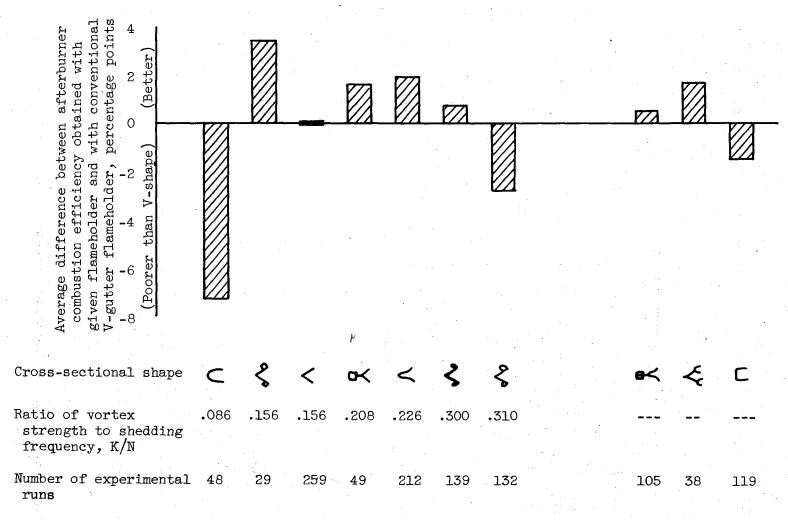
Figure 37. - Average difference in afterburner combustion efficiency obtained with various flameholder shapes.

(a) Engine afterburner tests (ref. 26).

(b) Simulated afterburner facility (ref. 2).
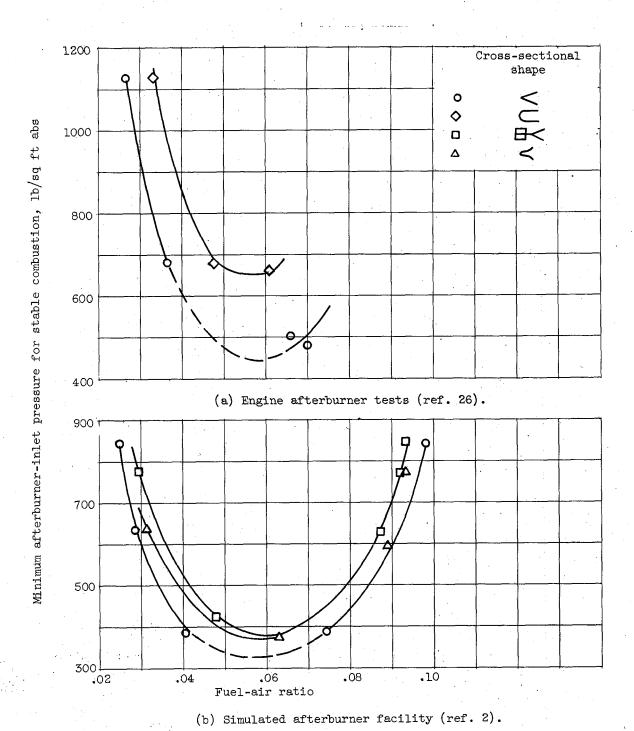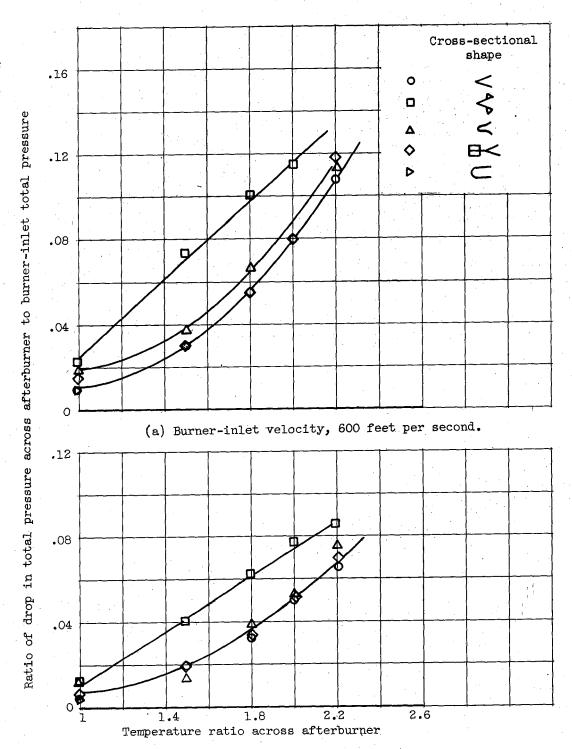
Figure 38. - Effect of flameholder cross-sectional shape on blow-out limits.

3701

CU-16

(a) Burner-inlet velocity, 600 feet per second.
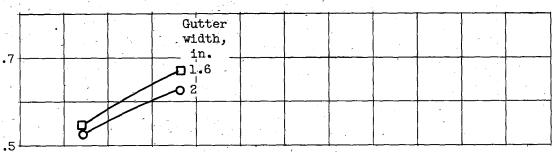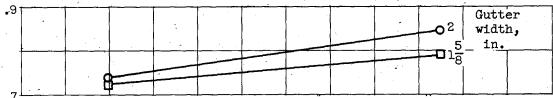
(b) Burner-inlet velocity, 500 feet per second.

Figure 39. - Effect of flameholder cross-sectional shape on after-
burner pressure loss. Blockage, 29 percent.
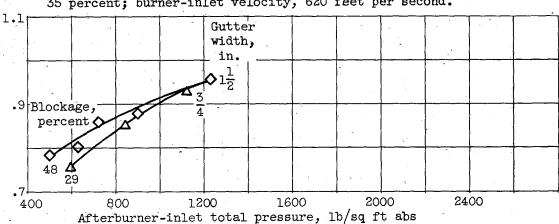
(a) Fuel-area ratio, 0.04; two-ring flameholder; blockage, 27 percent; burner-inlet velocity, 450 feet per second.
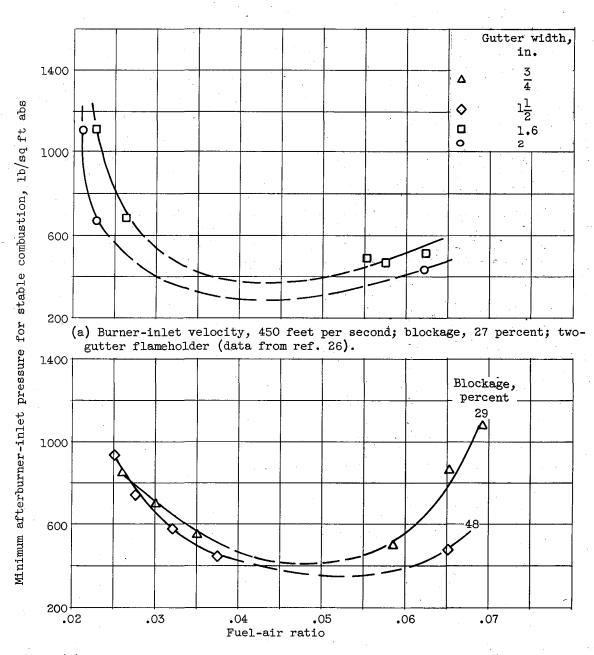
(b) Fuel-area ratio, 0.04; two-ring flameholder; blockage, 35 percent; burner-inlet velocity, 620 feet per second.

(c) Fuel-air ratio, 0.05; three-ring flameholder; burner-inlet, velocity, 520 feet per second.

Figure 40. - Effect of flameholder V-gutter width on afterburner combustion efficiency.

(a) Burner-inlet velocity, 450 feet per second; blockage, 27 percent; two-gutter flameholder (data from ref. 26).

(b) Burner-inlet velocity, 520 feet per second; three-gutter flameholder (data from ref. 27).

Figure 41. - Effects of flameholder gutter width on afterburner blow-out limits.
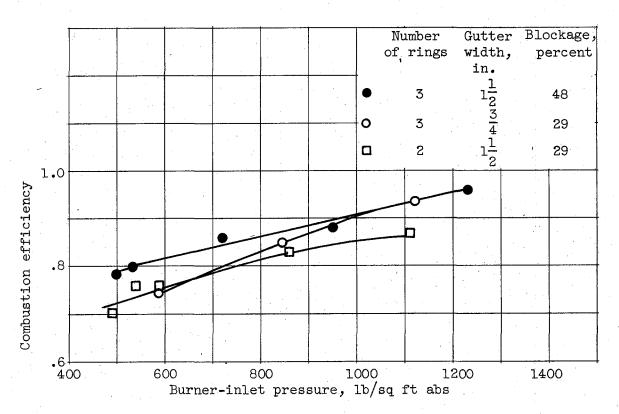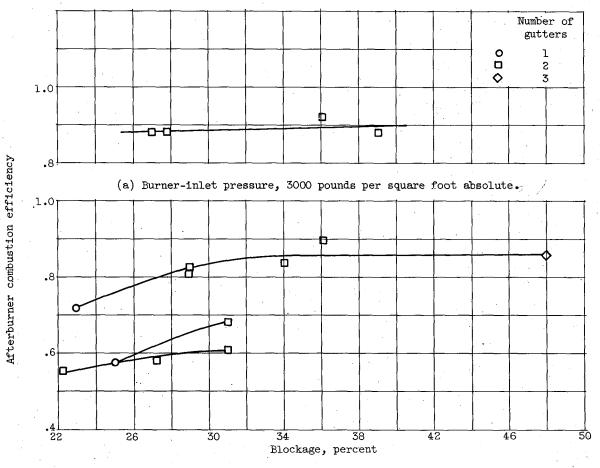
Figure 42. - Effect of number of gutters on afterburner combustion efficiency. Afterburner-inlet velocity, 520 feet per second; fuel-air ratio, 0.05.

(a) Burner-inlet pressure, 3000 pounds per square foot absolute.

(b) Burner-inlet pressure, 800 pounds per square foot absolute.

Figure 43. - Effect of blockage on afterburner combustion efficiency. Fuel-air ratio, between 0.04 and 0.05.
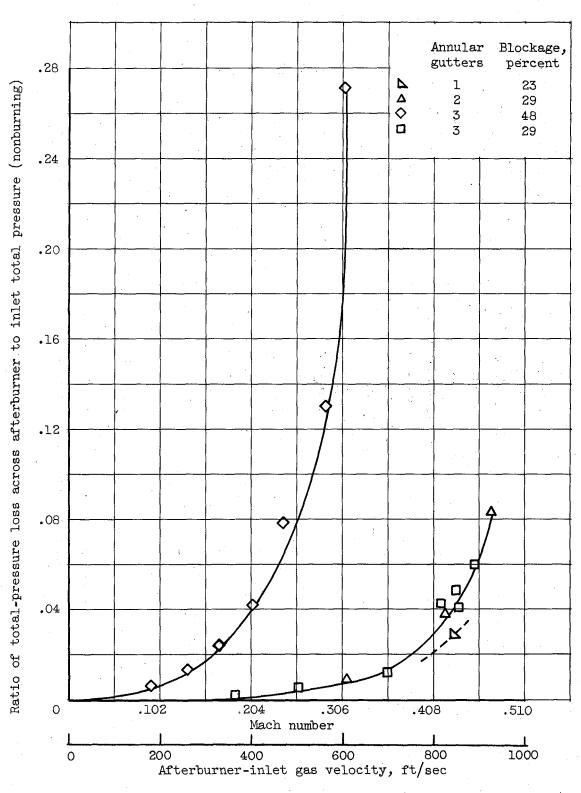
Figure 44. - Effect of afterburner-inlet gas velocity on nonburning total-pressure loss.
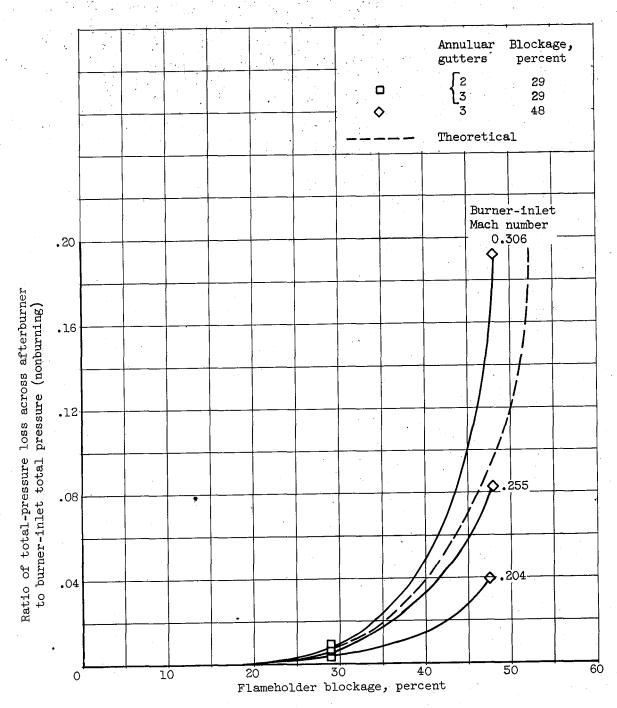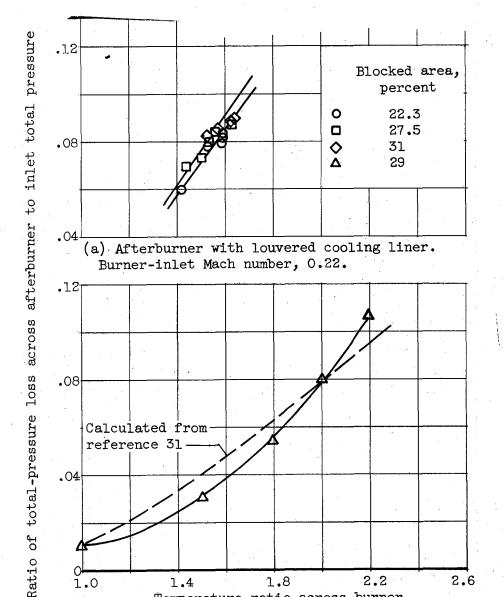
Figure 45. - Effect of flameholder blockage on nonburning total-pressure loss.

(a) Afterburner with louvered cooling liner. Burner-inlet Mach number, 0.22.

(b) Afterburner without cooling liner. Burner-inlet Mach number, approximately 0.30.

Figure 46. - Effect of temperature ratio and blocked area on pressure losses, with burning.
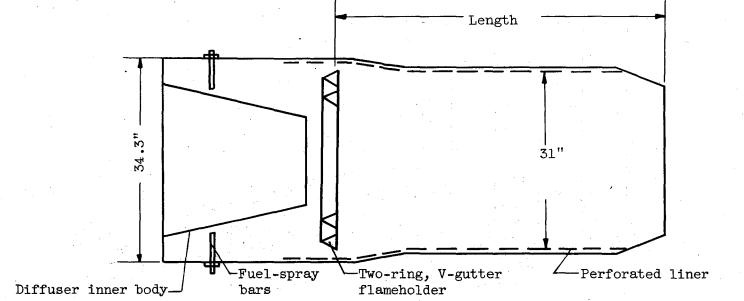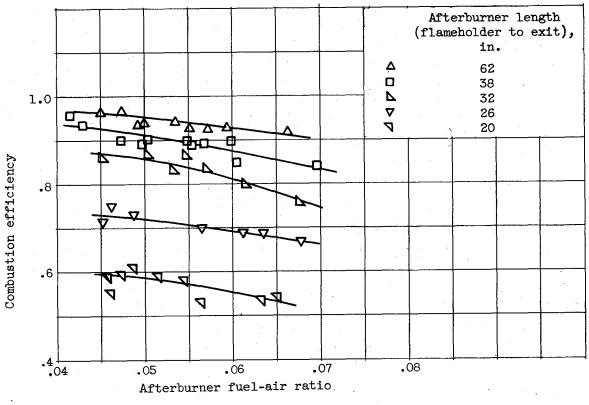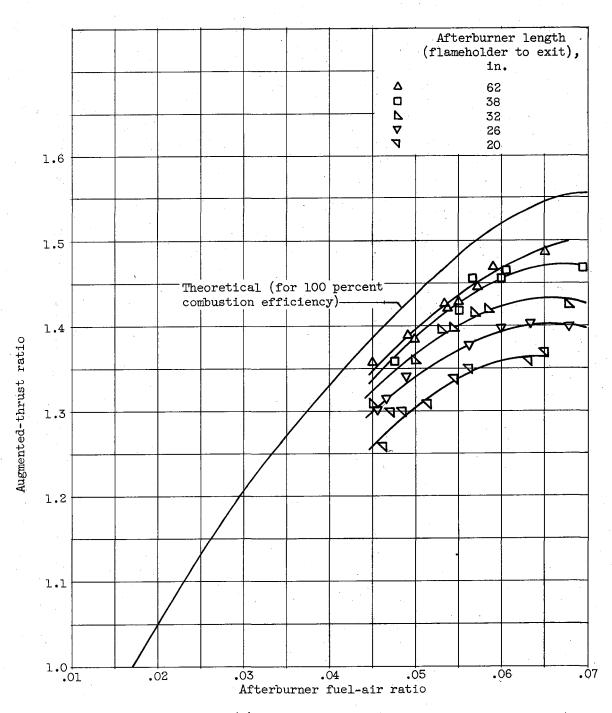
Figure 47. - Afterburner designed for take-off application.
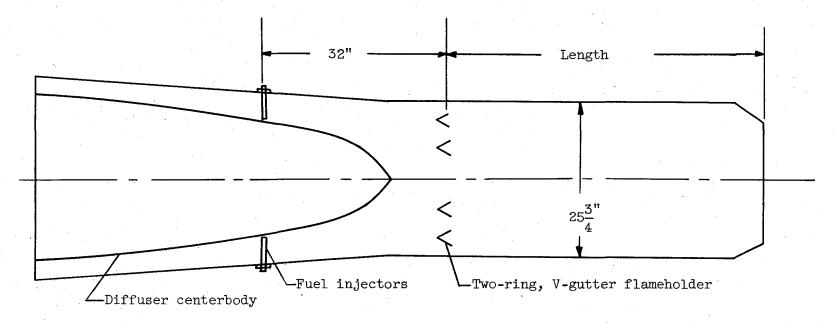
(a) Combustion efficiency.

Figure 48. - Effect of afterburner length on performance of take-off afterburner. Burner-inlet pressure, 3800 pounds per square foot absolute.
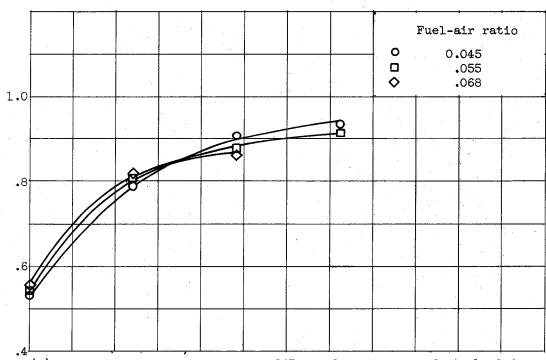
(b) Augmented-thrust ratio.

Figure 48. - Concluded. Effect of afterburner length on performance of
take-off afterburner. Burner-inlet pressure, 3800 pounds per square foot
absolute.
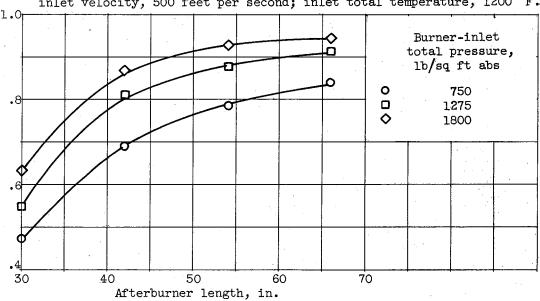
Figure 49. - Afterburner designed for high-altitude conditions.

3701

Combustion efficiency
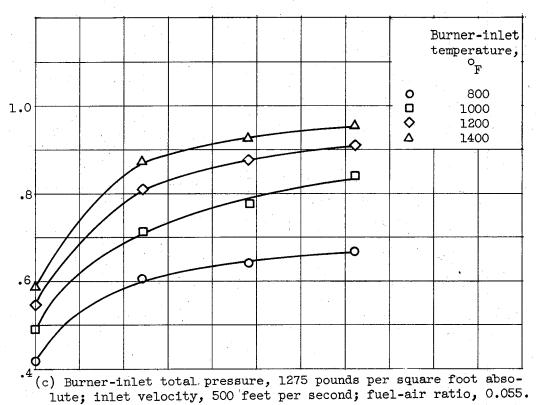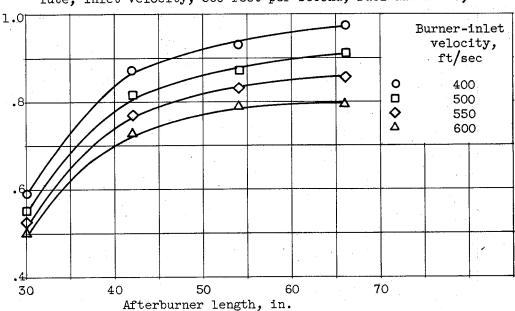
(a) Burner-inlet total pressure, 1275 pounds per square foot absolute; inlet velocity, 500 feet per second; inlet total temperature, 1200° F.

Afterburner length, in.

(b) Burner-inlet velocity, 500 feet per second; inlet temperature, 1200° F; fuel-air ratio, 0.055.
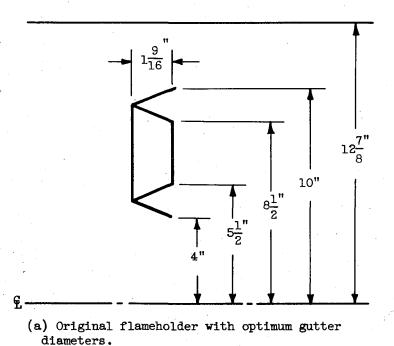
Figure 50. - Effect of afterburner length on performance of high-altitude afterburner.
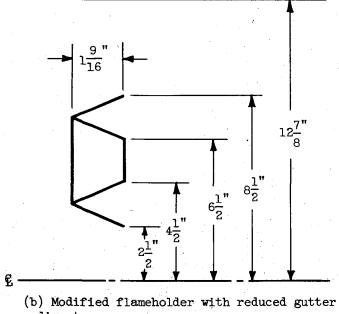
CONFIDENTIAL

(c) Burner-inlet total pressure, 1275 pounds per square foot absolute; inlet velocity, 500 feet per second; fuel-air ratio, 0.055.

(d) Burner-inlet total pressure, 1275 pounds per square foot absolute; inlet temperature, 1200° F; fuel-air ratio, 0.055.

Figure 50. - Concluded. Effect of afterburner length on performance of high-altitude afterburner.

(a) Original flameholder with optimum gutter diameters.
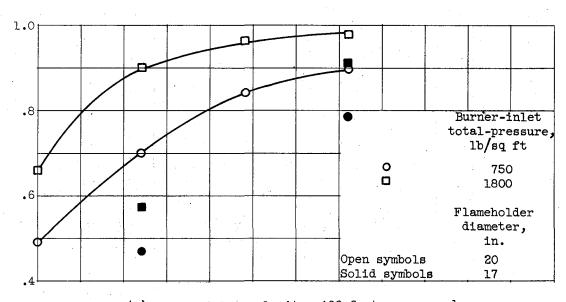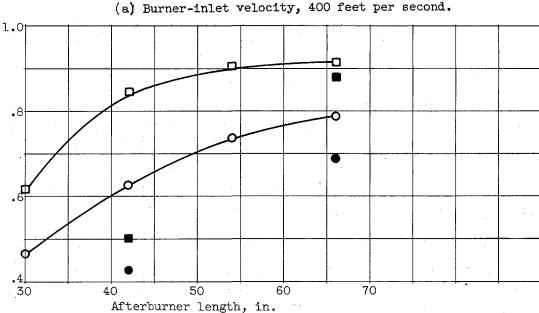
(b) Modified flameholder with reduced gutter diameters.

Figure 51. - Comparison of flameholders with optimum and reduced gutter diameters.

CONFIDENTIAL

Combustion efficiency

Burner-inlet
total-pressure,
lb/sq ft

O	750
□	1800

Flameholder
diameter,
in.

Open symbols   20
Solid symbols   17

(a) Burner-inlet velocity, 400 feet per second.

Afterburner length, in.

(b) Burner-inlet velocity, 550 feet per second.

Figure 52. - Effect of reduced flameholder-gutter diameter on combustion
efficiency. Burner-inlet total temperature, 1200° F; fuel-air ratio,
0.055.
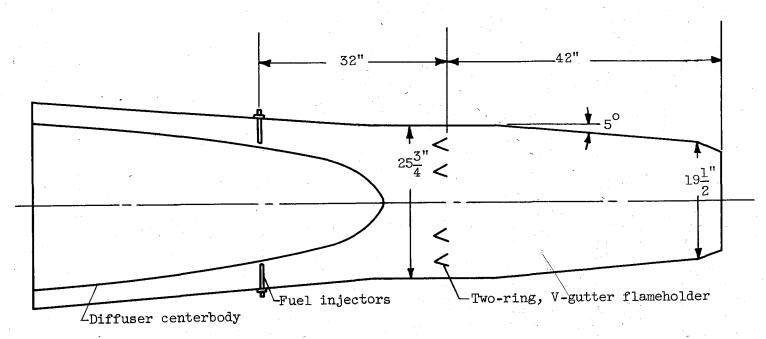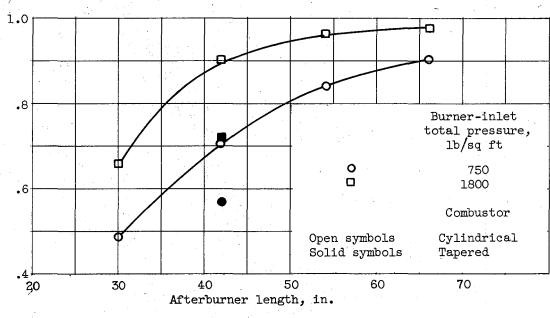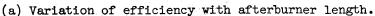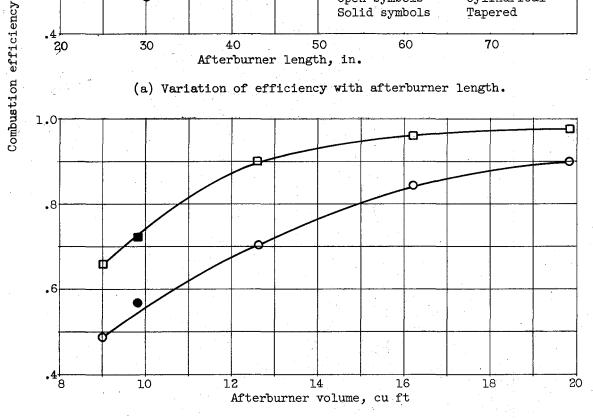
Figure 53. - Tapered afterburner designed for high-altitude operation.

3701

(a) Variation of efficiency with afterburner length.

(b) Variation of efficiency with afterburner volume.

Figure 54. - Effect of afterburner-shell taper on combustion efficiency.
Burner-inlet velocity, 400 feet per second; inlet total temperature,
1200° F; fuel-air ratio, 0.055.
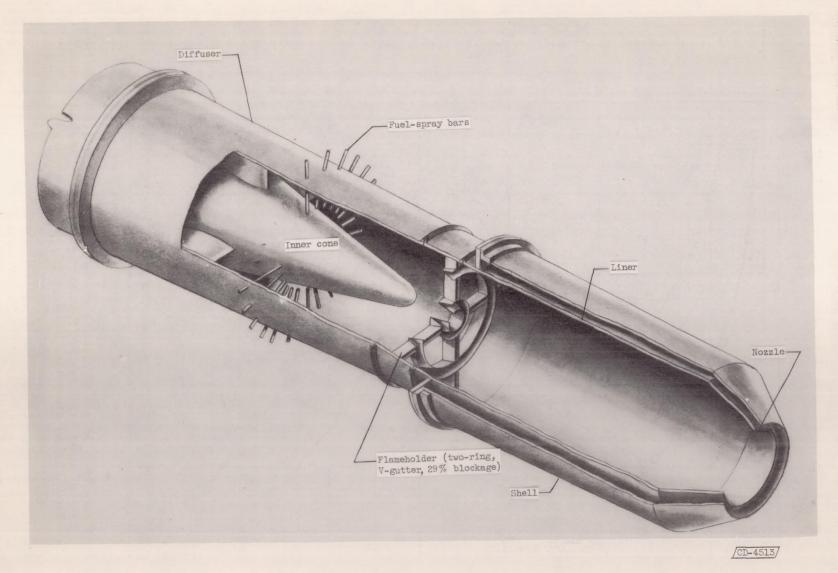
Figure 55. - Cutaway view of afterburner.
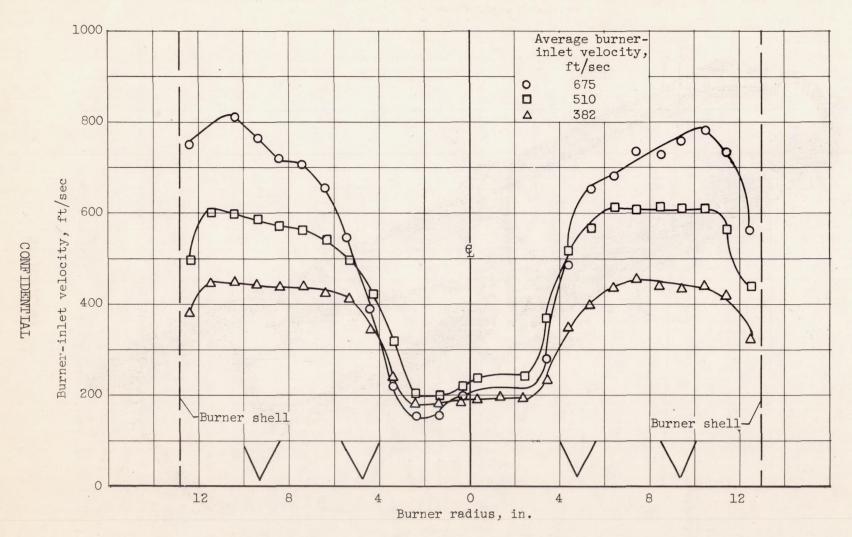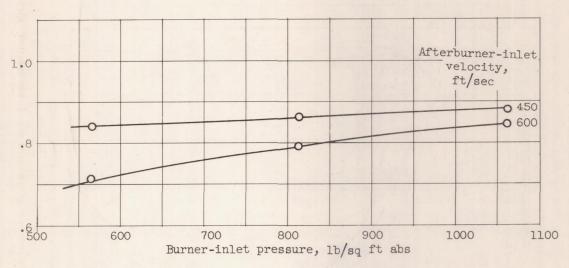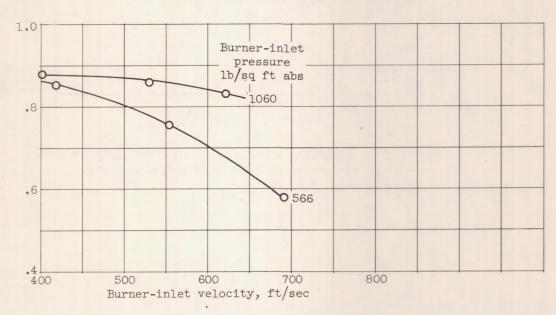
Figure 56. - Velocity profile at burner inlet showing relative location of flameholder gutters.

DECLASSIFIED

(a) Effect of burner-inlet pressure.

(b) Effect of burner-inlet velocity.

Figure 57. - Effect of inlet pressure and inlet velocity on combustion
    efficiency of afterburner. Blockage, 30 percent; V-gutter flameholder;
    fuel-air ratio, 0.047.
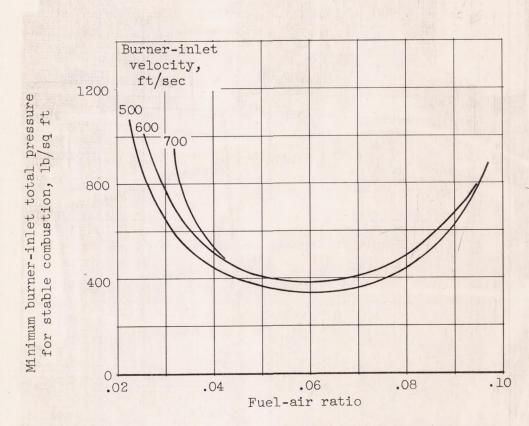
Figure 58. - Effect of velocity on stable operating
range of afterburner with 30-percent-blocked-
area V-gutter flameholder.
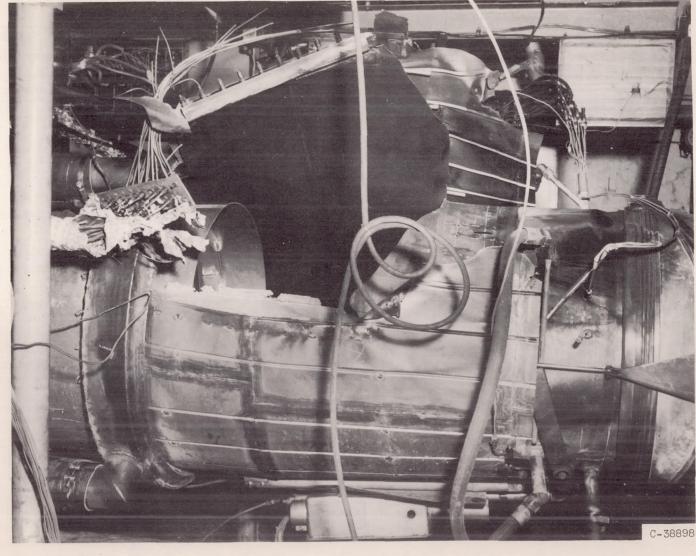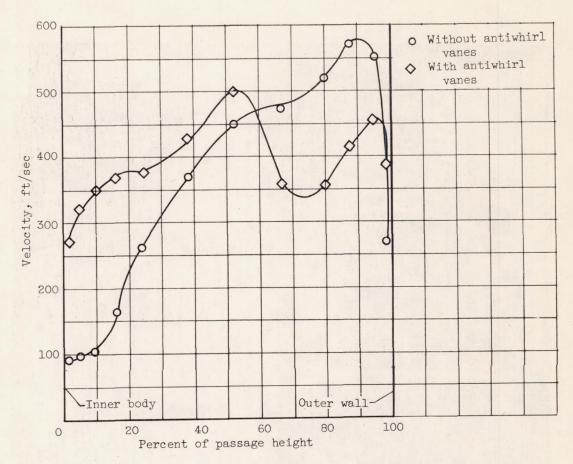
Figure 59. - Burner damaged by screech.

C-38898

(a) Diffuser-exit velocity profile.

(b) Screech limits.
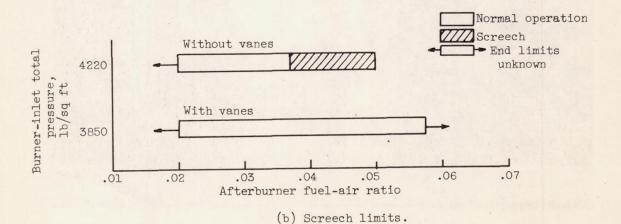
Figure 60. - Effect of radial distribution of velocity at afterburner
inlet on screech limits.
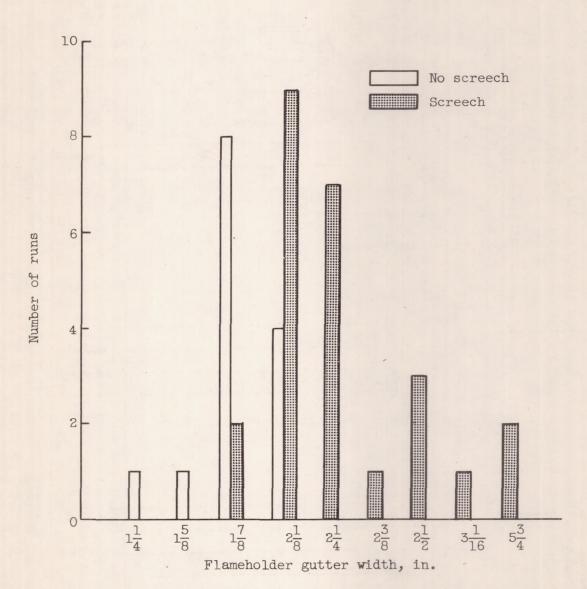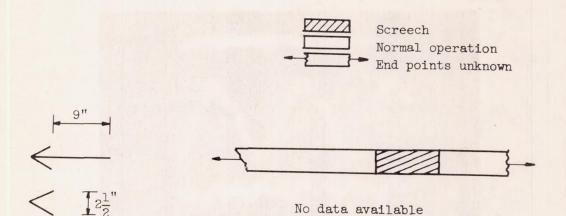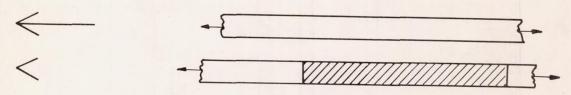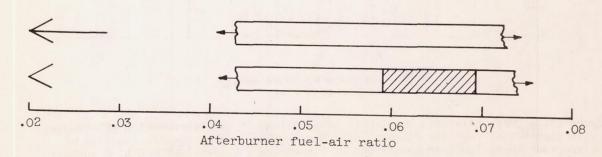
Figure 61. - Influence of flameholder gutter width on occurrence of screech. Burner-inlet total pressure, 3850 to 4220 pounds per square foot absolute; flameholder blockage, 32 to 40 percent of flow area.

(a) Burner-inlet pressure, 1080 pounds per square foot.

(b) Burner-inlet pressure, 990 pounds per square foot.
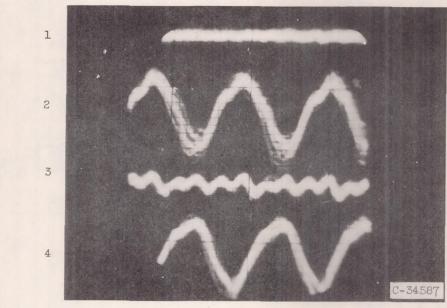
(c) Burner-inlet pressure, 870 pounds per square foot.

Figure 62. - Effect of flameholder splitter on screech limits.
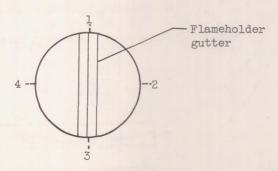
Figure 63. - Phase relations of screech oscillations in 26-inch-diameter afterburner with diametrical V-gutter flameholder. Microphones equally spaced; location of microphone taps, 1.0 inch downstream of flameholder; flameholder width, 8 inches; screech frequency, 650 cycles per second.

Pressure
node

Burner shell

Pressure
node

Particle paths
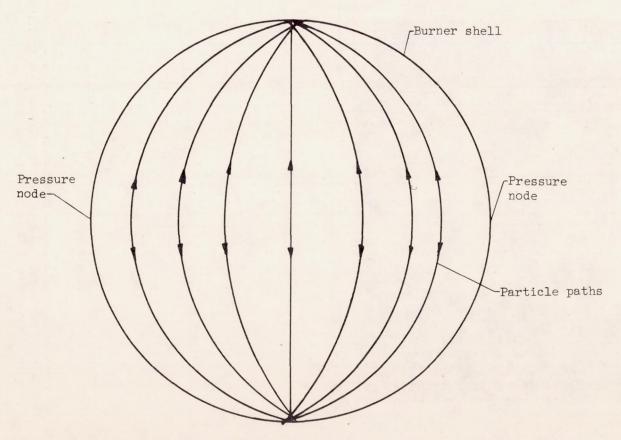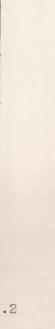
Figure 64. - Idealized cross section of afterburner, showing loci of wave-front
paths for first transverse mode of oscillation.
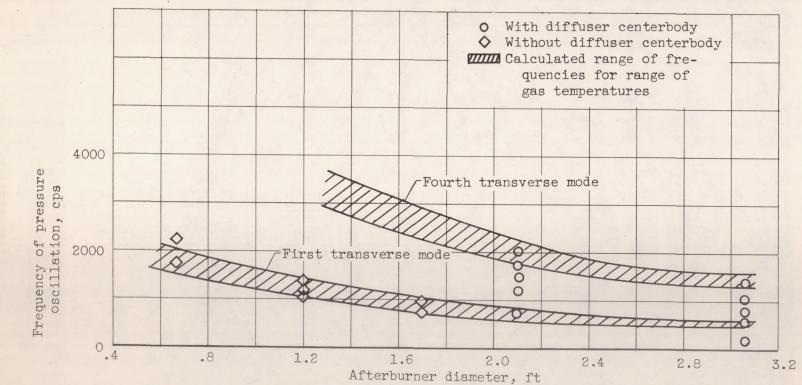
Figure 65. - Screech frequencies of afterburners of various diameters.

C-32755
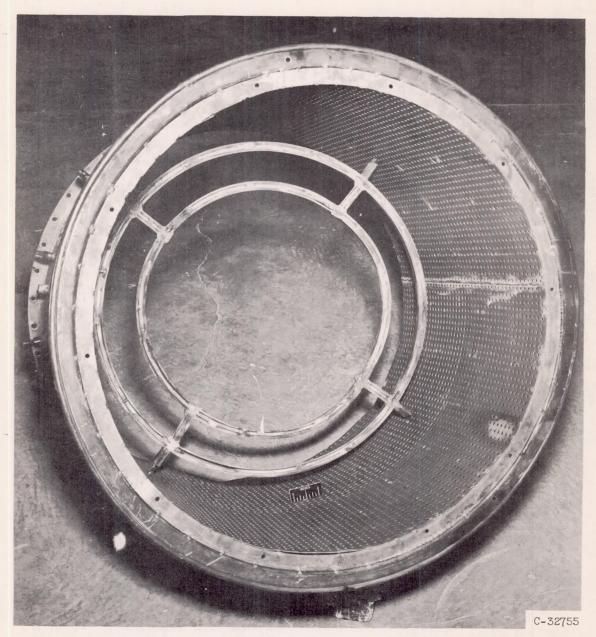
Figure 66. - Upstream view of perforated liner installed in 32-inch-diameter afterburner for suppression of screech.

3701
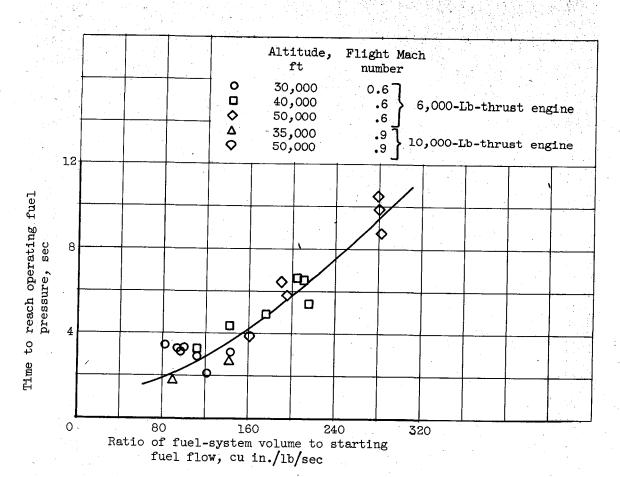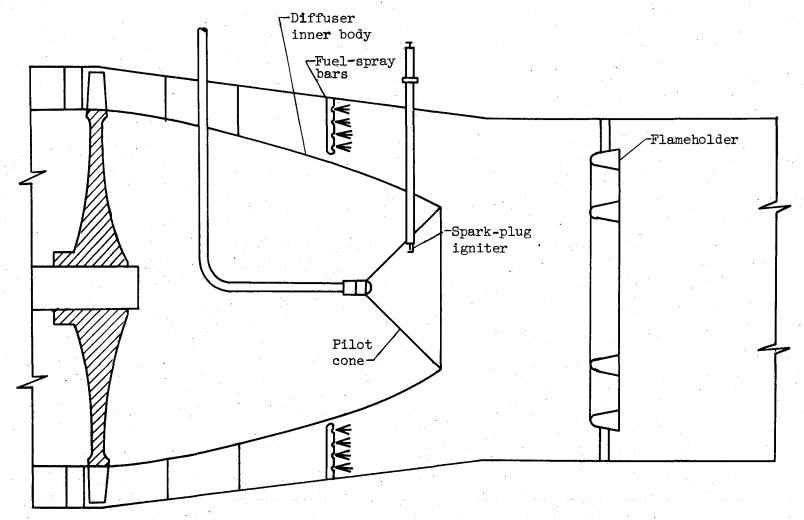
Figure 67. - Time required to reach operating fuel-manifold pressure for an afterburner start.

Figure 68. - Typical spark-plug igniter installation in afterburner.
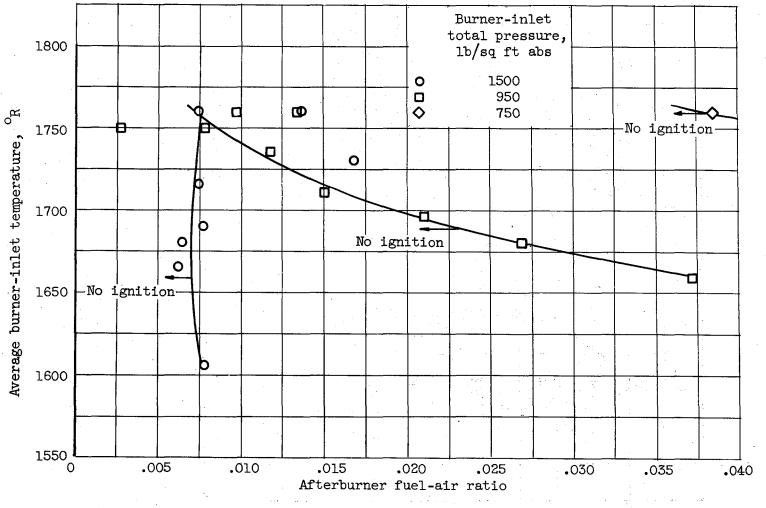
Figure 69. - Effect of afterburner-inlet pressure and temperature on limits of spontaneous ignition. MIL-F-5624 fuel with Reid vapor pressure of 7 pounds per square inch.
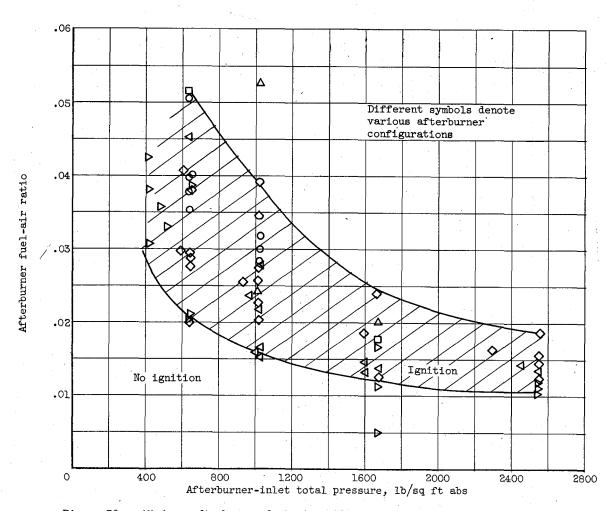
Figure 70. - Minimum afterburner fuel-air ratios at which autoignition occurred with several afterburner configurations. Fuel, MIL-F-5624 (AN-F-58); burner-inlet temperature, 1710° to 1760° R.
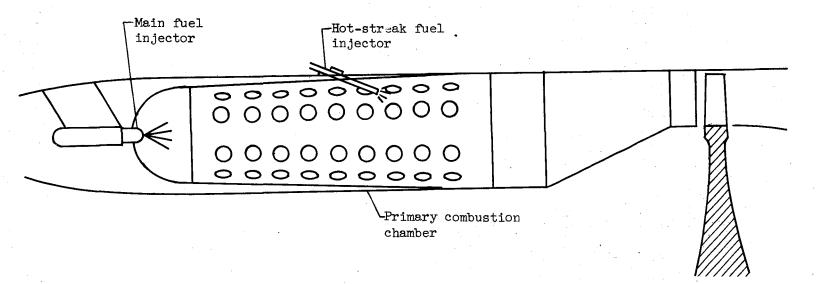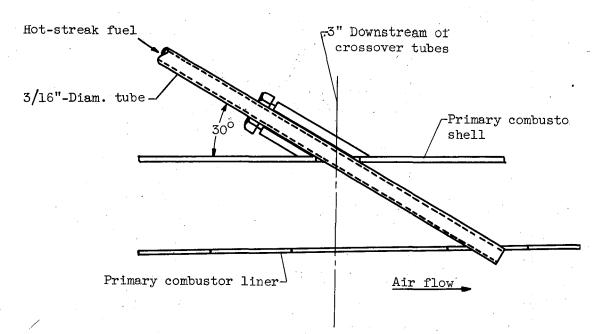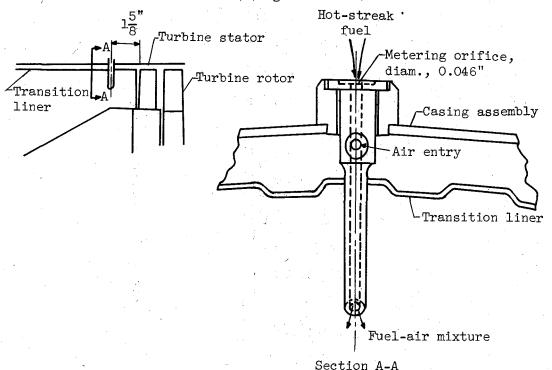
Figure 71. - Schematic diagram of hot-streak ignition system.

Hot-streak fuel

3/16"-Diam. tube

30°

.3" Downstream of crossover tubes

Primary combusto shell

Primary combustor liner

Air flow

(a) Igniter A.

1 5/8"

A

Turbine stator

Transition liner

A

Turbine rotor

Hot-streak fuel

Metering orifice, diam., 0.046"

Casing assembly

Air entry

Transition liner

Fuel-air mixture
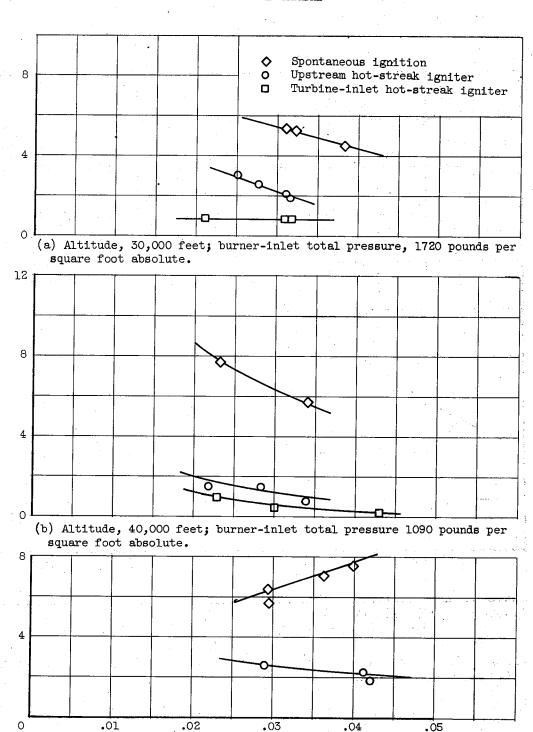
Section A-A

(b) Igniter B.

Figure 72. - Details of two hot-streak igniters.

DECLASSIFIED

3701

(a) Altitude, 30,000 feet; burner-inlet total pressure, 1720 pounds per square foot absolute.

(b) Altitude, 40,000 feet; burner-inlet total pressure 1090 pounds per square foot absolute.

(c) Altitude, 50,000 feet; burner-inlet total pressure, 660 pounds per square foot absolute.

Figure 73. - Effect of altitude on time for afterburner ignition. Flight Mach number, 0.6.
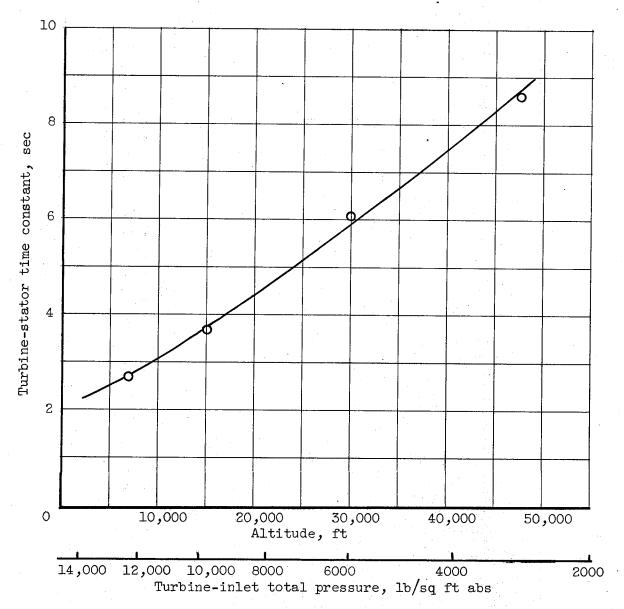
Figure 74. - Variation of turbine-stator time constant with altitude.
  Flight Mach number, 0.8.
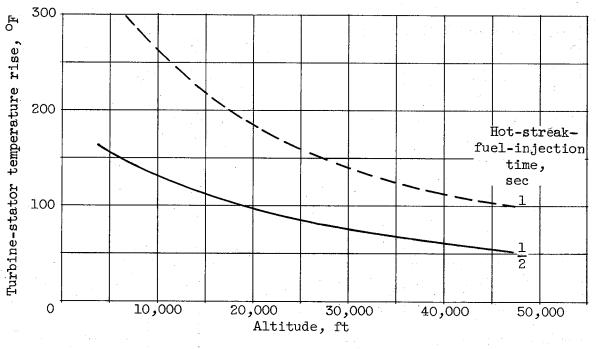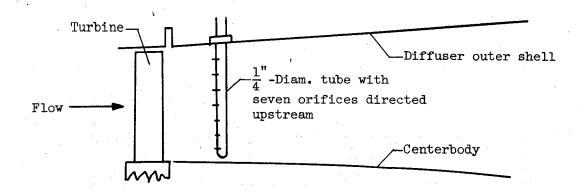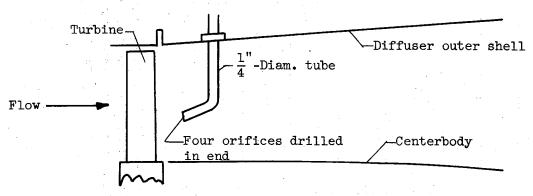
Figure 75. - Effect of hot-streak-fuel-injection time on variation
of turbine-stator-blade temperature rise with altitude. Initial
gas temperature, 2000° R; local gas temperature, 3000° R; equilib-
rium blade temperature equal to 0.93 gas temperature; flight Mach
number, 0.8.

(a) Configuration A, multiorifice bar.
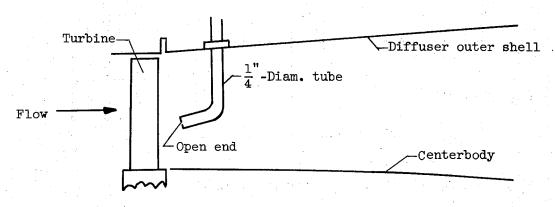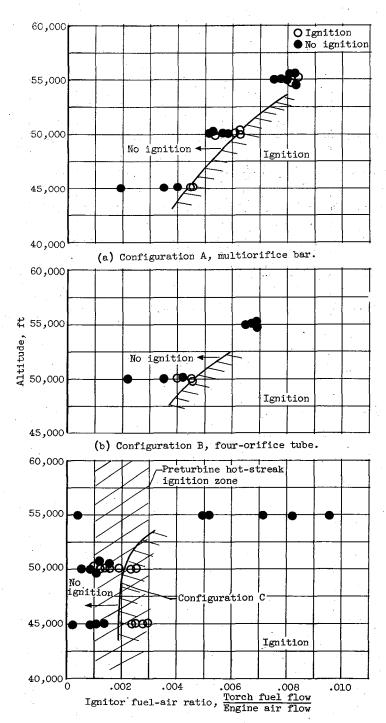
(b) Configuration B, four-orifice bar.
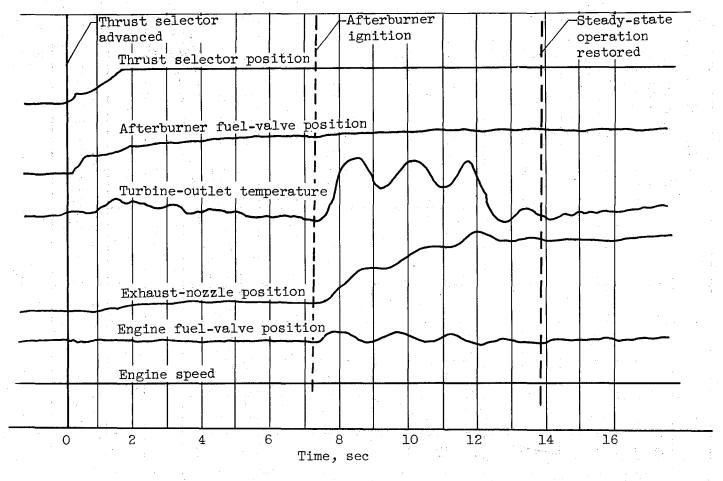
(c) Configuration C, open-end tube.

Figure 76. - Turbine-outlet hot-streak systems evaluated.

(a) Configuration A, multiorifice bar.

(b) Configuration B, four-orifice tube.

Ignitor fuel-air ratio, $\dfrac{\text{Torch fuel flow}}{\text{Engine air flow}}$

(c) Configuration C, open-end tube, compared with typical preturbine hot-streak configuration.

Figure 77. - Ignition limits of turbine-outlet hot-streak systems in comparison with typical pre-turbine hot streak. Turbine-outlet temperature, 1710° R.

Figure 78. - Oscillograph indications of control-parameter variations during afterburner ignition and transient to steady-state operation. Altitude 30,000 feet; flight Mach number, 0.6.

DECLASSIFIED

CU-21|back 3701
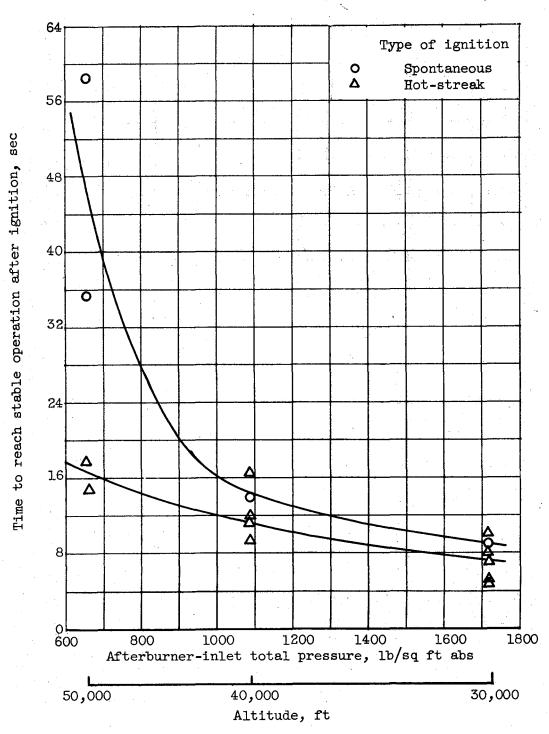
Figure 79. - Effect of afterburner-inlet total pressure on time to reach stable operation after ignition. Flight Mach number, 0.60.
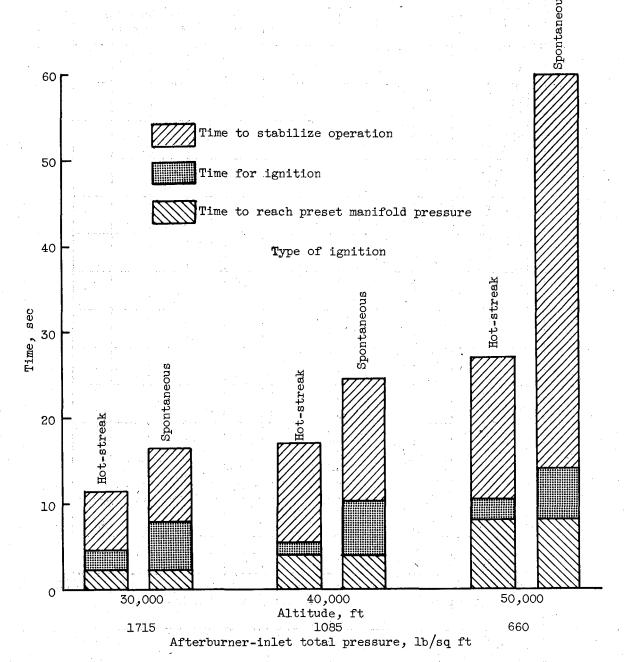
Figure 80. - Effect of altitude on over-all time required for afterburner
starting. Preset fuel-air ratio, 0.03; flight Mach number, 0.6.

Fuel-spray bars

Flameholder, 35 percent blockage; $1\frac{3}{4}"$ wide gutters

$25\frac{3}{4}"$

$57\frac{5}{8}"$
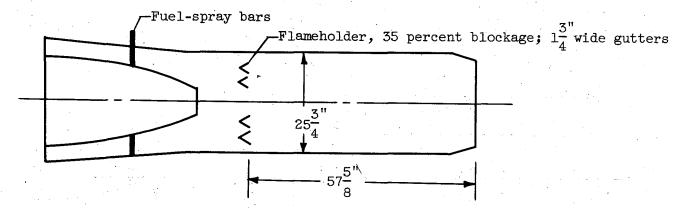
Figure 81. - Afterburner used with water-alcohol injection. Inlet velocity, 350 feet per second.
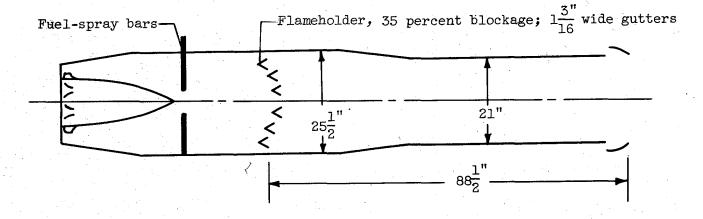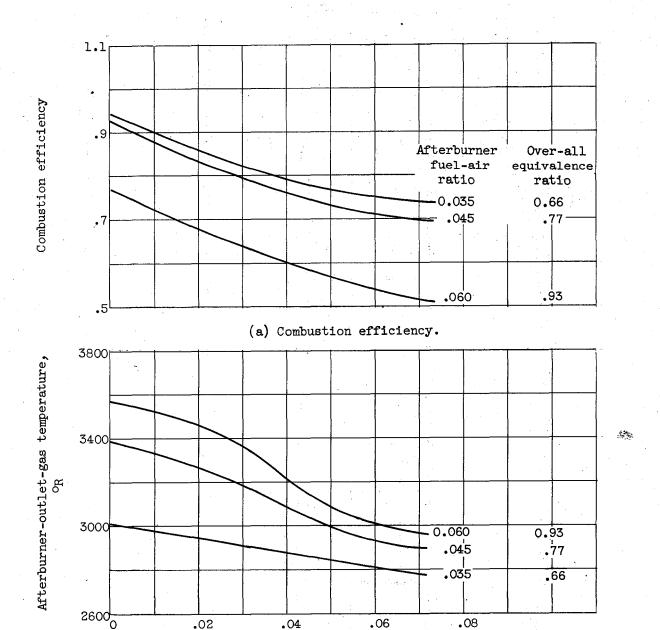
Figure 82. - Afterburner used with ammonia injection. Inlet velocity, 391 feet per second.

(a) Combustion efficiency.

(b) Afterburner-outlet-gas temperature.

Figure 83. - Effect of water-alcohol injection on afterburner per-
    formance.   Afterburner-inlet pressure, approximately 3800 pounds
    per square foot absolute.
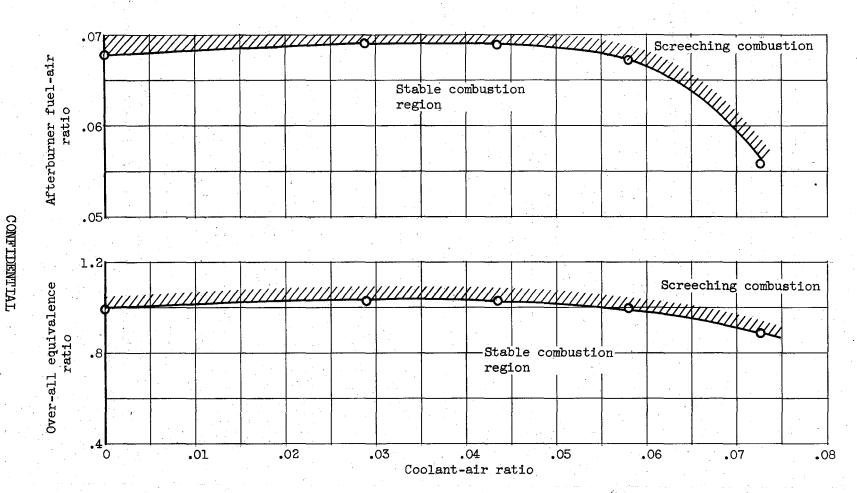
Figure 84. - Afterburner combustion stability limits with water-alcohol injection in compressor.

3701

CU-22
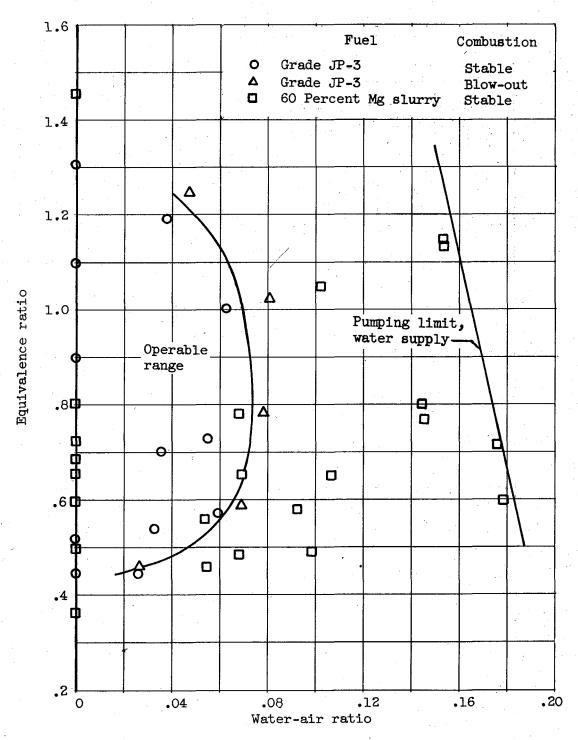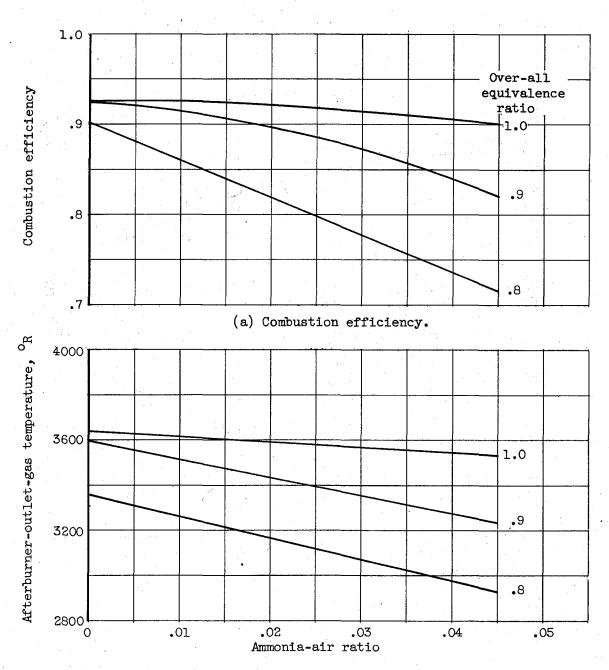
Figure 85. - Blow-out limits for JP-3 fuel and 60-percent
magnesium slurry fuel in 6-inch burner. Burner-inlet
velocity, 300 to 450 feet per second; burner-inlet pressure,
1100 to 1700 pounds per square foot absolute.

(a) Combustion efficiency.

(b) Afterburner-outlet-gas temperature.

Figure 86. - Effect of ammonia injection on afterburner performance.
Afterburner-inlet pressure, 1780 pounds per square foot absolute.

CU-22 /back   3701
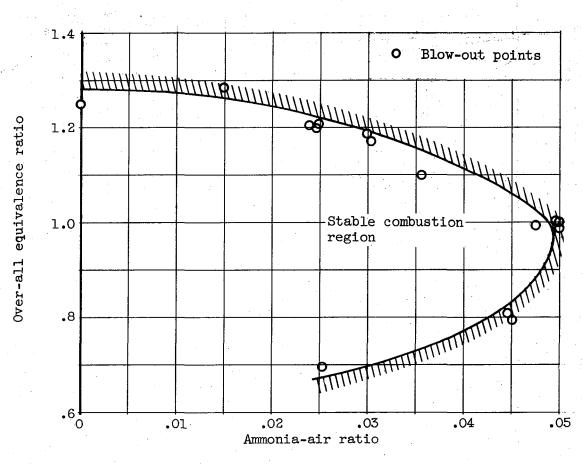
Figure 87. - Effect of ammonia-air ratio on blow-out limits. Afterburner-inlet pressure, 1780 pounds per square foot absolute.
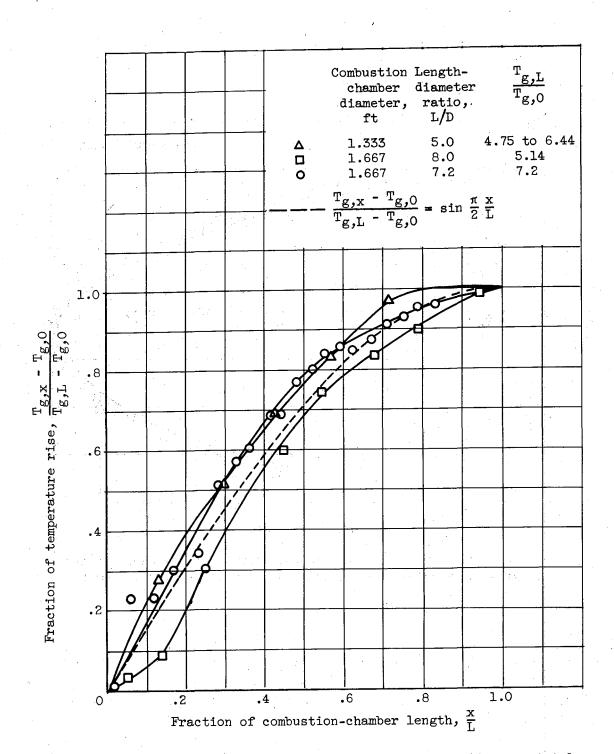
Figure 88. - Longitudinal distribution of combustion-gas total temperature for several ram-jet combustion chambers.

370L
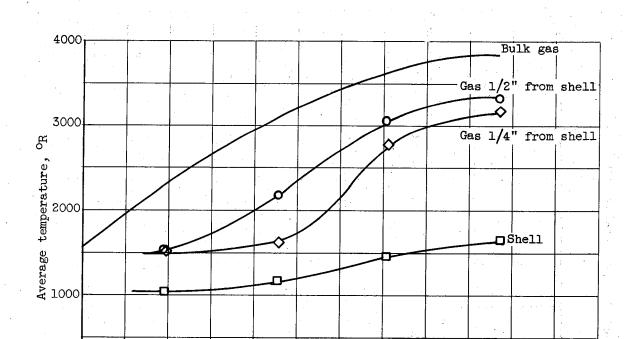
Figure 89. - Typical longitudinal profiles of gas and afterburner-shell temperatures. Outlet gas temperature, 3811° R; inlet cooling-air temperature, 537° R; cooling-air mass-flow ratio, 0.1374.
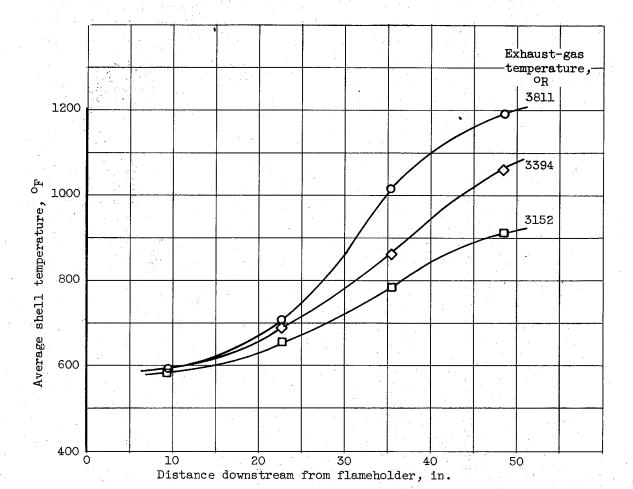
Figure 90. - Typical longitudinal profiles of afterburner shell tem-
perature for various outlet gas temperatures. Cooling-air mass-flow
ratio, approximately 0.14; inlet cooling-air temperature, approximately
520° R.

3701
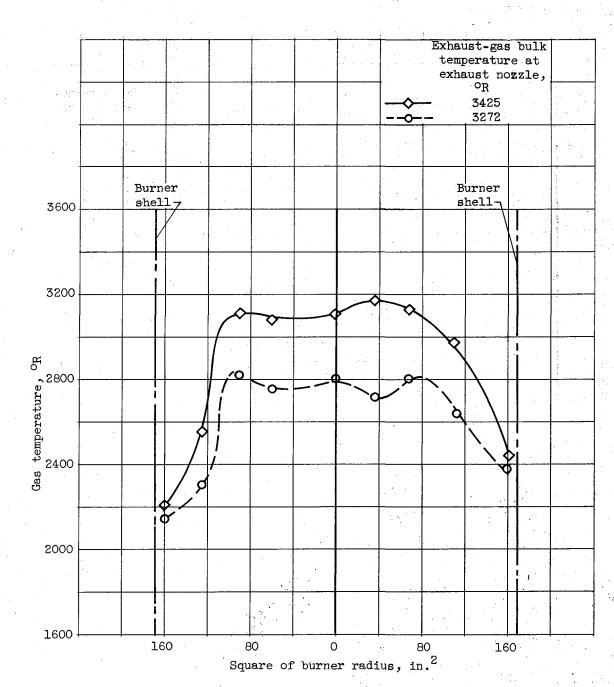
Figure 91. - Typical transverse profile of gas temperature 48 inches downstream of flameholder.

(a) Variation with operating time.
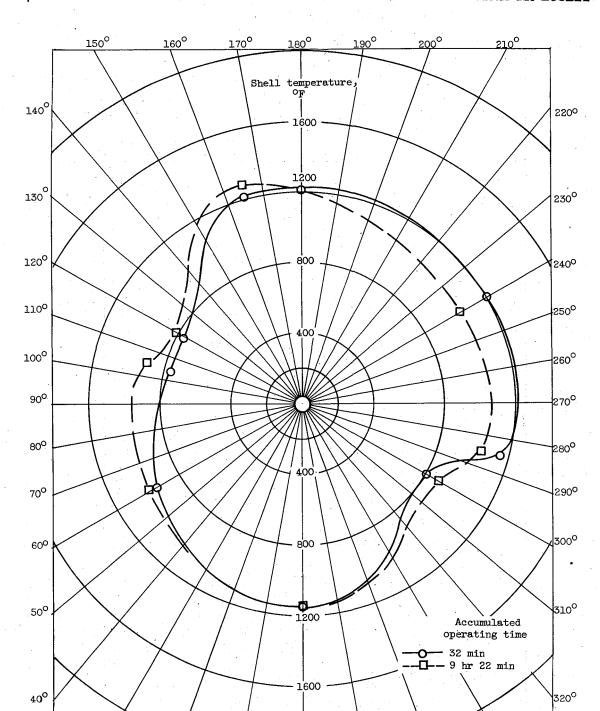
Figure 92. - Typical circumferential profiles of shell temperature 48 inches downstream of flameholder.

3701

CU-i23

(b) Variation with exhaust-gas temperature.
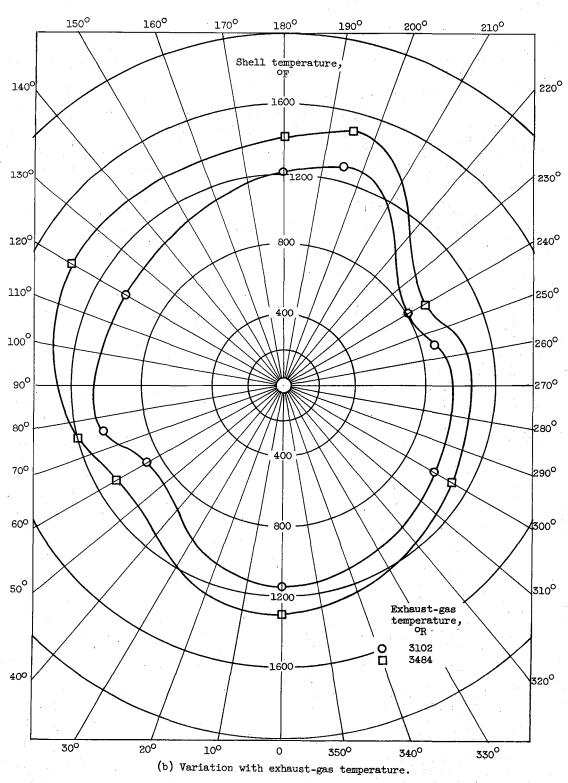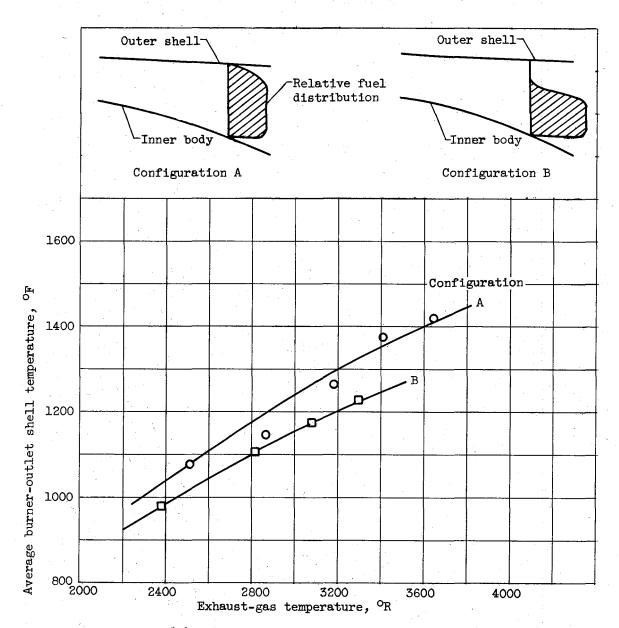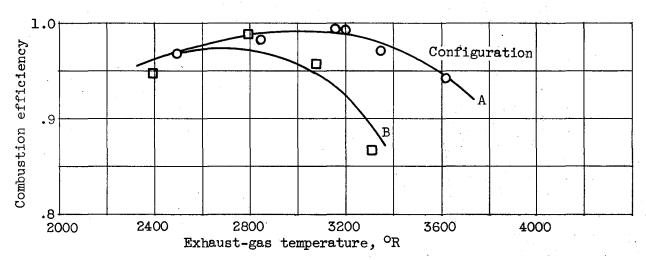
Figure 92. - Concluded. Typical circumferential profiles of shell temperature 48 inches downstream of flameholder.

(a) Effect on burner-outlet shell temperatures.
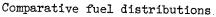
Figure 93. - Effect of fuel-air-ratio distribution on afterburner performance.

(b) Effect on combustion efficiency.

Figure 93. - Concluded. Effect of fuel-air-ratio distribution on afterburner performance.

Comparative fuel distributions

Configuration A　　　　　Configuration B　　　　　Configuration C
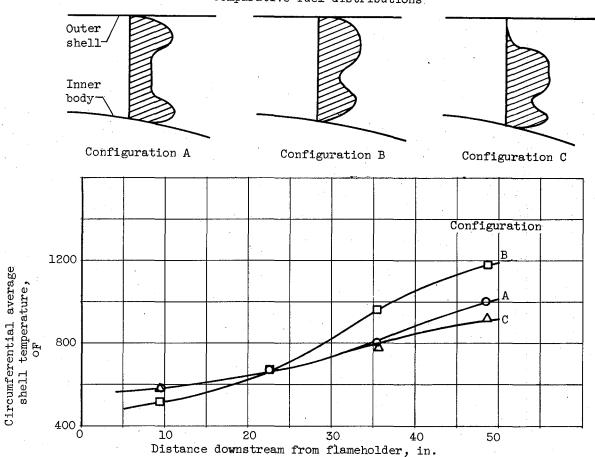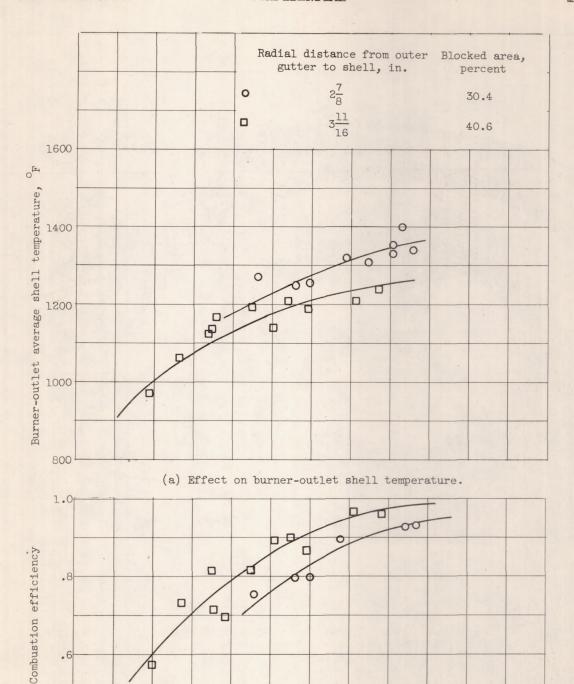
Figure 94. - Effect of radial fuel-air-ratio distribution on longitudinal profiles of afterburner-shell temperature.

(a) Effect on burner-outlet shell temperature.

(b) Effect on combustion efficiency.

Figure 95. - Effect of flameholder area distribution on afterburner
performance.

CONFIDENTIAL

Figure 96. - Downstream view of inner liner in afterburner.

C-24818

Symbol	Turbine-outlet temperature, °R	Burner length, in.	Liner passage width, in.	Reference
◇	1700	46	1/2	1
○	1735	54	1/2	48
□	1760	48	a3/4	Unpublished
–––– b	1700	48	1/2	46

aMaximum height of corrugated liner.

bCalculated from cooling correlation equation for 6-percent cooling-gas flow.
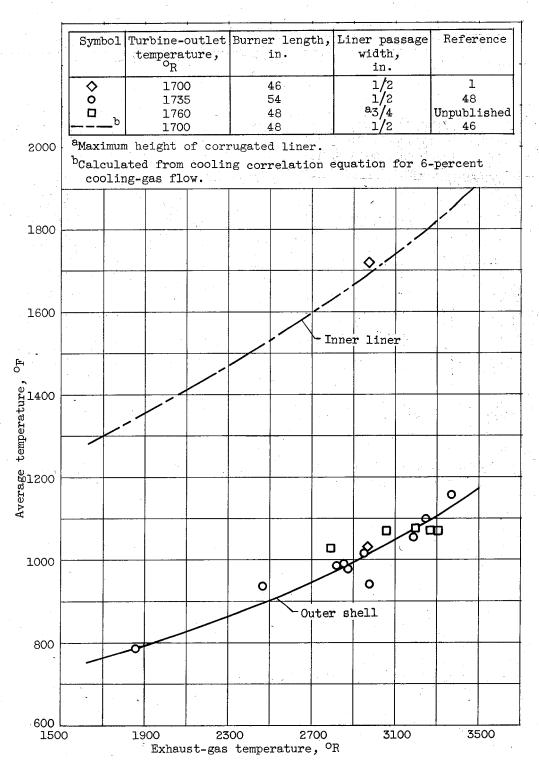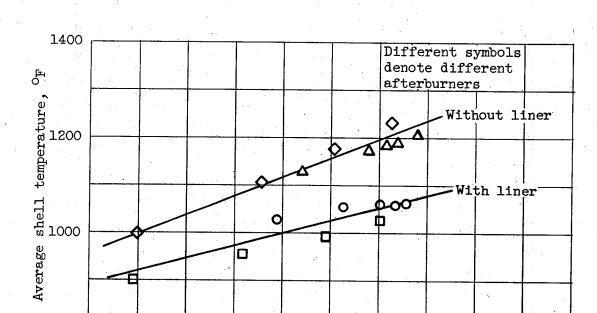
Figure 97. – Average temperatures of inner liner and outer shell of several typical full-scale afterburners at exhaust-nozzle inlet station. Liners extend entire length of combustion chamber.

Figure 98. - Effect of cooling liner on average temperature of burner shell at exhaust-nozzle inlet.
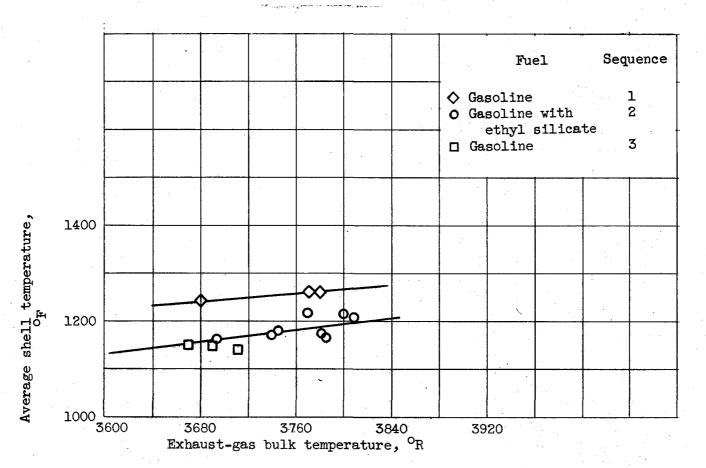
Figure 99. - Reduction in burner shell temperature by addition of 4 percent ethyl silicate in fuel.

3701

$$\frac{h_c D}{k_f} = 0.034 \left(\rho_f \, \frac{V_b D}{\mu_f} \right)^{0.8} \left(\frac{c_{p,f} \mu_f}{k_f} \right)^{0.4} \left(\frac{L}{D} \right)^{-0.1}$$

Vertical axis: $\dfrac{\text{Nusselt number} \left(\dfrac{\text{length}}{\text{diameter}} \right)^{0.1}}{(\text{Prandtl number})^{0.4}}$, $\dfrac{\left(\dfrac{h_c D}{k_f} \right) \left(\dfrac{L}{D} \right)^{0.1}}{\left(\dfrac{c_{p,f} \mu_f}{k_f} \right)^{0.4}}$

	Exhaust-gas temperature, $^\circ R$	Combustion-gas temperature at nozzle inlet, $^\circ R$
○	3845	3520
□	3435	3165
▽	3265	3025
◇	3240	2990
△	3060	2870

Modified Reynolds number, $\rho_f \dfrac{V_b D}{\mu_f}$
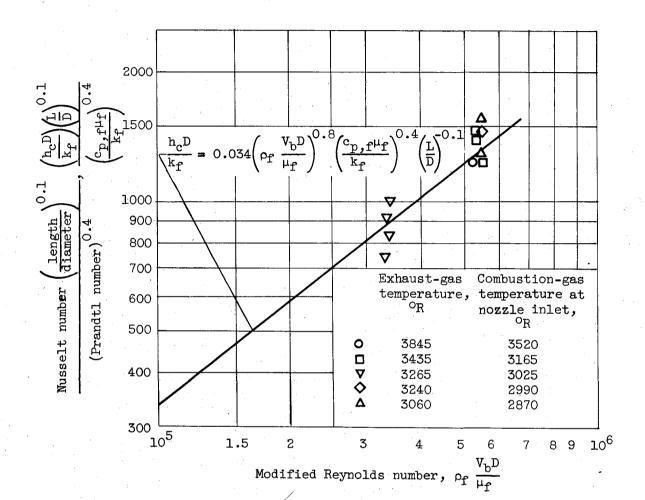
Figure 100. - Correlation of convective heat-transfer coefficient at exhaust nozzle inlet. Physical properties of air evaluated at film temperature T_f.

CU-24 | back   3701
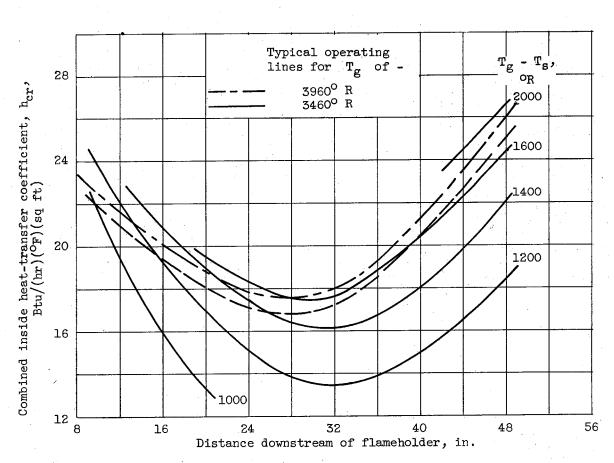
Figure 101. - Variation of combined inside heat-transfer coefficient along length of burner for typical afterburner with burner-inlet temperature of 1633° R. Burner-inlet pressure, 1400 pounds per square foot absolute.
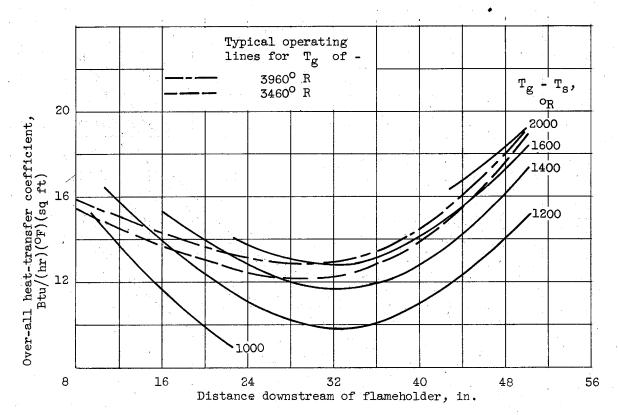
Figure 102. - Variation of over-all heat-transfer coefficient along
burner length for typical afterburner with burner-inlet temperature
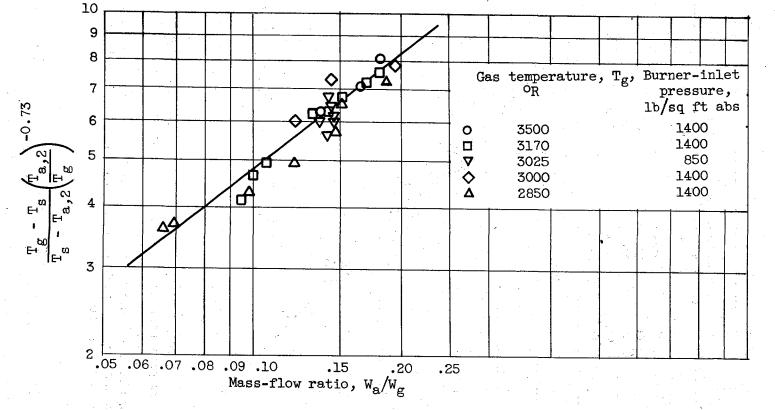of 1633° R; burner-inlet total pressure, 1400 pounds per square foot.

Figure 103. - Correlation equation for average afterburner shell temperatures at exhaust-nozzle inlet.
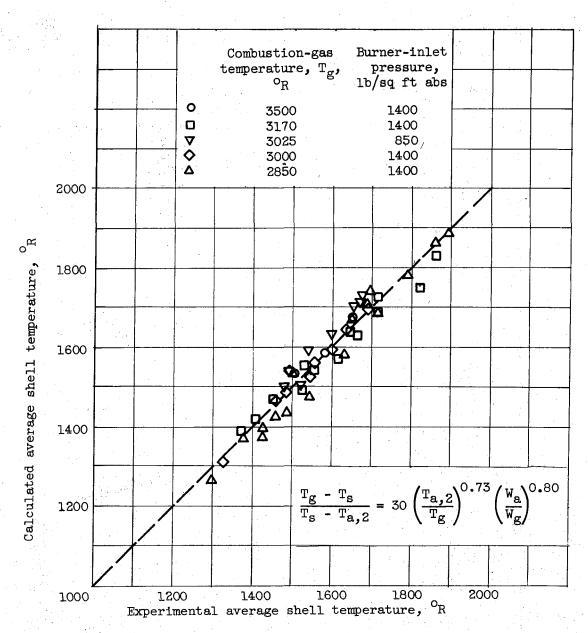
Figure 104. - Comparison of experimental shell temperatures at exhaust-nozzle inlet with temperatures calculated from correlation equation.
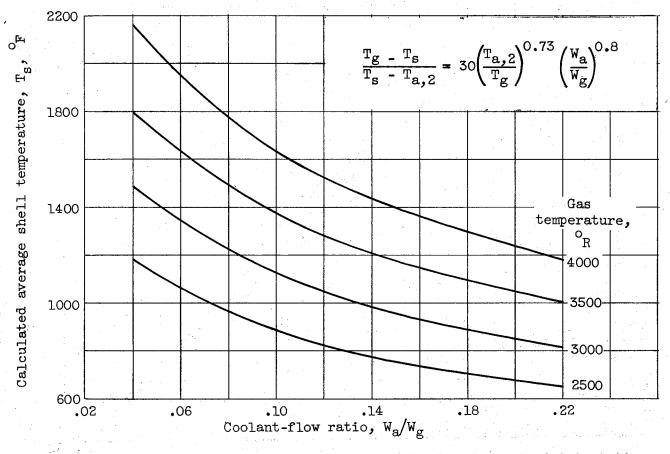
Figure 105. - Average shell temperatures at exhaust-nozzle-inlet station for range of exhaust-gas temperatures and mass-flow ratios as calculated from correlation equation. Cooling-air inlet temperature, 80° F.
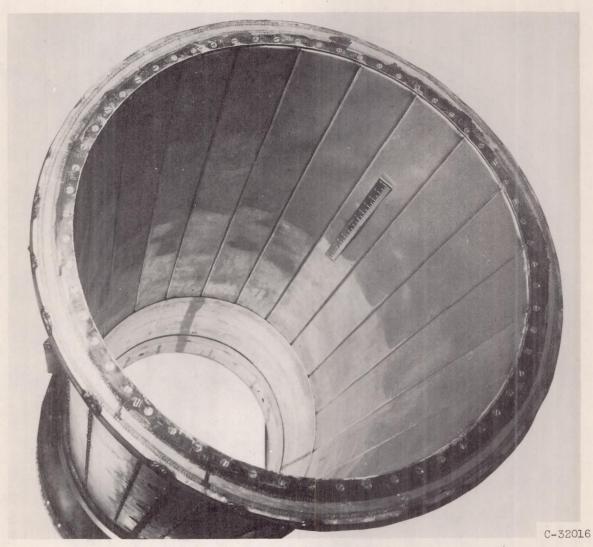
$$\frac{T_g - T_s}{T_s - T_{a,2}} = 30\left(\frac{T_{a,2}}{T_g}\right)^{0.73}\left(\frac{W_a}{W_g}\right)^{0.8}$$
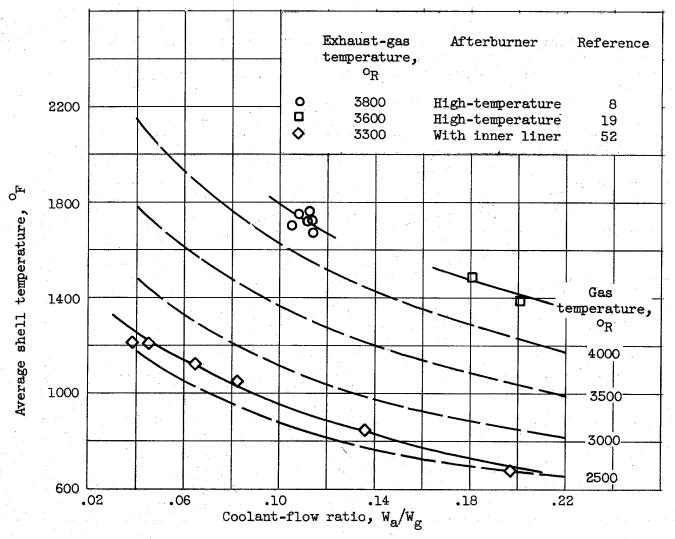
Figure 106. - Comparison of afterburner-shell temperature from correlation equation with available data from several afterburners.

C-32016

(a) Before cooling investigation.

Figure 107. - Interior view of experimental transpiration-cooled afterburner with porous combustion-chamber wall fabricated from brazed and rolled wire cloth. Exhaust nozzle removed.
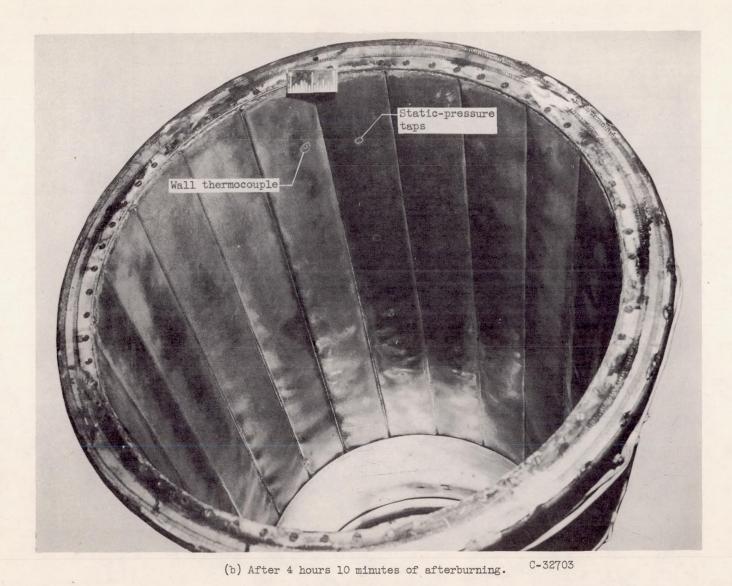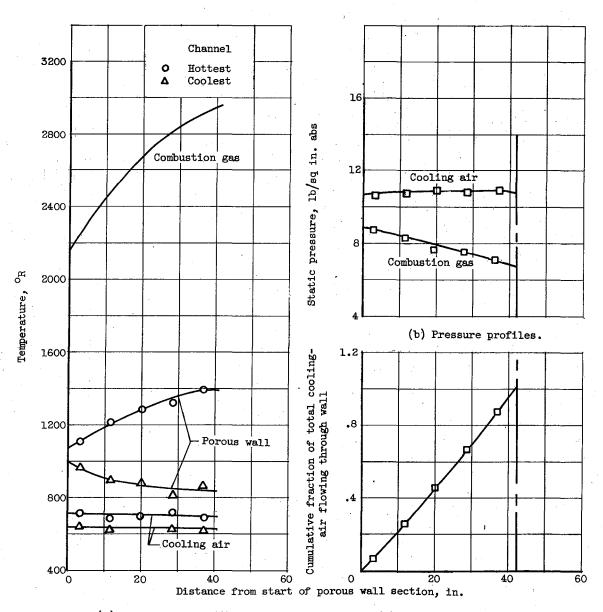
(b) After 4 hours 10 minutes of afterburning.   C-32703

Figure 107. - Concluded. Interior view of experimental transpiration-cooled afterburner with porous combustion-chamber wall fabricated from brazed and rolled wire cloth. Exhaust nozzle removed.

(a) Temperature profiles.

(b) Pressure profiles.

(c) Cooling flow distributions.

Figure 108. - Typical longitudinal profiles of temperature and pressure for wire-cloth afterburner. Exhaust-gas temperature, 2954° R; total cooling-air flow ratio, 0.0716.
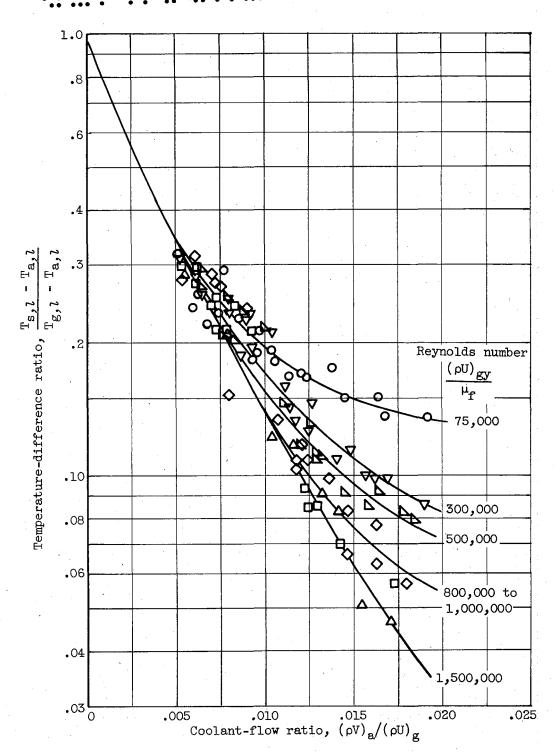
Figure 109. - Correlation of cooling data for wire-cloth afterburner. Reynolds number based on mass flow of combustion gas, distance from start of porous wall in flow direction, and viscosity at film temperature.
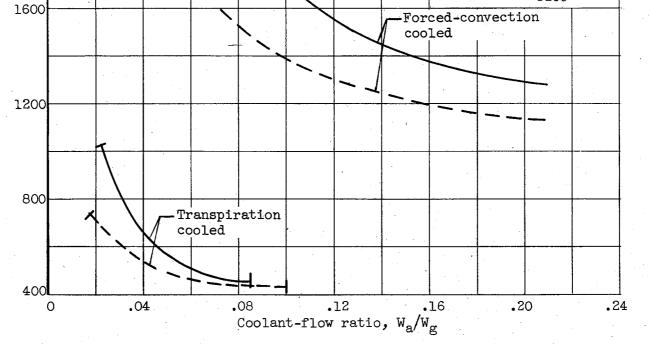
Figure 110. - Comparison of forced convection and transpiration cooling of typical afterburner. Uniform-permeability porous wall. Cooling-air temperature, 200 to 250° F for transpiration cooling and -16° F for forced-convection cooling.